UNIVERSITÉ DE MONTRÉAL

A STUDY ON THE CHARACTERISTICS OF VERTICAL ACCELERATIONS AND THEIR EFFECTS ON CIVIL ENGINEERING STRUCTURES

CONSTANTIN CHRISTOPOULOS
DÉPARTEMENT DES GÉNIES CIVIL, GÉOLOGIQUE ET DES MINES
ÉCOLE POLYTECHNIQUE DE MONTRÉAL

MÉMOIRE PRÉSENTÉ EN VUE DE L'OBTENTION
DU DIPLÔME DE MAÎTRISE ÈS SCIENCES APPLIQUÉES
(GÉNIE CIVIL)
AOÛT 1998

National Library
of Canada

Acquisitions and
Bibliographic Services

395 Wellington Street
Ottawa ON K1A 0N4
Canada

Bibliothèque nationale
du Canada

Acquisitions et
services bibliographiques

395, rue Wellington
Ottawa ON K1A 0N4
Canada

Your file Votre référence

Our file Notre référence

0-612-38666-X

Canada

UNIVERSITÉ DE MONTRÉAL

ÉCOLE POLYTECHNIQUE DE MONTRÉAL

Ce mémoire intitulé :

A STUDY ON THE CHARACTERISTICS OF VERTICAL ACCELERATIONS AND THEIR EFFECTS ON CIVIL ENGINEERING STRUCTURES

présenté par : CHRISTOPOULOS Constantin

en vue de l'obtention de diplôme de : Maîtrise ès sciences appliquées

a été dûment accepté par le jury d'examen constitué de :

M. TREMBLAY Robert, Ph.D., président

M. LÉGER Pierre, Ph.D., membre et directeur de recherche

M. FILIATRAULT André, Ph.D., membre et codirecteur de recherche

M. TINAWI René, Ph.D., membre

Στους γονείς μου,
σας ευχαριστώ για όλα.

À mes parents,
je vous remercie pour tout.

Remerciements

L'auteur désire remercier ses directeurs de projet M. Pierre Léger et M. André Filiatrault pour leur aide précieuse dans la réalisation de cette étude. L'étendue de leurs connaissances, la pertinence de leurs commentaires, leur dévouement pour leur travail, leur ouverture d'esprit, ainsi que leurs nombreuses qualités humaines ont été fortement appréciés.

L'auteur désire remercier Mme. Malama Tsiménis pour son soutien moral tout au long de sa maîtrise.

Enfin, l'auteur désire remercier le CRSNG et le FCAR pour l'aide financière attribuée à ce projet.

Résumé

Le présent travail de recherche traitant des caractéristiques des accélérations verticales et leurs effets sur les structures de génie civil est divisé en trois grandes parties. La première consiste en une étude sur les caractéristiques sismologiques des accélérations sismiques verticales. La deuxième est une investigation sur l'effet des accélérations verticales sur la réponse sismique d'un cadre d'acier résistant aux moments. Finalement, la dernière partie explore l'effet des accélérations verticales sur le glissement d'un barrage-poids.

Une revue de la littérature est effectuée en mettant l'accent sur : a) les aspects sismologiques, b) les observations historiques, c) les résultats expérimentaux, d) les résultats d'analyses numériques et e) les différents codes.

L'étude statistique sur les caractéristiques des accélérations verticales a été effectuée sur une banque de séismes historiques divisée en trois groupes. Le critère de sélection pour chaque groupe était le ratio a/v tel que défini par le CNBC (1995). Ce ratio, entre l'accélération de pointe au sol, a_g, exprimée en g, et la vitesse maximale au sol, v_g, exprimée en m/s, est une mesure du contenu fréquentiel du séisme, et caractérise la sismicité d'une région. Des valeurs de a/v élevées sont caractéristiques de séismes de l'est canadien, tandis que les valeurs de a/v moyennes et faibles représentent des événements de l'ouest du pays. Les paramètres étudiés incluent différentes mesures de la durée, la période prédominante de l'excitation, ainsi que des mesures d'énergie. Les spectres de réponse horizontaux et verticaux pour tous les séismes ont aussi été calculés et comparés. Utilisant les résultats de l'étude statistique, une méthode pour générer des accélérogrammes verticaux à partir de spectres horizontaux est présentée.

Des analyses non-linéaires sur un cadre résistant aux moments en acier de six étages ont été effectuées afin d'étudier l'effet des accélérations verticales sur la réponse sismique de

ce genre de structures. Le cadre est soumis à des accélérations typiques d'événements californiens à proximité de l'épicentre. L'accélération verticale n'a pas influencé la demande en ductilité en rotation des poteaux et des poutres. Toutefois, les valeurs de efforts axiaux maximum, dans les poteaux ainsi que le taux de déformation ont augmenté considérablement par la prise en compte des excitations sismiques verticales. Ces dernières étaient plus ressenties par la structure lorsque celle-ci demeurait élastique. Au fur et à mesure que la structure se plastifiait, l'effet des accélérations verticales à haute fréquence était filtré, jusqu'à devenir négligeable pour la structure.

L'effet des accélérations verticales sur le glissement d'un barrage-poids a été étudié. Le barrage de Paugan, un ouvrage d'environ 50 m de haut, a été choisi pour cette étude. La structure est soumise à des accélérogrammes historiques et synthétiques typiques de l'est et de l'ouest de l'Amérique du nord. Les accélérogrammes horizontaux synthétiques ont été générés pour être compatibles avec le spectre moyen des accélérogrammes historiques, tandis que les accélérogrammes synthétiques verticaux ont été générés selon trois méthodes : (1) calibration des accélérogrammes horizontaux, (2) réduction du spectre horizontal puis génération des accélérogrammes et (3) réduction du spectre horizontal ainsi que calibration des périodes puis génération des accélérogrammes. Les analyses ont été effectuées à l'aide d'un logiciel qui a été développé dans le cadre de ce travail afin de prédire le glissement et évaluer les facteurs de sécurité contre le glissement en incluant les accélérations horizontales et verticales. Dans ce logiciel, on modélise le barrage comme un corps rigide soumis à des accélérations bi-directionelles et pouvant glisser sur une surface rugueuse.

Lorsque seules les accélérations horizontales sont incluses dans le calcul, les séismes de l'ouest donnent des valeurs de glissement nettement supérieures aux valeurs obtenues avec les séismes de l'est. Pour le groupe de séismes de l'est, les résultats obtenus pour les

séismes synthétiques sont comparables à ceux obtenus pour les séismes historiques que ce soit en incluant ou non les accélérations verticales.

Les méthodes de génération basées sur la calibration de spectres ont donné des résultats satisfaisants. Pour les séismes de l'ouest, le glissement calculé pour les séismes synthétiques est supérieur à celui calculé pour les accélérogrammes historiques. Une discussion sur le facteur de corrélation entre les composantes horizontales et verticales est présentée, et la question de corrélation des pics est abordée.

Abstract

The present study is related to the incidence of vertical seismic excitation on the structural response of civil engineering structures. Three major research axes were considered: the characteristics of vertical ground motions, the effect of vertical accelerations on steel moment-resisting frames, and finally the effect of the vertical excitation on the sliding response of a gravity dam.

First, a review of previously published work on vertical seismic accelerations is presented. The following aspects are considered: a) the seismological aspect, b) historical evidences, c) experimental evidences, d) numerical evidences, and e) codes of practice.

The study on the characteristics of the vertical accelerations was performed on a series of historical accelerograms that were subdivided according to the NBCC (1995) definition of the a/v ratio. The ratio of the peak ground acceleration, a_g, expressed in g, over the peak ground velocity, v_g, expressed in m/s, is a measure of the frequency content of the excitation. A high a/v value is representative of eastern North American ground motions, whereas the low and intermediate values of this ratio represent western North American events. For these series of historical accelerograms, indices such as different measures of duration, predominant period, as well as spectral ordinates were computed and compared. Based on these results, a method consisting of shifting and reducing the horizontal spectrum to obtain the vertical one was proposed.

The non-linear analyses on a 6-story steel moment-resisting frame structure were performed for earthquakes typical of near-fault Californian ground motions. Special attention was given on determining the effect of the vertical excitation on the rotational ductility demand, but other response parameters such as the increase in the axial load and the strain rate effects were also examined. The vertical accelerations did not influence the

demand in rotational ductility nor the maximum horizontal floor deflections of the structure. Important increases in maximum axial loads in columns were noted, but they did not affect the structural response. The strain rate in columns and beams, was found to increase when vertical accelerations were included. The vertical accelerations were found to play a more important role in the elastic response of the structure. As yielding progresses in the structure during an earthquake, the effects of high frequency vertical accelerations were filtered out.

The effects of the vertical accelerations on the sliding response of gravity dams was investigated in a case study of the Paugan dam (50 m), subjected to historical and synthetic records typical of eastern and western earthquakes. The synthetic horizontal accelerograms were generated based on the mean acceleration response spectra of the historical earthquakes, whereas the vertical synthetic accelerograms were generated with three distinct methods. The first method consisted in simply calibrating the horizontal accelerogram by a value of 2/3. The second method consisted in calibrating the horizontal spectrum to obtain the vertical one, then generating the vertical accelerogram. The third consisted in shifting and reducing the horizontal spectrum to obtain a vertical spectrum used to generate vertical accelerograms. The analyses were performed with a computer program developed in the scope of this study to compute the sliding displacements as well as other performance indicators (i.e. sliding safety factors). This program uses rigid body dynamics to compute the sliding response of the dam, under both horizontal and vertical input accelerations.

Western type earthquakes were found to induce larger sliding displacements than eastern type earthquakes when only the horizontal component was applied. The vertical acceleration was found to play a more important role on the sliding displacement in the eastern earthquake group than the western one. For eastern type earthquakes, the synthetic accelerograms yielded results comparable to the results obtained from historical

records, for seismic analyses with and without vertical excitation. The vertical component generation methods based on calibration of the horizontal spectrum yielded structural response results comparable to the historical ones. For western type earthquakes, the sliding displacements computed with the synthetic records yielded values much larger than the values obtained with the corresponding historical records. A discussion on the correlation factor between accelerograms and the control of peak correlation is presented.

Condensé

Introduction

La multiplication des enregistrements d'accélérations sismiques multi-directionelles, combinée avec de récentes observations de dommages sur des structures de génie civil suite aux séismes de Northridge (1994) et de Kobe (1995), ont sérieusement remis en question l'hypothèse selon laquelle les accélérations verticales peuvent être négligées lors du calcul ou du dimensionnement sismique.

À la suite du séisme californien de Northridge, un débat animé s'est engagé entre les chercheurs qui ont attribué plusieurs ruptures inattendues, aux fortes accélérations verticales et ceux qui considèrent toujours que l'effet des accélérations verticales est négligeable. L'effet des accélérations verticales a souvent été négligé à cause de la nature impulsive de cette sollicitation et à cause des facteurs de sécurité de nos codes, qui garantissent une marge plus que suffisante dans la direction verticale pour résister à tout excès de charge provenant de ces accélérations.

Avec le développement de la puissance et de la vitesse de calcul des ordinateurs, plusieurs logiciels tels que Ruaumoko (1996) ont offert la possibilité d'inclure les accélérations verticales dans les analyses paramétriques. De pair avec la question de l'effet possible des accélérations verticales sur le comportement sismique, un effort important est aussi effectué pour caractériser ces sollicitations. En effet, vu le manque flagrant d'enregistrements pour certaines régions du monde, la génération d'accélérogrammes synthétiques devient une activité d'importance majeure, puisque les ingénieurs effectuent

de plus en plus des analyses dynamiques non-linéaires dans le temps pour étudier la sécurité sismique des ouvrages de génie civil..

C'est dans cette perspective que se situe le sujet de ce travail de recherche. D'une part, la question de l'effet des accélérations verticales sismiques sur les ouvrages de génie civil est traitée à travers des analyses paramétriques, et, d'autre part, la question de la nature et la définition des sollicitations mêmes est abordée.

Revue des connaissances actuelles sur les accélérations verticales

Dans une première partie (chapitre 2), un survol des travaux de recherche et d'observations antérieures est effectué, afin de faire le point sur l'état des connaissances sur ce sujet. Les articles et documents retenus portent sur cinq thèmes majeurs : a) les aspects sismologiques, qui traitent des caractéristiques intrinsèques comme le contenu fréquentiel, la durée et l'importance des sollicitations verticales par rapport aux sollicitations horizontales; b) les observations historiques suite à des séismes majeurs dans le monde; c) les résultats numériques couvrant l'effet des accélérations verticales sur plusieurs types de structures de génie civil et finalement d) l'aspect normatif de différents pays dans le monde, qui prévoient des clauses sur les accélérations verticales dans leur code du bâtiment respectifs.

À travers cette revue de la littérature, on peut s'apercevoir que l'état des connaissances sur le sujet se trouve à l'état embryonnaire, et surtout que les codes de différents pays n'offrent pas une méthode universelle, simple et précise, à l'ingénieur pour gérer la question des accélérations verticales. Il est évident qu'il existe une certaine confusion à ce qui a trait au sujet et que, plus souvent qu'autrement, les codes suggèrent de ne pas tenir compte de ces accélérations, à moins d'avoir un doute ou une indication que les

accélérations verticales pourraient avoir un effet important sur la réponse sismique des structures considérées. Certaines observations de dommages "historiques", comme par exemple durant le séisme d' El Asnam en Algérie (1980) pointent la nécessité de codifier les charges induites par les accélérations verticales.

Étude sur les caractéristiques des accélérations verticales

Dans la deuxième partie du mémoire (chapitre 3), les caractéristiques des accélérations verticales sont quantifiées à travers une étude statistique basée sur une banque de séismes historiques (Heidebrecht 1988), divisés en trois groupe selon le ratio a/v, où a est l'accélération de pointe au sol exprimée en g et v la vitesse maximale du sol exprimée en m/s. La subdivision de ces groupes permet de voir si les conclusions tirées sont applicables à tous genres de séismes, puisque le ratio a/v est une mesure du contenu fréquentiel de l'accélérogramme et représente les caractéristiques sismiques d'une région donnée (principalement l'est vs l'ouest).

L'étude statistique effectuée a permis de tirer plusieurs conclusions sur les caractéristiques du mouvement sismique vertical, comme par exemple sa nature plus impulsive, à plus haute fréquence et à plus basse amplitude que les mouvements du sol horizontaux.

Il est aussi apparu qu'une valeur de 2/3 pour représenter le ratio de l'accélération de pointe au sol verticale sur l'accélération de pointe au sol horizontale est une bonne approximation de la moyenne obtenue dans cette analyse. Toutefois, l'écart type sur cette mesure est considérable, et l'accélération verticale maximale peut, dans certains cas, amplement dépasser la valeur maximale horizontale. Parmi les conclusions tirées, il importe de souligner que les accélérations verticales sont des mouvements oscillatoires,

dont le contenu fréquentiel est beaucoup plus élevé que celui des accélérations horizontales.

Les statistiques ont été réalisées sur les accélérogrammes, mais aussi et surtout sur les spectres de réponse calculés avec 5 % d'amortissement critique. L'approche spectrale présente des avantages importants par sa simplicité et permet à l'ingénieur de rapidement estimer l'effet d'un séisme sur une structure. Cette approche est, dans la majorité des cas, suffisante et sécuritaire pour le calcul sismique des ouvrages. De plus, le spectre représente une empreinte "sismique", puisqu'il caractérise le mouvement attendu dans une région. C'est pour cela que la plupart des méthodes de génération d'accélérogrammes synthétiques sont basées sur la compatibilité du spectre du mouvement généré avec le spectre de réponse cible représentant la région.

Par observation des spectres des accélérogrammes retenus pour notre étude et considérant une idée développée pour des séismes californiens par Bozorgnia et al. (1992), une méthode pour définir un spectre cible vertical pour une région donnée à partir du spectre horizontal représentant la région est proposée. Le spectre horizontal est en général bien documenté, soit par des spectres proposés par les différents codes, soit par lissage de spectres moyens obtenus d'accélérogrammes historiques pour les régions où les enregistrements sont plus nombreux.

Deux facteurs qui viennent modifier le spectre horizontal pour obtenir le spectre vertical sont introduits, soit: Sf ou facteur de périodes et Rf ou facteur de réduction. Le facteur de période, Sf, vient réduire l'abscisse du spectre qui est l'axe des périodes, pour ramener le pic spectral horizontal vers des fréquences plus élevées. Le facteur de réduction vient diminuer l'amplitude du spectre horizontal, pour respecter le ratio des amplitudes observées lors des analyses statistiques.

Afin d'illustrer le processus, un exemple est montré où des accélérogrammes horizontaux et verticaux sont générés pour la ville de Montréal. La ville de Montréal appartient au groupe de a/v élevé, et les accélérogrammes ont été générés avec le programme SIMQKE (1976), et en se basant sur le spectre horizontal proposé par le CNBC (1995) pour Montréal, et le spectre réduit et pondéré pour le vertical.

Une fois les accélérogrammes générés, une question très importante est traitée, celle de la simultanéité ou la combinaison des composantes horizontales et verticales. La corrélation des deux accélérogrammes est le paramètre qui influence le plus la réponse de la structure, lorsque les accélérations verticales sont incluses dans l'analyse. Si la corrélation n'est pas correctement contrôlée lorsque des accélérogrammes synthétiques sont utilisés, la réponse peut être grandement sous ou sur estimée. Le calcul de la corrélation, ainsi qu'une méthode simple pour induire le degré de corrélation souhaité entre deux accélérogrammes, sont présentés. Cette méthode n'est pas utilisée pour la génération d'accélérogrammes dans le chapitre 5, car suite aux calculs de glissement effectués sur un barrage, il ressort que ce paramètre bien qu'important d'un point de vue sismologique n'est pas tout à fait relié à l'effet des accélérations combinées sur la réponse structurale.

Afin de mieux définir la corrélation des pics d'accélération significatifs à la réponse structurale étudiée, une nouvelle mesure de la corrélation est proposée, le PCF, "Peak Correlation Factor" pour tenir compte seulement de la simultanéité des pics, plutôt que de la corrélation de l'accélérogramme au complet, qui peut contenir plusieurs secondes d'accélération non-significatives pour la structure, mais fortement corrélées, pouvant biaiser le facteur de corrélation conventionnel.

Analyses paramétriques sur un cadre rigide en acier

Le deuxième axe d'intérêt de cette étude est l'estimation et la quantification des dommages structuraux supplémentaires, induits par la présence des accélérations verticales. Dans le cadre de cette étude, puisque tous les cas potentiels de dommages causés par les accélérations verticales relevées lors de la revue de littérature ne pouvaient être examinés, deux types de structures, correspondant à deux axes de recherche de la section de structure de l'École Polytechnique de Montréal, ont été choisies, soit un cadre rigide en acier et un barrage poids.

Un bâtiment de six étages composé de cadres en acier rigides résistant aux moments, a été retenu par ce qu'il a fait l'objet, suite au séisme de Northridge (1994) en Californie, de plusieurs études visant à expliquer des ruptures survenues dans ce genre de structures. De plus, dans la littérature, il est mentionné qu'une augmentation de 10 % sur la demande en ductilité en courbure des poutres et des poteaux est attribuée à l'inclusion des accélérations verticales dans les analyses (Broderick et al. 1994).

Les résultats obtenus dans ce projet ne concordent pas avec cette observation. Il semblerait que les accélérations verticales ne jouent pas un rôle important dans la réponse globale des cadres rigides résistant aux moments, sous des sollicitations à proximité de l'épicentre de type "near fault" typiques de la Californie. Selon les calculs effectués, la demande en ductilité en courbure, ainsi que les déplacements maximum des étages ne sont pas affectés. Toutefois, les accélérations verticales jouent un rôle important sur d'autres paramètres. Les charges axiales de compression et de tension maximales dans les poteaux sont grandement augmentées par la présence des accélérations verticales. L'augmentation en moyenne pour les cinq séismes utilisés est de 85% pour le cas de la compression, et de 26.8% lorsque la tension est étudiée. Ces augmentations importantes des charges axiales maximales n'affectent pas le comportement global de la structure. Les cadres rigides résistant aux moments sont dimensionnés pour être sollicités par des

moments très importants, et sont largement surdimensionnés pour reprendre les charges axiales. Cependant il est possible que l'augmentation de charge axiale observée pour cette structure à cadres rigides soit semblable à l'augmentation observée sur une structure de mêmes dimensions, mais formée d'éléments rotulés et contreventés de type treillis. Dans ce cas, le critère de dimensionnement est plutôt la charge axiale, cette augmentation de charge axiale attribuée aux accélérations verticales pourrait alors être très importante.

Un autre point important, soulevé lors des études paramétriques, est le fait que les sollicitations provenant des accélérations horizontales et verticales sont déphasées. L'augmentation de charge axiale, qui réduit la limite élastique selon les courbes d'interaction moment - charge axiale, est à une fréquence plus élevée que la variation du moment qui plastifie la section. Ce moment de plastification est principalement dû aux sollicitations horizontales. Ceci empêche les deux phénomènes (augmentation de la charge axiale et du moment) de se coupler et diminue ainsi l'influence des accélérations verticales. Il est évident qu'un contenu fréquentiel rapproché entre la réponse axiale et la réponse en moment induirait beaucoup plus de plastification dans la structure. Ceci peut être influencé par une sollicitation sismique où le contenu fréquentiel des accélérogrammes horizontaux et verticaux sont rapprochés.

Un effet important des accélérations verticales sur la réponse structurale est l'augmentation marquée du taux de chargement et de déformation, surtout au début du séisme, lorsque la structure répond dans le domaine élastique. En effet, lorsque les accélérations verticales sont incluses dans le calcul, en utilisant une formule proposée par Wakabayashi (1984) pour calculer la limite élastique en fonction du taux de déformation, on constate qu'en début de séisme, la limite élastique F_y peut passer d'une valeur initiale de 290 MPa à une valeur de 320 MPa. Cette augmentation marquée de F_y peut causer une augmentation importante du moment plastique, sans toutefois modifier la résistance ultime de l'acier. Ceci a comme conséquence de rendre le matériau fragile et de favoriser une rupture sans dissipation d'énergie par fissuration et propagation rapide de fissures

dans l'acier. Une telle rupture, où même une série de fissures qui endommageraient les sections d'acier dans les premières secondes du séisme, pourraient favoriser une réponse sismique inadéquate et dangereuse puisque la structure perdrait sa capacité de se déformer plastiquement.

De plus, dans la philosophie de dimensionnement sismique des poutres faibles-poteaux forts, le dimensionnement des poteaux qui, en théorie, ne doivent pas se plastifier afin d'éviter la formation de mécanismes, est basé sur les moments nominaux des poutres qui s'y attachent. L'augmentation de ces moments nominaux, induite par l'augmentation de la limite élastique, augmente la sollicitation des poteaux et peut provoquer leur plastification. Ceci est bien sûr considéré comme un mécanisme et peut entraîner des ruptures fragiles et catastrophiques. Le dimensionnement des soudures, normalement composées de matériau plus résistant mais aussi plus fragile que le métal de base, est basé sur le moment maximum provenant des poutres que l'assemblage doit reprendre. Une augmentation de ce moment peut causer des ruptures fragiles ou un endommagement sérieux de la soudure durant les premières secousses importantes du séisme.

Dans les résultats de nos analyses, que ce soit au niveau du taux de chargement ou de la fréquence d'oscillation de la charge axiale des poteaux, l'effet des accélérations verticales est beaucoup plus important au début du séisme, où la structure répond dans le domaine élastique. En effet, au fur et à mesure que la structure se plastifie, elle filtre les hautes fréquences, jusqu'au point où elle devient complètement insensible à la sollicitation verticale de haute fréquence. On peut clairement apercevoir sur les historiques des charges axiales, que bien qu'au début du séisme la réponse avec accélérations verticales et la réponse sans accélérations verticales sont très différentes, à partir du milieu et progressivement jusqu'à la fin de l'enregistrement, les deux réponses deviennent de plus en plus identiques.

Effet des accélérations verticales sur le glissement d'une structure de barrage-poids

Dans le cadre de l'évaluation de plusieurs barrages construits il y a 20 ans et plus, un effort important a été effectué pour évaluer la performance sismique de ces ouvrages dimensionnés selon des règles de calcul sismique qui diffèrent grandement des pratiques actuelles. Dans cet effort d'évaluation des barrages existants, la question du choix d'accélérogrammes, ainsi que l'importance des sollicitations multi-dimensionelles ont émergé. Dans notre travail, nous avons examiné la question de l'effet des accélérations verticales sismiques sur le facteur de sécurité au glissement et la magnitude des déplacements sismiques relatifs entre le barrage et sa fondation.

Afin de pouvoir effectuer des analyses numériques de glissement en incluant les sollicitations horizontales et verticales simultanément, un logiciel a été développé basé sur une modélisation de corps rigide du barrage. Le logiciel considère deux modes possibles durant le séisme, soit un mode "non-glissement" où la structure ne glisse pas et suit intégralement le mouvement du sol, et un mode "glissement", lorsque la résistance disponible en friction à l'interface barrage-fondation est dépassée par les forces d'inertie. Le logiciel vérifie à chaque pas de temps, en considérant les accélérations horizontales et verticales, si la structure est en mode "non-glissement" ou en mode "glissement". Lorsque la structure entre dans le mode "glissement", un algorithme classique de type Newmark-Beta à accélération linéaire est utilisé pour intégrer les équations de mouvement. Une fois le glissement engendré, il ne prend fin que lorsque a) l'accélération horizontale est inférieure à l'accélération critique et b) lorsque le signe de la vitesse du bloc devient à la fin d'un pas de temps négatif. Lorsque ceci est le cas, le glissement cumulé est ramené à la valeur du pas de temps précédent, et une correction est rajoutée pour tenir compte du fait que, pendant un pas de temps où la vitesse est négative à la fin du pas mais positive au début, une certain glissement a lieu entre le début du pas de temps et le moment où la vitesse devient nulle, avant de passer dans le négatif.

Le logiciel calcule aussi le facteur de sécurité au glissement à chaque pas de temps, ainsi que la position de la résultante à la base du barrage. Cette dernière mesure est un indicateur de la possibilité que, durant le séisme, sur la surface de contact il y ait des régions en tension, que ce soit en amont ou en aval. De plus, cette mesure est aussi un indicateur du potentiel de renversement du barrage.

Le barrage de Paugan, un ouvrage de 50 m de haut, a été choisi comme structure de référence (voir Ghrib et al. 1997), et les charges ont été calculées selon les hypothèses présentées au chapitre 5.

Les analyses ont été effectuées pour deux groupes de séismes, soit un groupe représentatif de l'est canadien, et un groupe représentatif de l'ouest.

Une première série d'analyses a été réalisée sur des séismes historiques correspondant aux groupes de séismes respectifs. Une seconde série d'analyses a été effectuée sur des séismes synthétiques générés de différentes façons, afin d'appliquer les méthodologies présentées au chapitre 3 de ce travail. Tous les séismes ont été calibrés pour une accélération horizontale de pointe au sol de 0.25 g. Les durées respectives pour chaque groupe de séismes synthétiques ont été ajustées par essai et erreur, en calculant à chaque fois les durées significatives et en comparant avec les valeurs moyennes correspondantes aux séismes historiques.

Une fois les accélérogrammes historiques calibrés et les accélérogrammes synthétiques générés, les analyses ont été effectuées pour calculer le facteur de sécurité au glissement, le glissement relatif entre le barrage et la fondation et la position de la résultante verticale..

En examinant d'abord les séismes historiques sans les accélérations verticales, il est évident que les accélérogrammes du groupe de l'ouest sont beaucoup plus critiques pour le glissement du barrage-poids. En effet, en accord avec d'autres résultats rapportés dans

la littérature (Tinawi et al. 1998), le contenu fréquentiel plus élevé des séismes de l'est est moins critique, car c'est la durée des impulsions significatives qui influence le glissement total, et non pas nécessairement le PGA de l'accélérogramme.

En comparant le glissement horizontal moyen des séismes historiques au glissement moyen obtenu avec les accélérogrammes horizontaux synthétiques, on remarque que pour le groupe de l'est, il y a une grande similitude. Pour le groupe de l'ouest, les accélérogrammes synthétiques donnent des valeurs de glissement nettement supérieures à celles obtenues avec les accélérogrammes historiques. En calculant certains paramètres des accélérogrammes comme la racine carrée de la somme des carrés (RMSA) et l'intensité Arias, ainsi que la période prédominante, on remarque que les accélérogrammes générés pour le groupe de l'ouest, malgré leur bonne compatibilité avec le spectre cible, présentent des caractéristiques très différentes des accélérogrammes historiques. En effet, les accélérogrammes historiques sont grandement influencés par deux ou trois impulsions très importantes, qui marquent et influencent le spectre de réponse. Les accélérogrammes synthétiques, générés par un processus mathématique, sont beaucoup plus uniformes à ce qui a trait aux amplitudes et au contenu fréquentiel du mouvement durant le séisme. Il est évident qu'une même réponse spectrale peut être obtenue avec différents accélérogrammes, et nos résultats de glissement indiquent à quel point il est important de calculer et comparer les indices des accélérogrammes générés aux accélérogrammes historiques, même si la compatibilité des spectres de réponse est respectée.

Pour les séismes historiques, on remarque que les pourcentages d'augmentation du glissement obtenu avec l'ajout des accélérations verticales est plus important pour les séismes de l'est que ceux de l'ouest. Les contenus fréquentiels des accélérations horizontales et verticales qui sont plus rapprochés pour les séismes de l'est et le PGA vertical plus important pour les séismes de l'est expliquent ce résultat.

Parmi les trois méthodes proposées pour la génération des accélérogrammes verticaux, les méthodes basées sur les spectres ont donné des résultats beaucoup plus réalistes et plausibles en comparaison avec les séismes historiques. En effet, il ressort clairement de nos résultats que la méthode qui consiste à pondérer un accélérogramme horizontal par une valeur de 2/3 pour obtenir un estimé de l'accélérogramme vertical est inacceptable, car la corrélation parfaite entre les deux signaux est beaucoup trop critique.

Deux méthodes de calcul du spectre vertical basé sur le spectre horizontal on été examinées: la méthode de calibration spectrale (reduced) et la méthode de calibration spectrale et de réduction de l'axe des périodes (shifted and reduced). Pour le groupe de l'est la méthode "shift and reduced" donne des résultats plus proches des résultats obtenus avec les accélérogrammes historiques. Toutefois, pour les calculs de glissement effectués, il serait difficile de justifier de façon pratique l'effort de calcul nécessaire pour appliquer cette méthode, vu le peu de différence avec la méthode de calibration spectrale (reduced). Le barrage a été modélisé comme un corps rigide. Il est cependant probable que, lors d'un calcul dynamique sur une structure flexible il pourrait y avoir une amplification dans la direction verticale. Dans ce cas, la méthode "reduced" sous-estimerait l'effet de l'amplification dynamique verticale, puisque le pic spectral serait à des périodes plus hautes, soit celles correspondant au pic spectral horizontal.

Les résultats obtenus sur le facteur de sécurité au glissement confirment d'une certaine façon que la combinaison de la "règle du pouce" du 30%, largement utilisée en pratique, donne des résultats comparables aux combinaisons les plus critiques obtenues avec les analyses pas-à-pas dans le temps. Cette règle est utilisée pour le calcul pseudo-statique du facteur de sécurité contre le glissement. Elle consiste à appliquer simultanément 100% de la force d'inertie horizontale maximale basée sur l'accélération de pointe au sol horizontale (PGAH) avec 30% des forces d'inertie verticales maximales, basées sur l'accélération de pointe au sol verticale (PGAV). Cette approche tient compte de la faible

probabilité que les sollicitations maximales dans les deux directions, horizontale et verticale, se produisent simultanément.

Toutefois, il est intéressant de noter que pour le groupe de l'est, la combinaison 100% horizontal avec 30% vertical a donné des facteurs de sécurité comparables à la combinaison 30% horizontal avec 100% vertical. Ceci indique qu'il serait judicieux de calculer les deux combinaisons avec la règle du 30% pour les calculs effectués pour des séismes de l'est.

Le calcul du facteur de corrélation des pics (PCF), défini dans le chapitre 3 pour différents séismes, est un paramètre qui indique le degré de sollicitation dû à l'effet simultané des accélérations horizontales et verticales. En calculant le nombre de pas de temps où le PCF est supérieur à une valeur significative pour la structure étudiée, un estimé de la sévérité de la combinaison des accélérogrammes horizontaux et verticaux peut être obtenu. Le PCF peut être aussi un indicateur de la compatibilité entre un accélérogramme synthétique et un accélérogramme historique. En effet, la compatibilité des spectres étant une condition nécessaire mais non suffisante pour assurer des mouvements générés réalistes et cohérents, le PCF peut devenir un paramètre d'évaluation pour les générations de séismes multi-directionels.

Le calcul des durées significatives, de la période prédominante, et de l'énergie d'un accélérogramme synthétique sont des points de repère pour évaluer sa ressemblance avec un mouvement historique. De la même façon, le PCF peut être un indicateur de la corrélation entre deux accélérogrammes synthétiques, et peut être un paramètre pour évaluer si l'effet des deux composantes d'accélérogrammes synthétiques est comparable à l'effet des deux composantes d'un séisme historique.

TABLE OF CONTENTS

LIST OF TABLES

LIST OF FIGURES

LIST OF APPENDIX

CHAPTER 1

Introduction

1.1 Overview

In recent earthquakes, due to better equipped seismological stations, a considerable amount of data on the vertical components of ground motion was recorded and made available for further studies. Some of these studies suggest that this component may account for considerable structural damage. Following the 1994 Northridge earthquake in California, where the largest ever vertical accelerations in an urban region were recorded, many questions were raised concerning the state of practice in structural design. Recent investigations have shown that the commonly used 2/3 ratio between vertical and horizontal acceleration amplitudes may grossly underestimate the effect of vertical acceleration in certain frequency ranges. Lawson (1994) stated that the current safety factors applied to vertical static loads in the Uniform Building Code (1991), and the 2/3 ratio between the horizontal and vertical excitations may be sufficient to insure a safe design. In addition, many studies show that the coupling of horizontal and vertical accelerations may influence the structural behaviour. As will be seen in Chapter 2 of this thesis, where a review of previous work is presented, the debate has sparked a number of specific case studies, but the conclusions reached are insufficient to fully asses or codify the effects of vertical seismic accelerations on the seismic response of civil engineeriring structures. A review of current code provisions in many countries in the world (Paz 1994), reveals there is no consensus in the best way to approach this problem.

In the effort to generate synthetic accelerograms to match target spectra for different regions to evaluate the safety of structures through time-history analyses, the problem of

incorporating the vertical component in a simple and realistic way arises. In regions where extensive data is available, the difficulty lies in adapting predicted results to fit the horizontal and vertical spectrum simultaneously. Added to this, the occurrence of the maximum responses for each of the components must be evaluated in a realistic way to avoid too severe or insufficient correlation between the two components.

In regions where available data is poor, attenuation relationships for both components must be derived. Some studies suggest methods where the two components are coupled, while others drive each component separately. References concerning the different approaches are presented in Chapter 2.

1.2 Objectives

In this study, an assessment of the current state of knowledge and research done on the characteristics and effects of vertical seismic excitation on civil engineering structures is attempted by reviewing previously published work. Pertinent information has been synthesized and grouped according to different subjects of interest.

The main objective of the study is to develop a simple and reliable approach for engineers who need to include vertical accelerations in their calculations and study the modeling parameters that have fundamental significance in the seismic structural response.

It is also attempted through this study to show the important role that vertical accelerations could play in assessing the seismic performance of building and gravity dam structures, and how current code provisions or rules of the art may lead to under or overestimation of results.

Finally, it is attempted to convince design engineers that vertical accelerations should be considered as playing an important role in the seismic behaviour of all structures until proven otherwise, and not the opposite.

1.3 Scope of study

At first, a literature review on several the aspects pertaining to vertical seismic accelerations and their effect on structures is presented (Chapter 2), emphasizing 5 major topics : a) seismological aspects, b) historical evidences, c) experimental evidences, d) numerical evidences, and finally e) code provisions.

In the first part of our study (Chapter 3), the characteristics of the vertical component of seismic ground motions are investigated through statistical analyses of three groups of earthquakes.

Based on these characteristics, a method for constructing a reliable vertical response spectrum from the corresponding horizontal spectrum is developed.

In the second part of our study emphasis is given more on the effect of vertical ground motion on structures. Two different structures are examined through numerical calculations: a 6-story moment resisting steel frame structure subjected to near fault ground motion (Chapter 4), and a gravity dam structure analyzed for ground motions typical of eastern and western North America (Chapter 5).

Finally, in Chapter 6, a summary of the thesis is presented as well as conclusions and recommendations for future work on this topic.

CHAPTER 2

Review of Literature

2.1 Seismological aspects

In several recent seismological studies, the emphasis has been put on the nature of the earthquake ground motion to better predict the ground motion characteristics that may occur at a given site. In fact, engineers have made great progress in developing structural design procedures to resist economically earthquake induced forces. However the important question that remains is: which earthquake, with which characteristics, will hit the structure in its life span? In the literature, many different approaches could be found based: (1) on attenuation formulae and response spectra, (2) on observed and recorded data, and (3) on fault properties like the rupture mechanism, the distance to the fault, or the magnitude of the fault rupture. The information that covered the horizontal (H) and vertical (V) components of ground motions could be investigated considering six different aspects : (1) intensity of the H/V ratio, (2) frequency content, (3) duration, (4) coherency between the H and V components, (5) generation of synthetic ground motions, and (6) propagation of S and P waves. Previous work on these various aspects is described below.

2.1.1 Intensity of H/V ratio

Bardet and Davis (1997), while analyzing the Van Norman Complex records obtained during the 1994 Northridge earthquake, noted that the vertical acceleration reached maximum peaks comparable to those of the horizontal acceleration. Furthermore, they noted that the occurrence of these peaks was almost simultaneous, and corresponded to the end of the first pulse of the earthquake.

In the study by Mohammadioun and Mohammadioun (1996), the H/V ratio was compared for different cases. The two major parameters being the magnitude and the distance to the source. Comparison of H/V ratio was made for two groups of magnitudes 5-6 and >6 events, and for distances to the source of 5 km, 5-10 km, and for 10 -50 km. The authors stressed the presence of abnormally high velocities for lower accelerations in the horizontal direction for sites where the vertical component of the ground motion was relatively strong. The idea of a non-linear behaviour of soils could explain the H/V ratio, and its dependence on the site location. Considering the fact that the horizontal acceleration is predominantly due to the propagation of shear waves and that the vertical one consists mostly of compressional waves, the authors based their conclusions on certain observations. Near the fault, in the event of a strong ground motion, horizontal accelerations seemed to saturate at values of 0.45 g - 0.5 g when the soil behaviour becomes non-linear. The vertical component was unaffected, and may even be amplified in regions of strong soil non-linearity. The saturation of the horizontal component leads to a transfer of energy towards lower frequencies, causing the observed increase in peak velocities and displacements.

In the Preliminary Reconnaissance Report of the Canadian Association for Earthquake Engineering (1997) on the Hyogo-Ken Nanbu (Kobe) Earthquake of January 17, 1995 in Japan, the authors observed that the peak vertical acceleration was not affected by liquefaction, and high vertical accelerations were transmitted to the surface despite liquefaction of the underlying soils. Furthermore, the authors noted the similarities between the Kobe seismic event and a subduction earthquake that could occur in Western Canada, with the same widespread soil liquefaction.

An interesting approach was suggested by Ohno and Konno (1996) who used a spectral transfer ratio that directly relates the vertical acceleration component as a multiple of the

horizontal one. This method was based on the observation that the duration of the vertical components were similar to those of the horizontal, but that the former built up faster. Following the analysis of data for both vertical and horizontal components of some earthquakes, they found that this ratio could be taken as equal to 0.6 for shorter periods, 0.5 for longer periods, and could be calculated by log-log interpolation for medium periods.

The horizontal accelerogram is computed first with one of the commonly used methods. Using the transfer ratio, the vertical accelerogram is then derived. Furthermore the authors stated that since the horizontal component propagated mainly as S-waves and the vertical as P-waves (Takahashi et al. 1992) the difference in the horizontal and vertical components must appear in the site factor. These transfer ratios were established for soft rock with a shear wave velocity $V_s = 700$ m/s.

In an analysis of the extensive data recorded during the Northridge earthquake, Hudson et al. (1996) reached the following conclusions concerning the ratio of vertical to horizontal spectral ground motions. The ratio was found in general to decrease with distance to the fault. The strongest ratios were found for short periods, and near fault distances. After reaching a peak in the small period range, the ratio decreased and then increased into the longer period range. For long periods there is no significant decrease with distance.

2.1.2 Frequency content

Research by Lachet et al. (1995) suggested that there was a direct link between the H/V ratio and the geological conditions of the site. This experimental study, where ambient white noise and strong motions were used, correlates the H/V peak of the site to the geological conditions. The authors concluded that H/V peak is located at a particular

position (spectral period at which peak occurs) in the frequency domain, and that this position could be a characteristic of a site.

2.1.3 Duration

Ohno and Kohno (1996) state that the duration of the vertical component is similar to that of the horizontal component. It was further noted that the former builds up faster.

In the study by Atkinson (1992) the duration t_d in seconds for distances greater than 200 km from the source was taken as $t_d = 1/f_0 + 0.05$ R where f_0 is the corner frequency of the source spectrum, and R the hypocentral distance in km at distances greater than 200 km. The author states the importance of the duration of earthquakes in Eastern North America (ENA) since for a given Fourier spectrum, the peak ground acceleration and response spectral amplitudes depend on the duration of the earthquake, because the total value of energy must be spread out in the time domain. These conclusions reached on the duration are also applicable and of interest for the vertical component, since an earthquake is a single multi-dimensionnal event.

2.1.4 Coherency between H and V

Penzien and Watabe (1975) showed that the three components of ground motion are independent. This conclusion is reached if the motion is expressed in a principal axis system. Furthermore, the same intensity function is used for the three components of the motion. It is also important to note that an analyzed structure must have its principal axis coinciding with those of the input ground motion.

Chen and Lee (1973) computed statistics on the correlation factor between the three components of 104 real strong motion recordings. They concluded that considering the

three components as independent is not a realistic estimate of the coherency, especially between the horizontal and vertical ground motions. They further suggested that the inconsistency between their conclusion and the one reached by Penzien and Watabe, was most probably due to the fact that the three intensity functions were taken as the same. Based on their statistics they suggested a low correlation factor between the horizontal and vertical components in the range of 0.16 to 0.2.

Some methods have been proposed to generate low-correlated accelerograms.

Levy and Wilkinson (1973) suggest that a first time history can be generated from a spectral density function at a frequency increment $\Delta\omega$. The second time history is generated by using the same spectral density function, but choosing the frequencies midway between the frequencies used in the generation of the first accelerogram. This method yields accelerograms that are reasonably correlated, but is not very realistic since both time histories are generated from the same spectral density function.

Furthermore, it was noted that when the correlation coefficient is defined as a function of the time lag between the start of the first and second accelerograms, by varying the time lag, a different correlation coefficient could be found. In fact, by moving one accelerogram on the time scale the correlation coefficient could be varied until the desired correlation is obtained.

2.1.5 Generation of synthetic ground motions

Many studies have focused on the problem of simultaneously generating accelerograms or response spectra for the vertical and horizontal components of ground motion. Some of these studies used the spectral approach, where equations like the one Ghosh (1987) suggested:

$$S = A + B \cdot M + C \cdot M^2 + D \cdot R + E \cdot R^2 \qquad (2.1)$$

where S is the normalized spectral value and A, B, C, D and E are constants, and M and R represent the magnitude of the earthquake and the distance from the source, respectively. This method does not account for the mechanistic side of the earthquake, but fits recorded data, to generate a representative spectrum. The form of the equation is chosen to account for the oscillatory variation of spectral amplitude with respect to both M and R. The value of S, for a given period and damping ratio, is obtained by a calibrated sum of spectral responses corresponding to recorded events. The author suggests independent analysis for the vertical and the horizontal components, to be coherent with previous results that suggest that the shapes of these two components are different. By computing the constants and plotting them, it was difficult to correlate the two responses by this approach. These results are derived from a series of 59 horizontal and 30 vertical accelerograms from thirteen earthquakes in the Western United States. Such a method can be applied to regions where available data is extensive, but would be insufficient and unrepresentative for regions with fewer recordings like Eastern Canada. Furthermore, the facts that the mechanistic side of the rupture is not considered, and that all results are given the same importance may have lead to poor predictions.

The other approach, as opposed to the spectral method, consists of generating time history accelerograms for both directions, to fit a target spectrum, by calibrating results on observed values through projected probability distributions of relevant parameters. Bruna and Riera (1988) suggested a general formula to obtain a 3 dimensional time dependent array of the three acceleration components as a sum of 'i' 3-dimensional arrays corresponding to "i" frequencies f_i, number of cycles (n), arrival times and final times. The proposed function is :

$$a_{ij}(t) = A_{ij} \bullet \sin(2\pi f_i t) \bullet \sin(\pi t / t_{di}) \bullet u(t-t_{ai}) \bullet u(t_{bi}-t), \quad (2.2)$$

with i corresponding to the number of independent functions and j = 1 to 3 (3 dimensions: 2 horizontal and 1 vertical). A is the amplitude, t_a, t_b, and t_d are the arrival time, the final time, and the i-wave duration, respectively , and u (t) denotes Heavyside's unit step function.

The result is obtained by summing the contribution of each term :

$$a_j(t) = \sum_{i=1}^{N} a_{ij}(t) \quad (2.3)$$

The suggested procedure consisted of selecting N, generating f_i for i = 1 to N from the $F_f(v)$ probabilistic distribution, determining the values of n_i and t_{ai}, computing A_{ij}, and finally adjusting the values of A_{ij} to improve the fit to the target spectra.

In a study by Atkinson (1992) on the characteristics of ground motions in Western Canada the H/V acceleration amplitude ratio was found to be a stable site characteristic, dependent on the velocity profile of the site. Furthermore, the ratio was also found to be independent of earthquake magnitude and distance, as well as source location or mechanism. Thus, a correlation between the two components could be obtained if the shear wave velocity profile of the recording site is known. For frequency ranges f = 0.5 Hz to 10 Hz, a smooth solid curve was adopted for Western Canada:

$$\log(H/V) = 0.07 + 0.25 \log f, \text{ with : } 0 < \log (H/V) < 0.25 \quad (2.4)$$

In a different study by Atkinson (1992) where the characteristics of Eastern Canadian earthquakes were examined, the following correlation was derived :

$$\log (H/V) = 0.0519 + 0.117 \log f \qquad (2.5)$$

Kitagawa et al. (1996) suggest a different approach. The horizontal and vertical accelerations are derived separately, by first obtaining a basic response spectrum. The spectrum is then multiplied by a seismic activity coefficient, a longer period coefficient and a soil amplification coefficient. These coefficients are derived independently for both directions according to the nature of the site, since no direct correlation could be developed.

An interesting observation on the similarities and the compatibility of horizontal and vertical spectra and a method for deriving vertical spectra from horizontal ones are proposed in an article by Bozorgnia et al. (1996). The authors state that the ratio of 2/3 grossly underestimates the V/H ratio for short periods and overestimates it for long periods. Following a comparison of peak ground accelerations for the vertical and horizontal motions, they noted that the vertical component is richer in high frequencies. Furthermore the shapes of the spectra are similar except that the horizontal spectrum is shifted towards the longer period range. This observation suggests that it is possible to approximate the vertical spectrum by shifting and calibrating the horizontal one to fit the characteristics of the vertical component. This method is simple and effective, but a large amount of earthquake records are required to calibrate the spectra.

2.1.6 Propagation of P and S waves

The experimental study of Abe and Watanabe (1996) suggests that, as an earthquake propagates near the surface, incident angles at the boundaries of soil layers are decreasing. This would explain the disagreement of some theoretical values with observed values on the spectral V/H ratio. The fact that, at the boundary of layers during

the propagation from a depth of 4 km, S-waves change into P-waves and vice-versa may explain the difference in observed spectral ratios. Vertical motion occurring after the arrival of S waves is strongly influenced by deep ground structures and the incident angle to the deep half space layer.

Amirbekian and Bolt (1995) used the value of f_{max} to compare the horizontal and vertical responses, where f_{max} corresponded to the superior frequency cutoff, for example frequencies superior to the corner frequency. The differences of f_{max} for the two components is believed to be closely tied with the difference in the intrinsic attenuation of P and S waves within the basin. P waves (direct or converted from S-waves) are believed to mainly influence the vertical motion, while S waves affect mostly the horizontal motion. For alluvial basins where the ratio of P to S velocities was commonly above two, the ratio of f_{max} was also found to be above two. The observations suggested that the high frequencies in the vertical direction could be attributed to the conversion of S waves to P waves at the bottom of a layered alluvial basin, near the source.

2.2 Historical evidences

Recorded data showed the importance of the vertical component in many earthquakes. In fact, in some seismic events the vertical accelerations exceeded the horizontal ones.

The question that puzzled engineers was whether or not the vertical components, as important as they may have been intensity wise, were responsible for structural damage. Historical evidences show that the vertical components were indeed directly the cause of a number of important failures, and that it also influenced indirectly the behaviour of structures resisting the horizontal components of ground motions.

2.2.1 El Asnam earthquake in Algeria (October 10th 1980)

The most revealing example of the effect of vertical accelerations, as described by Despeyroux (1982), is the 1980 El Asnam, Algeria earthquake. The quake is described as a sudden vertical impulse with high frequency vibrations of short duration. There is no recorded data to confirm the visual observations, but reliable testimony helped the author determine that the vertical accelerations were about 1g, and that the horizontal ones reached values of only 0.25 g to 0.30 g.

Many horizontal cracks due to the eccentric vertical loadings and vertical cracks due to the splitting under vertical compression were frequently observed at the site. A water tank in the El Asnam region provided proof that most of the damage was due to the vertical component of the earthquake. The upper panels of the structure buckled under the increased vertical compression and fell off the tower, while the lower panels that would have been damaged by strong horizontal motions remained intact.

There was practically no example of failure by repetition of displacement cycles, with plastic hinging, and transformation of structures into mechanisms. Most of the ruptures occurred in a brittle way, even for structures that were designed according to the French antiseismic "Recommandations AS55" (1954) and "Règles Parasismiques PS69" (1969). These codes were developed according to the philosophy of large plastic deformations in the occurrence of a major seismic event. The reason for the brittle failures was mainly the suddenness of the seismic attack, and the fact that the maximum vertical accelerations (which occurred first) were separated from the maximum horizontal accelerations by a very short time period. Most of the structures that were severely damaged did not loose their initial shape, since they did not have time to oscillate before rupture occurred.

2.2.2 Great Hashin Earthquake in Kobe Japan (January 17, 1995)

In the preliminary investigation report of the Kobe earthquake disaster by Bardet et al. (1995), extensive recorded data showed the presence of an important vertical ground acceleration. Numerous shear failures of reinforced concrete columns were attributed to the high vertical acceleration. The Hanshin expressway bridge in Nishinomiya, the reinforced concrete wall of the bank along the road from Meriken Park to JR Motomachi station, and the piers of the Hanshin expressway all presented shear failures that were also attributed to the large vertical accelerations. A large number of bridge piers were similarly damaged although they were designed according to recent earthquake codes.

2.2.3 Sanriku earthquake in Japan (December 28, 1994)

In a report by Shioi and Sakajiri (1996) the same observations were reported. Big shear cracks in columns supporting large vertical loads were attributed to importance of the up-down motion. The authors also noted that the horizontal ground motion had a predominant period of 0.3 s. while the vertical excitation had high accelerations in the 0.125 s range.

2.2.4 Northridge earthquake in California (January 17, 1994)

In a paper summarizing the damage of parking structures during the 1994 Northridge California earthquake, Hawkins and Inverson (1994) stated that much of the observed damage could not solely be explained by the horizontal accelerations. In fact the near fault recordings showed that the vertical component was greater then expected, and that most damage was due to the combined effects of horizontal and vertical ground shaking. It was noted that the vertical strong shaking began about 3 seconds before the horizontal strong shaking, thus imposing significant vibrations to large span areas prior to the arrival

of the horizontal strong shaking. It was further noted that the duration of the vertical acceleration was relatively important, and that multiple near peak accelerations were recorded.

For the near fault area, simple calculations for a typical 2 to 3 story parking structure indicated that a horizontal acceleration of 0.4 g was sufficient to induce structural damage, but that failure and rupture of the structure was only expected at 0.85 g. This acceleration level was never reached for the structures that collapsed during the earthquake.

The authors suggested that the collapse of these structures may be explained by the presence of high vertical accelerations, and by the interaction of the forces produced by the horizontal and vertical accelerations.

2.3 Experimental evidences

A 1:20 scale, 15 story reinforced concrete frame tube structure building was tested by Jiwei et al. (1994). A comparison between results obtained soliciting the structure with only the horizontal acceleration and the combined horizontal and vertical accelerations suggested that in the elastic domain the effect of the vertical component was negligible on the horizontal displacements and acceleration response. In the inelastic domain the decrease in axial load caused by vertical accelerations was important especially at the column/beam connections. Furthermore, in a study by Kohzu and Suita (1996) on a steel moment resisting single story frame, a single or few excursions of the joints were necessary under the combined action of vertical and horizontal accelerations to cause failure. The concept of strain rate, and the influence of the vertical component of earthquake motions are discussed.

Kohzu and Suita (1996), noted that in the 1995 Kobe earthquake in Japan, the area close to welded beam-to-column connection presented brittle fractures in many steel structures. Following an experimental study, the authors concluded that the joints suffered the impulsive force and the simultaneous action of the horizontal and vertical ground motions, resulting in brittle failures caused by single or few excursions of the joints. The vertical acceleration component significantly influenced the stress-strain response at the critical sections. Both, the horizontal and the vertical components especially for near source sites, increased the strain rate in the connections. It was shown experimentally that the yield strength of the butt welded joint increases much more than the yield strength of the base metal with increasing strain rate, while both ultimate strengths remain unchanged with increasing strain rate. This induces a loss of ductility in the welded area of the connection relatively to the base metal section, thus favoring brittle fractures.

Agbabian et al. (1994), following an experimental study on one-third-scale models of multistory buildings, found that the coupling of the vertical and horizontal accelerations caused failure in beam-column connections prior to attaining the full resisting capacity of the beam sections. They noted that the vertical motion combined with overturning moments in the joint regions caused reduced column compression or even tension, that significantly reduced the concrete contribution to the shear resistance. In addition, marked effects on the shear deformation capacity, yield point, cracking pattern, ultimate capacity, and ductility in the panel zones were noted. A difference of 30% to 50% in the deformability were also recorded. The authors further stated that code provisions may be unconservative in the consideration of the vertical ground motion, since extensive data show that peak accelerations in the vertical direction may well exceed those of the horizontal direction, and that the frequency contents are quite different.

In a study of RC beams, Mohit and Shimazu (1987) showed that under the effect of combined vertical and cyclic horizontal loadings, the two extreme ends of the beams lost

their rotational stiffness, thus causing a gradual increase of the vertical deflections. The midspan deflections were found to increase from 70% to 140% after the first yield of critical sections in RC portal frames, under the working vertical and cyclic lateral loads. Furthermore, it should be noted that the vertical deformation of beams is not addressed by code provisions for earthquake resistant design.

2.4 Numerical evidences

The numerical evidences on the effect of vertical accelerations on structures can be divided in three major categories related to: (1) buildings, (2) bridges, and (3) dams. These three types of structures have very distinct structural behaviour, and respond differently (because of natural periods and the shape of the vibration modes) to seismic excitations.

2.4.1 Buildings

In a study by Paglieti and Porcu (1985), the concept of vertical eccentricity is introduced. The vertical eccentricity corresponds to a lateral offset of the center of mass from the center of rigidity in elevation along a horizontal floor element. Using an analytical model, this study shows that the vertical eccentricity induces rocking motions, which combined with the vertical motion, increases the axial load in columns by more than 30 % in certain cases.

In a different study by Gupta and Hutchinson (1994), the effect of coupling the vertical and the horizontal accelerations was examined with respect to the frequency ratio of the excitations. The coupling of the two components was more critical for frequencies that were closer to each other.

Orabi and Ahmadi (1988) stated that the relation between the effects of horizontal and vertical accelerations on the structure were due to the P-Delta effects for columns that bared a stress larger than 80% of Euler's load. This concept may not be relevant since columns are never designed to work under such high axial loads, but considering the inelastic behaviour in the occurrence of a major earthquake, such loads may indeed occur. In addition, it was noted that for low damping ratios the effect of vertical ground acceleration was important, and that it became insignificant for high damping ratios.

Asano and Torii (1992) examined a 30-story building incorporating a large cantilever with different analysis methods to reach a safe design for the horizontal accelerations, the coupling of torsionnal effects, and the vertical accelerations. The authors suggested following this analysis that large elements, like cantilevers that are directly affected by vertical accelerations, may vibrate excessively during an earthquake. These elements should be designed to remain in the elastic domain even under the action of severe seismic loading. Gravity and live loads in affected elements should remain under 40 to 50 % of the yield stress.

In an analytical study by Yamanouchi and Hasegawa (1996) on 2-story, 4-story and 8-story buildings designed according to the old and new Japan design codes, the vertical ground motion was found to affect the deflections at the center of beams, but did not significantly affect the overall frame response. It was also noted that the vertical acceleration had a more significant effect on the most heavily loaded interior columns, since the exterior columns were affected primarily by the horizontal motion.

2.4.2 Bridges

Following the failure of many bridges after the San Fernando earthquake in 1971, a large amount of research was made to determine the reasons for these failures. The same major

deficiencies identified were, lack of ductility, small seat width at expansion joints, lack of horizontal ties, and inadequacy of abutments and wing walls. Most of the damage was due to structural vibrations. Most of the work done on the dynamic response of these structures considered only the horizontal earthquake components. Many recordings indicate that most of the damage may have been caused by vertical accelerations. Saadeghvaziri and Foutch (1991) noted that during the Cape Mendocino California offshore earthquake in 1983, the peak vertical acceleration at the center of a bridge span was 10 times larger than that at the abutment, while it was only 2 times larger in the horizontal direction. After performing dynamic analyses on a number of model bridges, the authors concluded that vertical accelerations have a significant effect on bridges, by increasing the damage and even by inducing new damage patterns. In columns and piers, owing to uncoupled variations of the axial and lateral forces, the hysteresis loops are very unstable and asymmetric. On one hand the increased axial forces cause an increase in stiffness that in turn causes an increase in the shear and moments carried by the columns, increasing the possibility of failure in the column, the foundations, and abutments. On the other hand, the decreased axial forces, that could even be reversed into tensile forces, causing a weak beam-strong column behaviour, which reduces the shear capacity of concrete favoring a shear failure in the cross section. These results are given further importance, since there have been reports of unexpected yielding of columns for many bridges in past earthquakes. In the abutments and connections, varying forces due to vertical vibrations, that may exceed three times the usual loading, are not accounted for in current codes. In addition provisions for foundations and expansion joints are sometimes insufficient for vertical motions.

2.4.3 Dams

Léger and Leclerc (1996), studied the response of gravity dams to earthquake ground motions. When combining the effects of horizontal and vertical accelerations (vertical

peak ground acceleration (PGA) calibrated to 2/3 of the horizontal PGA), it was found that the vertical component did not appear to be critical in the seismic response of gravity dams since it increased the stresses by approximately 10 %. Nevertheless, it was noted that the vertical component caused a variation in the cracking pattern that influenced the large displacement response of the separated upper part of the dam. It was further noted that by reversing the sign of the vertical component when coupling it with the horizontal component may cause significant changes in the response, which emphasizes the question of coherency between the two components.

Kido et al. (1997) studied the performance of the Hitokura Dam during the 1995 Kobe earthquake. The results that were the most coherent with the real behaviour of the structure were obtained with simulations including both the horizontal and the vertical components of the seismic motion. However, the vertical acceleration did not affect significantly the results in terms of the stress conditions in the dam during the earthquake.

2.5 Code Provisions

Paz (1994) summarized the seismic provisions of countries having earthquake design codes, 17 of which had clauses dealing with the vertical component of the earthquake motion. Some of these clauses were more detailed than others, but in general the vertical component was given a very limited importance compared to the horizontal one. Table 2.1 presents a summary of the clauses related to vertical accelerations in these 17 codes.

All the codes that include a clause on vertical accelerations specified a limited number of structural cases where the clauses should be taken in account. Some codes, for example the Australian one (1993), leave the responsibility to the designer to determine whether or not to consider vertical earthquake components. The paragraph reads : " ... only if the nature of the structure shows that it could be significant (considering the vertical

component)." The elements to be considered for applying vertical accelerations, specified by the other codes, are the following:

- Columns in a structural frame bearing large vertical loads, with increased vertical flexibility (Algeria, Russia, Romania, Costa Rica).
- Cantilevered elements (Russia, Romania, Italy, Costa Rica, Bulgaria, Argentina)
- Balconies (Argentina)
- Roofs with large spans (Argentina)
- Bridges (Russia, Bulgaria)
- Any structural element with span greater than 20 m to 24 m (Argentina, Bulgaria, Russia, Spain, Italy, Costa Rica)
- Brick or stone structures (Bulgaria)
- Flat Plates (Costa Rica)
- Prestressed elements (Greece, Peru)
- Beams or cantilevers with large shear forces (Romania)
- Slab floors supported directly on columns (Romania)
- Arches (Russia)
- Masonry (Russia)
- Girders acting as column supports (Greece)

2.5.1 Intensity of vertical accelerations

The vertical excitation component, when considered, is treated in many different ways, each method being adapted to the general seismic provisions of the country with respect to the horizontal component.

In general, most of the methods uses a percentage of the seismic weight, or a dynamic amplification factor multiplied by the seismic weight, to compute a static vertical seismic force to be applied at the center of mass of the considered element. Other methods describes the vertical acceleration component as a fraction of the horizontal one, in terms of accelerations or even spectra.

Each Code has a different approach in considering the intensity of the vertical component. Most of the codes specify a single value, for example the Australian code (1993) states that the vertical acceleration should be taken as 0.5 the horizontal acceleration. Other codes have different amplification factors for each seismic zone, like the seismic code of Argentina, where the value of C_v (vertical seismic amplification coefficient) varies from 0 24 to 1 20 for the 4 seismic zones of the country.

Some other codes vary the intensity of the vertical force to be considered according to the type of structure. The Bulgarian code, for example, specifies an amplification factor of 2 for cantilevered elements. The Bulgarian code also correlates the value of the vertical acceleration (or vertical force used for design) to the peak ground acceleration for the region, through the factor C_v. The Italian Code has a vertical amplification factor of 0.2 for buildings with floor spans greater than 20 m and for horizontal thrust elements, and a factor of 0.4 for cantilevered elements.

It is important to note that the loads induced by the vertical accelerations are not specified as a function of the period of the analyzed element or structure. This point will be further investigated in this project.

2.5.2 Load Combinations

In terms of load combinations (Horizontal + Vertical) very few codes have specific considerations. Those which do, stress the need to consider both the effects of the up and down motions.

The Argentina Code uses two general combinations :

1) $1.3 \quad E_w \pm E_s$ (2.6)

2) $0.85\ E_w \bullet E_s$ (2.7)

E_w : Gravity forces

E_s : Seismic forces

Although these combinations do not specify directly the combination of the forces induced by the vertical and horizontal accelerations, with respect to the vertical acceleration, equation 2.6 accounts for the increased loads in the gravity direction added to the static vertical loads, while equation 2.7 considers the effects of the upward forces induced by vertical accelerations acting against the gravity forces.

The Chinese code suggests a combination between the horizontal and the vertical design forces:

1.3 Horizontal + 0.5 Vertical (2.8)

The Costa Rica code suggests a more specific load combination including the two horizontal orthogonal components, H_1 and H_2 and the vertical one, Vert :

1) $100\%\ H_1 + 30\ \%\ H_2 + 30\ \%$ Vert (2.9)

2) 100% Vert + $30\ \%\ H_1 + 30\ \%\ H_2$, (2.10)

if the vertical vibration mode is considered to be a primary one.

The Italian code has a different approach on load combination. The SRSS combination rule is used to obtain a single component. They suggest this combination rule for both the force and the displacement components.

2.5.3 Evolution of the National Building Code of Canada (NBCC)

In the commentary to the NBCC (1975) published in 1977, it is stated that the vertical accelerations represents 30 % to 60% of the horizontal ones, and could be even higher for near fault regions. It is also stated that vertical accelerations can induce instability or an unusual reduction of safety coefficients for some structures. When such a problem is expected, the code suggests that a dynamic analysis be carried out.

This clause remained unchanged through the edition of NBCC (1980) and NBCC (1985). In the NBCC (1990), the clause was changed and stated that the vertical accelerations vary between 2/3 and 3/4 of the horizontal accelerations. It is further stated that cantilevered structures or buildings that are deemed sensitive to vertical accelerations should be designed following a dynamic analysis. The NBCC (1995), kept this clause unchanged.

Table 2.1 summarizes the clauses covering the vertical acceleration in the codes of the above discussed countries.

Table 2.1: Summary of Code provisions for effects of vertical accelerations (after Paz, 1994) (pages 25 through 31)

Country	Vertical Component	Load Combinations	Other Considerations
ALGERIA Règles Parasismiques Algériennes (RPA-1988)	Not Specified	1) $D + L \pm E$ 2) $0.8\ D \pm E$ 3) $D + L \pm 1.2\ E$ Combination of vertical and horizontal not specified	For columns in a structural frame bearing large vertical loads
ARGENTINA Reglemento INPRES-CIRSOC103 (1991)	$F_{vert} = \pm C_v \gamma_d W$ γ_d : risk factor (1, 1.3 or 1.4) C_v : vertical seismic coeff. W:weight of structural component **Cases 1 and 2** : C_v given by table, function of seismic intensity zone **Case 3 :** Vertical acceleration spectrum obtained from horizontal one by : $S_{a\ vert} = f_v * S_{a\ hor}$ f_v obtained from table, function of seismic zone C_v obtained from spectrum.	1) $1.3\ E_w \pm E_s$ 2) $0.85 \pm E_s$ E_w : Effect of gravity forces E_s : Seismic effect Combination of vertical and horizontal not specified	**Case 1** : Cantilevers and balconies **Case 2** : Building roofs with large spans and horizontal prestressed elements **Case 3** : Structures with lateral projections
AUSTRALIA Australian Standards 1170.4 (1993)	$V_{accel} = 0.5\ H_{accel}$ **unless** data of vertical to horizontal ratio of recorded accelerograms shows different values	Not specified	For structures type D and E The type of structure depends on : 1) the importance of the structure, 2) the soil structure resonance factor, 3) the

			acceleration coefficient of the site.
BULGARIA Code for Design of Buildings and Structures in Seismic Regions. (1987)	Vertical seismic forces to be taken as a fraction of the horizontal ones **For buildings** 1)The vertical seismic forces taken as 15 % of seismic weight for low seismicity regions, and as 30 % for high seismicity regions 2) For cantilevered elements the vertical seismic force is taken as $2.C.K_c.Q$ Q: Weight of element C : importance coefficient (values of 0.75, 1, 1.5) K_c : Seismic coefficient representing the ratio of the ground peak acceleration to the gravitational acceleration. (varies between 0.05 and 0.27) $2.C.K_c$ varies from 7.5 % to 81 %	Not specified for structures For masonry : 100% H + 100% V	Horizontal or inclined cantilevers Superstructures of bridges Structures as frames, arches, trusses, and plate roofs with a span equal or greater than 24 m. Buildings and structures susceptible of overturning or sliding Brick or stone structures
CANADA NBCC (1995)	Vertical accelerations taken as 2/3 to 3/4 of horizontal accelerations	1.D + 1.E 1.D + (1.L+1.E) for storage areas 1.D + (0.5.L+1.E) for other occupancies	Gravity load requirements are sufficient to resist up down motion.

CHINA Code for Buildings and Structures (1989)	**High rise buildings and structures** $F_{EV} = \alpha_{vmax} . W_{eq.}$ F_{EV} : Total vertical force α_{vmax} : taken as 65% of α_{hmax} W_{eq} : equivalent weight taken as 75% of total seismic weight Vertical distribution of vertical seismic force : $F_{vi} = (W_i H_i / \Sigma W_i H_i) F_{EV}$ **Flat network roof structures and large span trusses** $F_v = W_{seismic} * \alpha_v$ α_v : varying from 0.08 to 0.25 Wseismic : total seismic weight **Long cantilever and other large-span structures** For the two highest seismic intensity regions, VIII and IX, vertical forces are taken as 10% and 20% respectively of the total seismic weight.	1) 1.3 Horizontal 2) 1.3 Vertical 3) 1.3 Horizontal + 0.5 Vertical	High rise buildings and structures Flat Network Roof structures and large span trusses

COSTA RICA Còdigo Sismico de Costa Rica (1986)	Vertical (acc.) = 2/3 of Horizontal	1) 100% H_1 + 30% H_2 + 30% V 2)If vertical vibration mode is considered to be a primary one : 100% V + 30 % H_1 + 30 % H_2	Usually neglected except for following cases : Increased flexibility in the vertical direction due to large axial loads Flat plates Long span beams Cantilevers
GREECE Greek Seismic Code (1992)	1) Computing of the fundamental period of the element in the vertical direction by Raleigh's method. 2) Vertical accelerations computed with the following formula : $F_{vi} = \frac{W \bullet \varepsilon_v \bullet m_i \bullet y_i}{\sum (m_i \bullet y_i)}$ W: total weight ε_v: seismic coefficient = 0,7• $\varepsilon_{horiz.}$ m_i : lumped mass at degree of freedom I y_i : deflection at degree of freedom i under a static load of (m_i.g), where g is the gravitational acceleration	Simple superposition of loads induced by vertical accelerations in horizontal and vertical directions. Vertical forces computed by the described method can be used irrespective of the method used to compute the horizontal earthquake forces.	Ignored except for the following cases : Prestressed concrete Girders acting as column supports Design of Slabs
INDIA IS-1984	Vert. (acc.) = 0.5 Hor. (acc.)	$F_{seismic}$ = 100 % Hor + 100 % Vert	Applied only when a vertical component analysis is deemed necessary

IRAN Iranian Code for Seismic Resistant Design of Buildings (1988)	$F_v = (2 \cdot A \cdot I/R_v) \cdot W_p$ A : design base acceleration 0.2 to 0.35 I : importance factor Wp : Dead load plus total live load Rv : reaction coefficient (2 for RC elements and 2.4 for cantilevers)	$F_{seismic}$ = 100% Hor + 100% Vert Consider both up and down motions separately.	
ISRAEL Israel Standard , IC-413 (1994)	$F_v = \pm 2/3\ Z\ .\ W$ (for cantilevers) $F_v = W_{min} - 1.5 \cdot Z \cdot I \cdot S \cdot W$(prestressed elements) W_{min} : minimal load on prestressed element W : dead load Z, I, S : seismic coefficients		Cantilevers Prestressed elements
ITALY Norme Technique per le Construzioni in Zone Sismiche (1986)	$F_{vi} = K_v \cdot I \cdot W_i$ I : importance factor W_i: weight of considered element K_v : vertical amplification factor ± 0.2 for cases 1 and 2 ± 0.4 for case 3	$\alpha = (\alpha_h^2 + \alpha_v^2)^{1/2}$ $\eta = (\eta_h^2 + \eta_v^2)^{1/2}$ α : single force component (bending force, shear force, torsionnal moment) η : single displacement component h: index specifying horizontal component v: index specifying vertical component	Case 1 : buildings with floor spans greater than 20 m. Case 2 : horizontal thrust elements Case 3 : Cantilevers

PERU Peruvian Code (1977)	$F_v = C \cdot W$ W: weight of analyzed element C : 0.3 for zone 1 0.2 for zone 2 0 for zone 3 (not considered)	Not specified	All vertical elements Prestressed elements Cantilevers
ROMANIA P100-91 (1991)	$F_v = C_v \cdot Q_i$ C_v : amplification factor = $\pm 2 \cdot K_s$ K_s is a zone factor corresponding to the ratio of the maximum seismic acceleration to the acceleration of gravity Q_i : gravitational load	Effects of vertical and horizontal seismic forces are not superimposed.	Columns with large axial forces Beams Cantilevers with large shear forces Slab floors supported directly on columns
SPAIN Comisiòn Permanente de Normas Sismicas (1991)	$F_{vert\,i} = v_i \cdot W_i$ $v_i : \chi \cdot c$ c: basic seismic coefficient χ : seismic intensity factor W_i : concentrated weights	Not specified	Beams with large spans When shape of structure requires it
Russia (former USSR) SNIP-II-7-81 Code (1982)	$S_{ik} = K_1 \cdot K_2 \cdot S_{oik}$ S_{ik} : seismic force at level k K_1 : coefficient of allowable damage K_2 : structural coefficient $S_{oik} = Q_k \cdot A \cdot \beta_i \cdot K_\varphi \cdot \eta_{ik}$ Q_k : seismic weight at level k A : zone factor β_i : dynamic coefficient for mode I K_φ : stiffness coefficient η_{ik} : distr. factor for mode i at level		Horizontal and inclined cantilevers Bridges Frames, arches, trusses and space roof structures with span greater than 24 m. Structures analyzed for overturning or sliding masonry structures.

	k **For vertical** : $K_{\varphi} = 1$ and $K_2 = 1$		
YUGOSLAVIA Technical Regulations for Design and Construction of Buildings in Seismic Regions (1981)	$F_v = K_v \cdot W$ W : total weight K_v : 0.7 K K : Total seismic coefficient for horizontal direction	Not specified	Effects of vertical acceleration to be ignored except for elements with very large spans.
AASHTO (U.S. bridge code)	If F vert > 50 % and < to 100% of the gravity forces, hold down devices must be designed for 10 % of the gravity loads. If F vert > 100 % of the gravity loads then hold down devices must be designed for 120 % of the difference between the vertical force and the gravity forces, or for 10 % of the permanent loads.		These specifications are applied to the vertical seismic force due to longitudinal seismic load. No consideration of a vertical component of the seismic solicitation is specified.

Chapter 3

Seismological Aspects

3.1 Introduction

In this chapter, some characteristics of earthquake ground motions are examined to better understand the relationships between the vertical and horizontal components. Once the relationships between these two components are established, a simple method for generating realistic input data for the vertical components of ground motion is developed, and a procedure to combine this component with the corresponding horizontal component in structural analysis is proposed. Therefore, the main objectives of this chapter are : (1) to obtain reliable vertical acceleration response spectra based on an assumed horizontal acceleration response spectra, and (2) to generate reliable vertical acceleration time histories to fit the computed spectra, taking into account the coherency criteria of the components of ground motion.

An existing data base of 45 pairs of horizontal and vertical acceleration records has been divided in three categories, according to the ratio of the peak acceleration to the peak velocity (a/v). The characteristics of the vertical components are first defined in terms of various intensity, frequency content, and duration indices. A statistical analysis is then carried out to define a shift factor, Sf, and a reduction factor, Rf, that could be applied to a horizontal response spectrum to obtain a reasonable approximation of the associated vertical response spectrum. The horizontal and vertical design response spectra are then used as targets to develop spectrum compatible ground motion time-histories suitable to perform step-by-step elastic or inelastic structural analysis. The coherency between the

horizontal and vertical components of ground motions have been considered in the development of the spectrum compatible accelerograms.

3.2 Selection of strong motion data

It is commonly accepted that the horizontal and vertical earthquake ground motions are quite different in terms of frequency content, since the former propagate mainly as shear-waves (S-waves), while the latter propagate as tension-compression waves (P-waves). To remain consistent with this fact, the earthquake data was divided in categories according to the frequency content of the horizontal strong motion data. The current edition of the National Building Code of Canada (NBCC, 1995) uses a similar classification for the seismic regions of the country. The zonal acceleration to velocity ratio Za/Zv used in the NBCC (1995) is directly related to the frequency content of earthquakes expected in a given region. In Eastern Canada the a/v ratio is usually high, corresponding to high frequency earthquakes, and thus high energy in the short period range. In Western Canada, the ratio is usually low or close to unity. Low a/v values indicate low frequency earthquakes and consequently high amplitudes in ground motion.

This categorisation was chosen because it remained consistent with the NBCC 1995 approach, and because in a study by Heidebrecht et al. (1988) a strong motion data base dividing the records in these three categories was established at McMaster University. The data base consists of 45 historical earthquake records, on firm ground, from North America, Eastern Europe and Japan.

The records are divided in three categories according to their acceleration-to-velocity ratio (a/v) : (1) high a/v >1.2, (2) intermediate 1.2 > a/v > 0.8, and (3) low 0.8 > a/v. These ratios are computed with the acceleration, a, expressed in g and the velocity, v,

expressed in m/s. Some characteristics of the earthquake records retained for this study are shown in Tables 3.1, 3.2 and 3.3.

Most of the previously published work on the vertical acceleration and its characteristics is based on California earthquakes, with intermediate to low a/v. By dividing the earthquake records in distinct groups, it is possible to establish if conclusions related to California events are applicable to all types of earthquakes.

Table 3-1: Characteristics of high a/v group

	Earthquake	*Date*	M_L	*Site*	*Epic. Distance (km)*	*a/v*	*PGA (g)*	*Direction*
1	Parkfield, CA	06/27/66	5.6	Trembior 2	7	1.86	0.27	N65W
2	Parkfield, CA	06/27/66	5.6	Cholame 5	5	1.70	0.43	N85E
3	San Francisco	03/22/57	5.3	Go.Gate Park	11	2.28	0.11	S80E
4	San Francisco	03/22/57	5.3	State Bldg.	17	1.67	0.05	S09E
5	Helena Mont.	10/31/35	6.0	Carrol Col.	8	2.03	0.15	N00E
6	Lytle Creek	09/12/70	5.4	Wrightwood	15	2.06	0.20	S25W
7	Oroville ,CA	08/01/75	5.7	Seism.Station	13	1.91	0.08	N53W
8	San Fernando	02/09/71	6.4	Pac. Dam	4	1.86	1.08	S74W
9	Nahanni CAN	12/23/85	6.9	Site 1 Invers.	7.5	2.38	1.10	LONG
10	Honshu, JAP	04/05/66	5.4	Hoshina A	4	2.43	0.27	N00E
11	M.Negro YUG	04/09/79	5.4	Albatros	12.5	2.63	0.042	N00E
12	B.Luka, YUG	08/13/81	6.1	S.St. B.Luka	8.5	2.31	0.07	N90W

Table 3-2 : Characteristics of intermediate a/v group

	Earthquake	*Date*	M_L	*Site*	*Epic. Distance (km)*	*a/v*	*PGA (g)*	*Direction*
1	Imp. Valley	06/27/66	6.6	El Centro	8	1.04	0.35	S00E
2	Kern County	06/27/66	7.6	Taft Lincoln	56	1.01	0.18	S69E
3	Kern County	03/22/57	7.6	Taft Lincoln	56	0.99	0.16	N21E
4	Borrego Mtn	03/22/57	6.5	San Onofocre	122	1.10	0.05	N57W
5	Borrego Mtn	10/31/35	6.5	San Onofocre	122	1.11	0.04	N33E
6	San Fernando	09/12/70	6.4	Holl. Storage	35	1.00	0.21	N90E
7	San Fernando	08/01/75	6.4	3407, 6th st.	39	0.99	0.17	N90E
8	San Fernando	02/09/71	6.4	234 Figueroa	41	1.19	0.20	N37E
9	East.C Honshu	12/23/85	6.1	Kashima	38	0.97	0.07	N00E
10	Monte Negro	04/05/66	7.0	Albatros	17	0.88	0.17	N00E
11	Mexico	04/09/79	8.1	El Suchil	230	0.91	0.11	S00E
12	Mexico	08/13/81	8.1	La Villita	44	1.17	0.12	N90E

Table 3-3: Characteristics of low a/v group

	Earthquake	*Date*	M_L	*Site*	*Epic. Distance (km)*	*a/v*	*PGA (g)*	*Direction*
1	Long Beach	03/10/33	6.3	Subway T.	59	0.41	0.10	N51W
2	Long Beach	03/10/33	6.3	Subway T.	59	0.37	0.06	N39E
3	Lower Cal.	12/30/34	6.5	El Centro	58	0.77	0.16	S00W
4	San Fernando	02/09/71	6.4	3550 Wil.	39	0.61	0.13	WEST
5	San Fernando	02/09/71	6.4	222 Figueroa	41	0.69	0.13	S37W
6	San Fernando	02/09/71	6.4	3470 Wil.	39	0.61	0.11	S90W
7	San Fernando	02/09/71	6.4	4680 Wil.	38	0.54	0.12	N15E
8	San Fernando	02/09/71	6.4	445 Figueroa	41	0.69	0.12	S38W
9	Mexico	09/19/85	8.1	Zihuatenejo	135	0.65	0.10	S00E
10	Mexico	09/19/85	8.1	Teacalco	333	0.70	0.05	N00E
11	Mexico	09/19/85	8.1	Mesa Vibrad.	379	0.36	0.04	N90W

Some of the earthquake records retained in this study present a very low Peak Ground Acceleration (PGA). The presence of records with very low PGA values may not be totally representative of larger strong motion events, but the paucity of strong motion data in the high a/v category (typical of Eastern North America) does not permit to form a large group of records based on major seismic events. Although small events may not trigger nonlinear response of rock soil mass while larger events may do so, it is believed that some of the characteristics derived from smaller events may be applied to larger events.

3.3 Indices to characterize earthquake records

Indices covering the three important aspects to structural engineers are examined : (1) amplitude of the motion, (2) frequency content of the excitation, and (3) duration and time of occurrence of maxima. The selected criteria are the following :

1) PGA : Peak Ground Acceleration (g)

2) Time of occurrence of the PGA (s)

3) Mc-Cann and Shaw duration (McCann and Shaw, 1979): the time span between the upper cut-off time and the lower cut-off time. The lower cut-off time is the time beyond which the reversed derivative of the cumulative RMSA (Root Mean Square of Accelerogram) is always decreasing. The upper cut-off time is the time beyond which the derivative of the cumulative RMSA (Root Mean Square of Accelerogram) is always decreasing.

4) Bracketed duration: the time between the first and last excursion of absolute value of acceleration above the cut-off acceleration (Bolt, 1973). (the cut-off was set at 0.05 g

except for records that had PGA values smaller than 0.05 g; for these records the bracket was set at 0.01 g).

5) Energy related duration: time necessary to attain 90% and 95% of the total energy. The energy is based on the Arias Intensity (defined below, eq. 3.2)

6) Trifunac-Brady Duration (Trifunac and Brady, 1975): the time necessary to accumulate between 5% and 95% of the total energy (energy also measured with the Arias Intensity).

7) Hudser Duration (Hudser, 1970): Defined as the time necessary to accumulate 90% of the total energy (energy also measured with the Arias Intensity)

8) Number of zero crossings (NZC)

9) Predominant period: the ratio of the total duration to 2 times the number of zero crossings.

10) a_{RMS}: Root Mean Square of accelerogram

$$a_{RMS} = \sqrt{\frac{1}{t_0} \cdot \int_0^{t_0} a(t)^2 \cdot dt} \qquad (3.1)$$

where a(t) is the acceleration, and t_0 is the total duration of the accelerogram.

11) Arias intensity, I_A (Arias, 1969):

$$I_A = \frac{\pi}{g} \cdot \int_0^t a(t)^2 \cdot dt \qquad (3.2)$$

where a(t) is the acceleration and t is the total duration.

12) Spectral Intensity based on acceleration (Tayebi, 1994): the area under the pseudo-acceleration spectrum between periods of s to 0.5 s for 5 % of critical damping.

13) Spectral Intensity based on velocity (Tayebi, 1994): the area under the pseudo-velocity spectrum between periods of 0.04 s to 0.5 sec for 5 % of critical viscous damping.

14) Correlation coefficient: cosine of the angle between horizontal and vertical accelerograms, considering a vectorial representation of the time series. The parameter is defined by dividing the scalar product of the two vectors by the product of their norms.

For each record, these parameters were computed for both the horizontal and the vertical components, and the vertical-to-horizontal (V/H) ratio was obtained for each parameter. For each a/v group of records, statistics of the V/H ratios were computed. Furthermore for each record, the acceleration and velocity response spectra for both horizontal and vertical components were plotted. The V/H ratios of spectral accelerations and spectral velocities were computed for all periods. For each a/v group of records, the average, average + 1 standard deviation (STDV), average - 1 STDV, maximum and minimum values of the V/H ratios of spectral accelerations were plotted.

3.4 Comparison of results

Scattered results were obtained for each a/v group of records. Nevertheless, a few trends could be noticed amongst the computed statistics.

3.4.1 Peak Ground Acceleration (PGA)

The V/H ratios of the PGA had a mean value of 0.7 for the high a/v group, 0.65 for the intermediate one, and 0.55 for the low one. This trend was also noticeable for the PGA

values of the average + 1 STDV, where the value for the high a/v group was 1.22, 1.00 for the intermediate one, and 0.73 for the low group. This could be explained by the fact that earthquakes in the high a/v group usually correspond to near fault events, where P-waves are predominant. The average distance to the fault for the records used in this group is 13.2 km. The vertical component of the earthquake motion is not significantly attenuated in near fault region, thus yielding vertical PGA values closer to the PGA values of the horizontal component. The intermediate and low a/v groups of records have average distances to the fault of 70.6 km, and 113 km, respectively. The increased distances from the fault causes P-waves to attenuate and thus reduce the vertical PGA (PGAV) comparatively to the horizontal direction one (PGAH).

The value of 2/3, usually suggested by building codes like the NBCC (1995) seems to be a good approximation of the average of the PGAV/PGAH ratio. However, the scatter of values may lead to considerable underestimation of the PGAV for certain events. In fact the max-min envelopes of the PGAV/PGAH ratio of the three a/v groups are :

(1) high a/v group : Max = 1.76, Min = 0.27,
(2) intermediate a/v group : Max = 1.35, Min = 0.34,
(3) low a/v group : Max = 1.02, Min = 0.34.

This indicates that the PGAV is predominant in some records. Thus making it necessary to find a more reliable way to estimate the vertical component of ground motion.

3.4.2 Frequency content

The frequency content of the horizontal and vertical records was monitored by the number of zero crossings, and the predominant period of strong shaking. In all three a/v groups, the average V/H ratio of the predominant period is about 0.8. This is consistent with previous results stating that the frequency content of the horizontal and vertical

components is different, and that the vertical accelerations are richer in high frequencies. By definition, each of the a/v group of records presents a different frequency content for the horizontal component. Since the V/H ratio of the predominant period stays constant at 0.8 in all three groups, it means that the vertical accelerations are affected in the same manner as the horizontal accelerations by the factors that influence the a/v ratio.

3.4.3 Energy

The V/H ratios of the root mean square of the accelerograms for the complete duration, the Bolt duration, the Trifunac effective duration, and the McCann and Shaw duration, are also constant at a value of 0.6 for all three a/v groups. Furthermore, the V/H ratio of the pseudo-absolute acceleration spectral intensity is also constant with a value of approximately 0.6 for the three a/v groups. These two results indicate that the total amount of energy generated by vertical accelerations is approximately 60 % of the amount of energy generated by the horizontal accelerations. However, since the frequency content of the horizontal and vertical components is different, it is more conclusive to compare the horizontal and vertical spectra, than the values of the PGA and root mean square of the accelerograms.

3.4.4 Correlation

The correlation factor, θ, is defined as the cosine of the angle between the horizontal and vertical accelerograms. A value of 1 indicates that the two accelerograms are not statistically independent (the two vectors are parallel), while a zero value indicates the complete independence of the components (the two vectors are orthogonal). The highest correlation factor was obtained for the high a/v group with a value of $\theta = 0.24$, whereas the intermediate and low groups had $\theta = 0.11$. The higher value of θ for the high a/v group may be due to the shorter fault distance for this group. The P-waves are therefore

less attenuated. The average V/H ratios for the above discussed parameters, for each of the groups of earthquakes, are presented in Tables 3-4, 3-5 and 3-6.

Table 3-4 : High a/v group, V/H ratios

		AV	*STDV*	*A+STD*	*A-STD*	*MAX*	*MIN*
PGA		0.66	0.45	1.11	0.20	1.76	0.22
Time of occurrence of PGA		1.15	0.61	1.76	0.54	3.00	0.45
McCann - Shah duration	t_1	1.17	0.63	1.80	0.54	2.82	0.12
	t_2	0.94	0.18	1.11	0.76	1.32	0.58
	Dur.	0.82	0.33	1.15	0.49	1.41	0.18
Bracketed duration		0.73	0.25	0.98	0.48	1.05	0.31
Energy related duration	*5%*	0.63	0.31	0.94	0.32	1.23	0.13
	90%	1.06	0.23	1.29	0.82	1.59	0.68
	95%	1.14	0.38	1.52	0.76	2.24	0.76
	Trifunac	1.35	0.59	1.94	0.76	2.94	0.74
	Hudser	1.06	0.23	1.29	0.82	1.59	0.68
Number of zero crossings		1.14	0.17	1.31	0.97	1.41	0.80
Predominant Period		0.89	0.15	1.04	0.75	1.26	0.71
Complete length of record	*Arias Int.*	0.60	0.25	0.85	0.35	1.06	0.26
	a_{RMS}	0.42	0.33	0.76	0.09	1.13	0.07
Bracketed Duration	*Arias Int.*	0.66	0.35	1.01	0.32	1.51	0.23
	a_{RMS}	0.48	0.48	0.96	0.00	1.75	0.03
Trifunac effective duration	*Arias Int.*	0.57	0.30	0.87	0.27	1.10	0.19
	a_{RMS}	0.42	0.33	0.75	0.09	1.13	0.07
McCann-Shaw duration	*Arias Int.*	0.56	0.28	0.84	0.29	1.08	0.21
	a_{RMS}	0.34	0.33	0.68	0.01	1.13	0.02
Spectral intensity Accel.		0.58	0.31	0.90	0.27	1.11	0.24
Spectral intensity Veloc.		0.71	0.48	1.19	0.24	2.16	0.28
θ		0.25	0.16	0.41	0.08	0.68	0.06

Table 3-5 : Intermediate a/v group , V/H ratio

		AV	STDV	A+STD	A-STD	MAX	MIN
PGA		0.66	0.33	0.99	0.34	1.35	0.34
Time of occurrence of PGA		1.11	0.92	2.03	0.19	2.62	0.01
McCann - Shah duration	t_1	0.87	0.86	1.73	0.00	2.55	0.01
	t_2	1.02	0.32	1.34	0.70	1.61	0.50
	Dur.	1.31	0.78	2.09	0.54	3.11	0.42
Bracketed duration		0.67	0.32	0.99	0.35	1.08	0.10
Energy related duration	*5%*	0.48	0.29	0.77	0.20	1.08	0.03
	90%	1.07	0.22	1.28	0.85	1.38	0.55
	95%	1.07	0.19	1.26	0.88	1.34	0.73
	Trifunac	1.21	0.33	1.54	0.89	1.77	0.76
	Hudser	1.07	0.22	1.28	0.85	1.38	0.55
Number of zero crossings		1.29	0.29	1.58	1.00	1.75	0.83
Predominant Period		0.81	0.19	1.00	0.62	1.21	0.57
Complete length of record	*Arias Int.*	0.64	0.23	0.87	0.41	1.07	0.34
	a_{RMS}	0.46	0.32	0.78	0.14	1.15	0.12
Bracketed Duration	*Arias Int.*	0.66	0.24	0.90	0.42	1.07	0.31
	a_{RMS}	0.36	0.36	0.72	-0.01	1.14	0.05
Trifunac effective duration	*Arias Int.*	0.61	0.27	0.88	0.34	1.10	0.26
	a_{RMS}	0.46	0.32	0.78	0.14	1.16	0.12
McCann - Shaw duration	*Arias Int.*	0.55	0.17	0.72	0.38	0.84	0.31
	a_{RMS}	1.18	1.73	2.90	-0.55	4.96	0.04
Spectral intensity (Accel.)		0.60	0.25	0.84	0.35	1.02	0.26
Spectral intensity (Veloc.)		0.49	0.15	0.64	0.33	0.77	0.24
θ		0.13	0.08	0.20	0.05	0.29	0.01

Table 3-6 : Low a/v group , V/H ratio

		AV	STDV	A+STD	A-STD	MAX	MIN
PGA		0.55	0.19	0.73	0.36	1.02	0.34
Time of occurrence of PGA		1.14	0.80	1.94	0.35	3.34	0.50
McCann - Shah duration	t_1	1.29	0.97	2.26	0.32	3.73	0.44
	t_2	0.95	0.16	1.11	0.79	1.25	0.66
	Dur.	0.87	0.26	1.13	0.61	1.33	0.52
Bracketed duration		0.68	0.34	1.02	0.34	1.00	0.05
Energy related duration	*5%*	0.73	0.44	1.18	0.29	1.42	0.18
	90%	1.12	0.17	1.29	0.95	1.43	0.85
	95%	1.10	0.10	1.20	1.00	1.30	0.94
	Trifunac	1.28	0.28	1.55	1.00	1.94	0.90
	Hudser	1.12	0.17	1.29	0.95	1.43	0.85
Number of zero crossings		1.22	0.22	1.44	1.00	1.71	0.99
Predominant Period		0.84	0.13	0.97	0.71	1.01	0.58
Complete length of record	*Arias Int.*	0.59	0.12	0.71	0.47	0.75	0.42
	a_{RMS}	0.36	0.14	0.51	0.22	0.56	0.17
Bracketed Duration	*Arias Int.*	0.55	0.20	0.75	0.35	0.84	0.12
	a_{RMS}	0.21	0.18	0.39	0.03	0.51	0.01
Trifunac duration	*Arias Int.*	0.55	0.14	0.69	0.41	0.74	0.38
	a_{RMS}	0.36	0.14	0.51	0.22	0.56	0.17
McCann - Shaw duration	*Arias Int.*	0.58	0.18	0.76	0.40	0.85	0.39
	a_{RMS}	0.30	0.17	0.47	0.13	0.52	0.11
Spectral intensity (Accel.)		0.59	0.22	0.81	0.37	1.09	0.34
Spectral intensity (Veloc.)		0.57	0.13	0.70	0.44	0.75	0.30
θ		0.11	0.09	0.20	0.02	0.22	0.02

3.5 Characteristics of horizontal and vertical response spectra.

For each earthquake record, the horizontal and vertical acceleration and velocity response spectra were computed for 5% damping. The V/H ratio of spectral acceleration (VSa/HSa) was plotted as a function of the period. For each a/v group, the average,

average +1 STDV, average -1 STDV, maximum and minimum envelopes of the (V/H) of Sa were plotted as a function of the period, as can be seen in Figures 3.1, 3.2 and 3.3.

All three groups exhibited peak ratios of VSa/HSa in the small period range (T < 0.25 s).

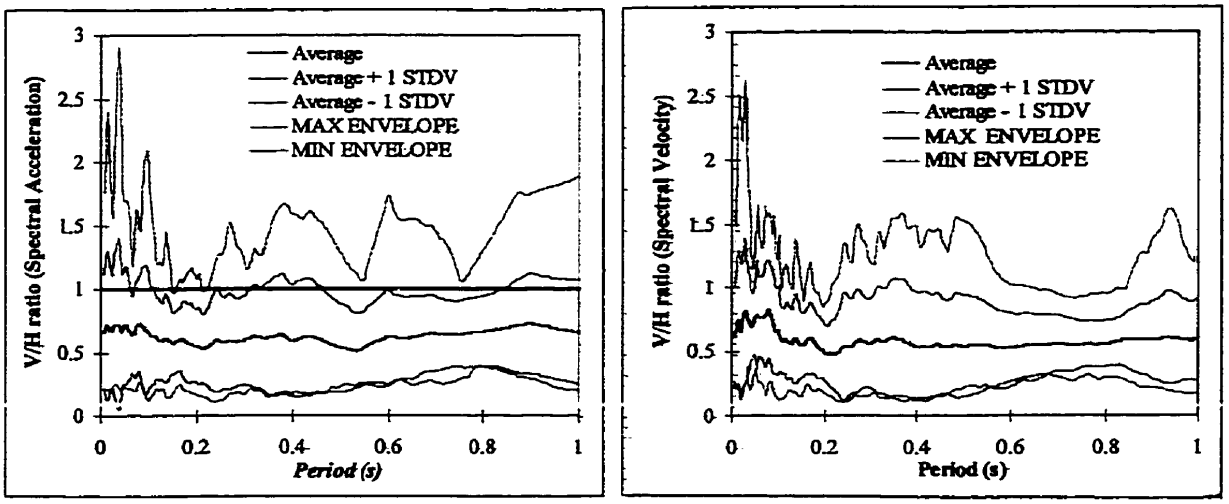

Figure 3.1: V/H ratio of Spectral acceleration and velocity (high a/v group)

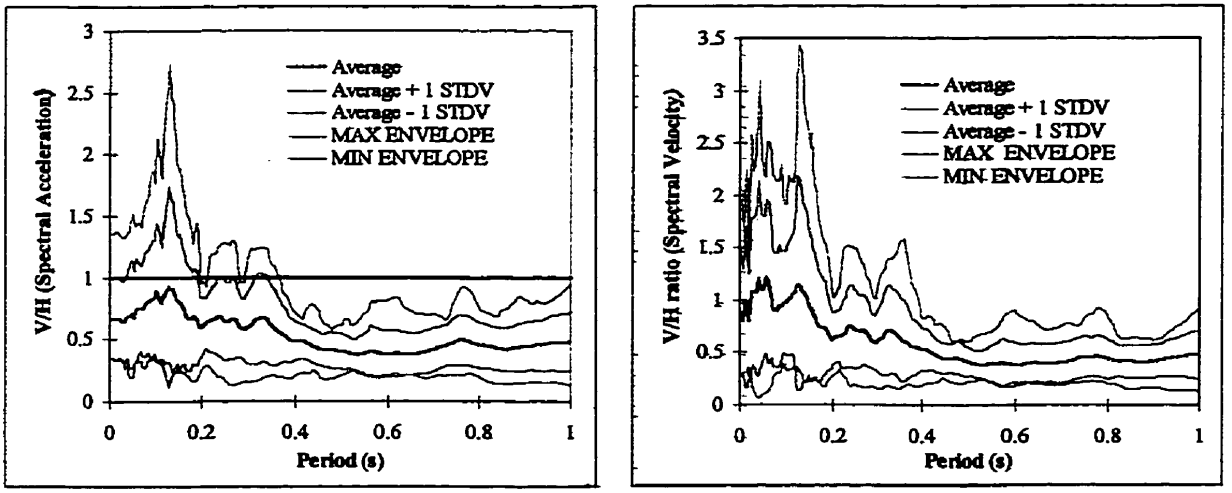

Figure 3.2: V/H ratio of Spectral acceleration and velocity (intermediate a/v group)

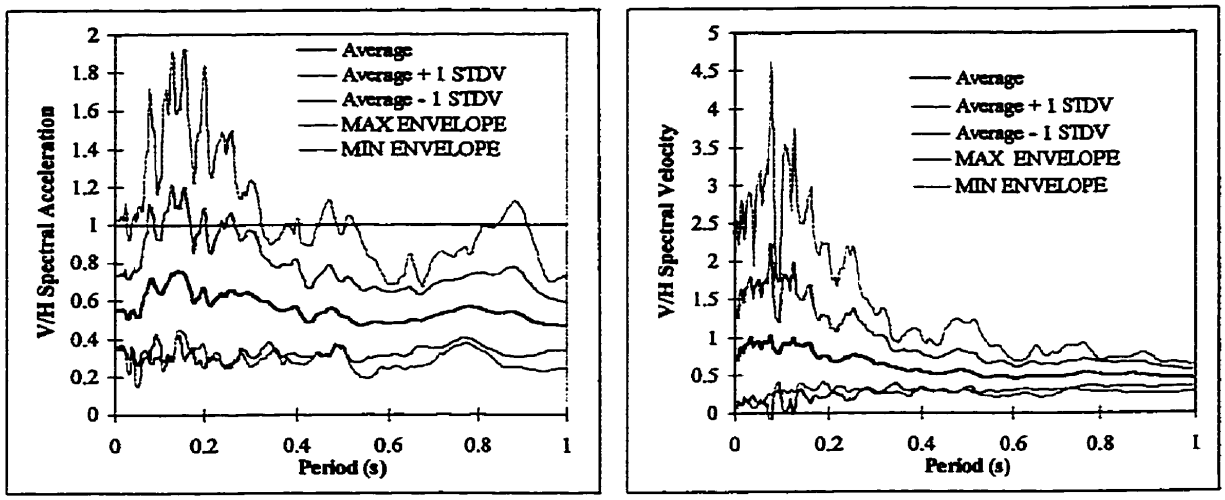

Figure 3.3 : V/H ratio of Spectral acceleration and velocity (low a/v group)

- **High a/v group of records :**

The average VSa/HSa ratio reaches a maximum of 0.75 for periods ranging from 0 s to 0.15 s. It then decreases to 0.5 at a period of 0.25 s. For periods between 0.25 s and 1 s the ratio is relatively constant at 0.6. The standard deviation is relatively high, and the average + 1 STDV curve follows the same form as the average curve, with an increase of 0.35 in the V/H ratio axis.

- **Intermediate a/v group of records:**

This group presents the most distinct VSa/HSa peak of the three groups. The maximum value of the VSa/HSa ratio is reached at a low period, but there is a build-up range before reaching the peak. The average VSa/HSa ratio builds up from an initial value of 0.65 at T = 0 s (corresponding to the group's average PGA) to 0.97 at a period of 0.15 s. It then decreases to 0.6 for a period of 0.25 s, and to 0.45 for a period of 0.5 s. The ratio remains constant at 0.45 from periods ranging from 0.5 s to 1 s . The standard deviation for this group is also relatively high, and the average + 1 STDV curve places the entire peak (0 s < T < 0.2 s) above a ratio of 1, with a maximum value of 1.7 at T = 0.15 s.

- **Low a/v group of records :**

This group presents also a build-up area in the low period range but the ratios are smaller. The initial average value of 0.55 at a period of 0 s increases to 0.75 for a period of 0.15 s. It then decreases to 0.58 for a period of 0.25 s, and to a value of 0.5 for a period of 0.5 s. The ratio remains constant for periods between 0.5 s and 1 s. Similarly to the two other a/v groups, the average + 1 STDV curve follows the same shape as the average curve, with a peak value of 1.2 at a period of 0.15 s.

In figure 3.4, the mean value of the V/H ratio of spectral acceleration is plotted for each group. The shape of the curves follow the trends discussed above. These curves are a smoothened representation of results presented in Figures 3.1 to 3.3.

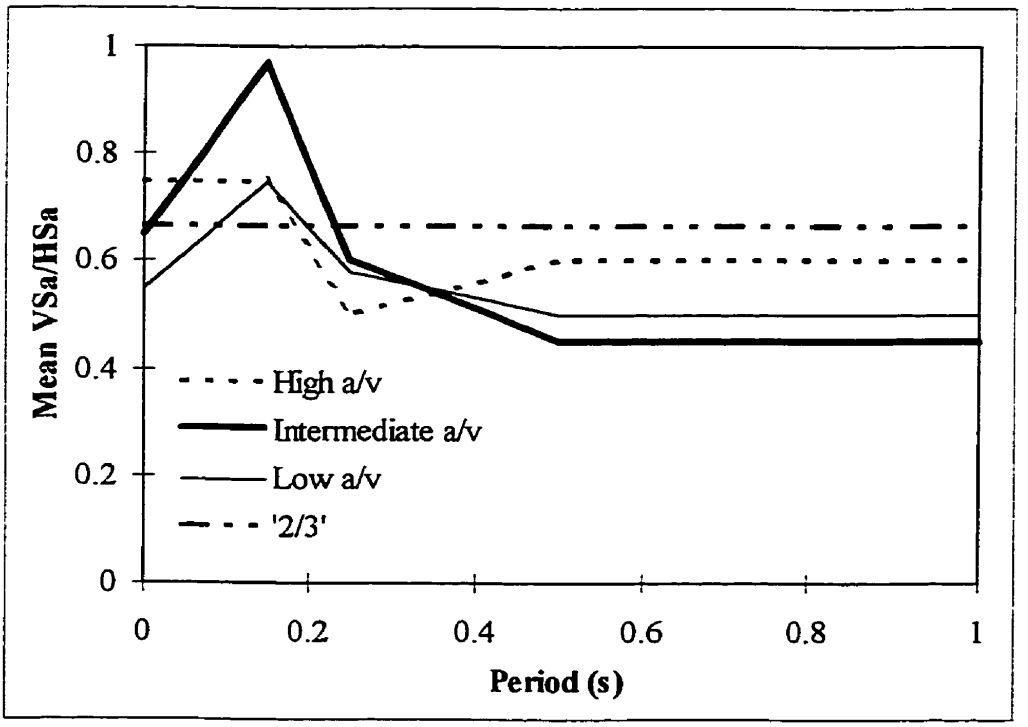

Figure 3.4 : V/H ratio of spectral acceleration for three a/v groups (average values)

Figure 3.4 shows that the VSa/HSa is greater in the short period range. In fact, for all three a/v groups for periods smaller than 0.25 s the V/H Sa ratio is greater than the value of 2/3. This value is usually applied to the PGAH to estimate the PGAV. It must be noted that when inspecting the shapes of the horizontal and vertical spectra for each record, the peaks of the acceleration response spectra do not occur at the same periods. Since the vertical acceleration is recognized as being richer in high frequencies, it could explain why the ratio is greater in this area.

The spectral acceleration at a certain period represents the peak acceleration effectively experienced by the structure. In fact the V/H ratio gives an estimate of the relative importance of the vertical component compared to the horizontal one. This measure is not indicative of the potential damage to a structure by the combined effect of the horizontal and vertical components of an earthquake, since the modes that will be influenced by the vertical direction input motion will be at a much higher frequency than those influenced by the horizontal component. These ratios are examined as indicators of how to obtain realistic vertical spectra from the corresponding horizontal ones.

In the following paragraphs, such a method is proposed through the use of shift and reduction factors to be applied to the horizontal spectra to obtain the vertical ones.

3.6 Generation of Shifted and Reduced Spectra (GSRS)

Following the idea proposed by Bozorgnia and Campbell (1996), and after analyzing the horizontal and vertical spectra plotted on a same graph for each earthquake, a similarity was noted in the shape of the spectra. As compared to the vertical spectra, the peaks of the horizontal spectra were usually shifted towards the longer period range. In general the peak horizontal spectral accelerations were higher than those of the vertical spectra.

Ohno et al. (1996) obtained vertical spectra by scaling the corresponding horizontal spectra by 0.6 for shorter periods, 0.5 for long periods and by a log-log interpolation for intermediate periods. This study was limited to records obtained from soft rock sites with a shear wave velocity of 700 m/s and could not be applied for all earthquakes, but the idea of obtaining the vertical spectra as a multiple of the horizontal one was retained. In the study by Bozorgnia and Campbell (1996), the same idea was used to generate the vertical spectrum from the horizontal one, but the method consisted in first shifting the horizontal spectra to the short period range by multiplying the period axis by a scaling factor, and then reducing the amplitudes of the spectra to approach a vertical target spectra.

Since this study was exclusively based on records from California earthquakes, it was decided to use the same methodology for the three a/v earthquake data groups previously considered. The idea was to see if a simple method could be used for each group to obtain the vertical spectra based on the horizontal ones. The period axis multiplier is defined as the Shift factor (Sf), and the amplitude calibrating multiplier is defined as the reduction factor (Rf).

To define Sf and Rf, the following methodology was used :

- Compute the vertical and horizontal absolute acceleration spectra for each earthquake.
- Compute the average acceleration response spectra for each a/v group, for both the horizontal and vertical components.
- Compute the values of Sf and Rf that minimize the sum of the squares of the errors between the shifted and reduced average horizontal spectra and the target average vertical spectra, for different ranges of the periods.

- Compile the values of Sf and Rf and compute the statistics for each group of earthquakes.
- Examine these results to determine Sf and Rf values that would result in an acceptable estimation of the real vertical spectra, from the horizontal spectra.

It was decided to use the average spectra for each group to compute Sf and Rf, instead of using the individual records and then compiling statistics for each group. This decision was based on the fact that our final goal is to generate spectrum compatible accelerograms, and that it is usually smooth average spectra that are used for generation. Furthermore, the method, which would be applicable to current design codes, would be used with code spectra which represent a smooth average of spectral ordinates that could occur within a prescribed probability.

A computer program GSRS-Generation of Shifted and Reduced Spectra (Christopoulos, 1998) was developed to compute optimum values of Sf and Rf. The optimization criteria was the sum of the squares of amplitude differences between the target vertical spectrum and the shifted and reduced spectrum. The program used the real spectra as input, and computed the optimum value of Sf and Rf by sweeping values of Sf ranging from 0.5 to 3 in steps of 0.1, and values of Rf ranging from 0.2 to 2 in steps of 0.1.

Initially the program computed the sum of the squares of amplitude differences for periods between 0 s and 1 s. Following the first set of results, it was decided that it was preferable to subdivide the period range in which the Sf and Rf factors where computed so that the peak spectral ordinates corresponding to the lower period values were not biased by the lower spectral ordinates corresponding to the higher period values.

The period range was subdivided into three groups :

1) from 0 to 0.25 s,
2) from 0.25 s to 0.5 s,
3) from 0.5s to 1s.

Although these ranges were used for checking how the factors behaved for different period values of the spectra, the period range from 0 s to 0.5 s which covers the most important range that includes the peak values of the spectral accelerations, and the complete range from 0 s to 1 s were also kept for comparison purpose.

The period limit of 1 s was retained because for periods longer than 1 s, there is no dynamic amplification. In fact after a period, T, of 1 s, the spectral acceleration falls bellow the value at T = 0 s, which corresponds to the PGA of the record. Furthermore, all the spectral peaks occur within the 0 s to 1 s range.

The choice of 0.5 s as a boundary for Sf and Rf calculations is also justified because NBCC (1995), 0.5 s is a boundary value that separates the long period structures from the short period structures, with respect to the equal displacement method.

Examining the computed values of Sf and Rf for each of the a/v groups as shown in Table 3-7, indicates that the values vary widely within the different period ranges. It was decided that, since the most important section was located in the 0 s to 0.5 s period range, and in order to obtain a reasonable match of the peak areas, the values of Sf and Rf computed for this period range only would represent the group.

Table 3-7 : Shift factors and reduction factors for the three a/v groups

Period	*High a/v*		*Inter a/v*		*Low a/v*	
Ranges	*Sf*	*Rf*	*Sf*	*Rf*	*Sf*	*Rf*
0 s to 0.25 s	2.05	0.85	2.00	0.55	1.50	0.55
0.25 s to 0.5 s	2.75	1.80	1.65	0.60	3.00	0.80
0 s to 0.5 s	***1.55***	***0.80***	***1.60***	***0.55***	***1.45***	***0.55***
0.5 s to 1 s	1.40	0.90	3.00	1.25	1.35	0.55
0 s to 1 s	1.50	0.80	1.55	0.55	1.35	0.55
AVERAGE	***1.85***	***1.03***	***1.96***	***0.70***	***1.73***	***0.60***

Figure 3.5 illustrates the proposed method. The computed Sf and Rf factors are applied to the horizontal acceleration response spectrum of the 1971 San Fernando earthquake record (Hollywood Storage) belonging to the intermediate a/v group to obtain the shifted and reduced spectrum which is compared to the vertical acceleration response spectrum (vertical target spectrum). The intermediate group values of Sf = 1.6 and Rf = 0.55, found in Table 3.7 were used for the shift and reduction.

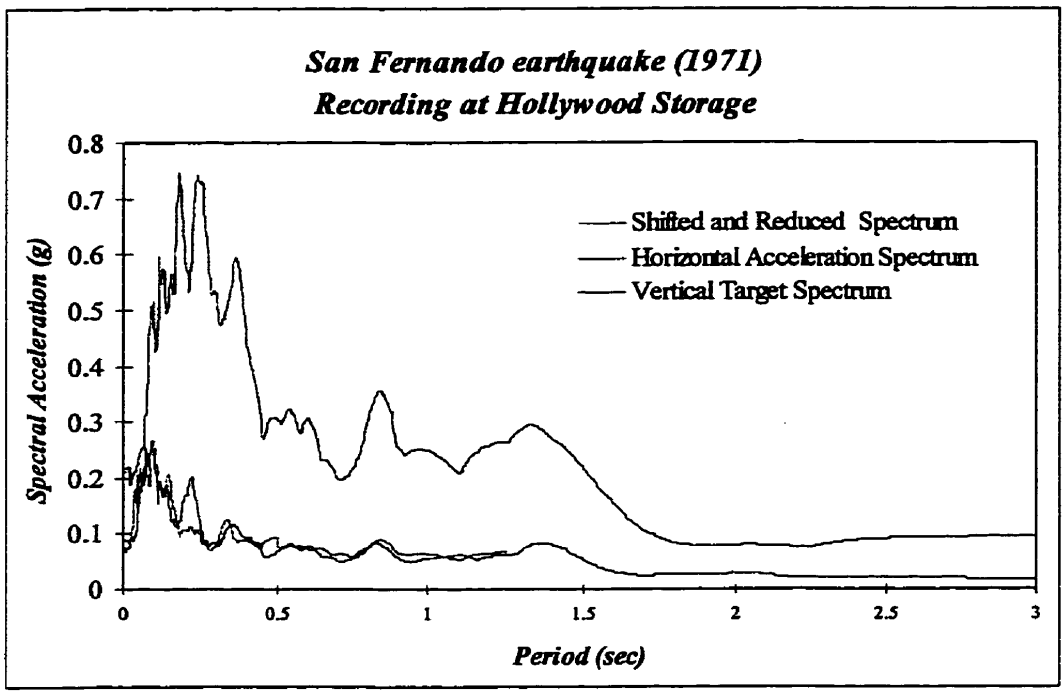

Figure 3.5 : Example of shifted and reduced spectrum

From the results presented in Table 3-7, one can see that the trend in Sf is directly related to difference in frequency content between the horizontal and vertical components. The lowest Sf corresponds to the high a/v group that represents near fault records. This result is coherent with the fact that the correlation factor, θ, between the horizontal and vertical accelerograms was found to be the highest for this group. Since it is mainly P-waves that influence the near fault recordings, it could be concluded that for this group of records, the response spectra of the two components of the ground motion are very similar. This is also verified by the fact that PGAV/PGAH ratio was found to be the highest for this group, and consequently the closest to unity. As the distance from the fault increases, for the intermediate and low a/v groups, the waves are attenuated in a more substantial way, and the horizontal and vertical components differentiate themselves more and more, whether it is frequency wise since the Sf increases, or amplitude wise, since the PGAV/PGAH ratio decreases.

Sf and Rf were also plotted in each group as functions of magnitude and distance, as well as the log of magnitude and the log of distance. No specific trend was found with respect to these parameters in each of the a/v groups.

3.7 Effects of damping

In this study, all results are based on an assumed critical damping ratio $\xi = 5\%$. Both the horizontal and vertical spectra are computed with this damping ratio, since it is the value recommended by NBCC (1995). However, it is recognized that ξ can vary from 2% to 10% depending on the materials and on the energy dissipation mechanism of the structural system.

To examine the effect of ξ on Sf and Rf, one typical record was chosen for two of the a/v groups of earthquakes. For each of these records, the horizontal and vertical spectra were computed for $\xi = 2\%$, 5%, and 10%. Then, Sf and Rf were computed from the spectra for each damping ratio.

As can be seen in Table 3.8, the values of Sf and Rf were practically unaffected by the different damping ratios. Since it is known that the damping ratio has a considerable effect on the acceleration spectra, it can be concluded that the horizontal and vertical spectra of an earthquake record are similarly affected by the damping ratio, thus making it possible to obtain shifted and reduced spectra for 2% damping for example, based on the horizontal spectra for 5% damping. In a study by Carr (1994) scaling factors for different damping ratios are proposed. Carr recommends, with 5% damping taken as unity, multipliers of 1.4 for 2 % damping, and 0.8 for 10 % damping. These values suggest that

the effect of the damping ratio is significant, since from 5% damping to 2% damping an increase in the response of 40 % is expected.

In the most commonly encountered structures, the load carrying mechanisms in the horizontal and vertical directions are not the same. In fact, seismic design emphasizes more on the dissipation of energy through horizontal resisting systems for dynamic loads, while the vertical mechanisms are designed to resist static gravity loads. Considering also

Table 3-8 : Effect of damping ratio on Sf and Rf

		0 s - 0.5 s		*0 s - 1 s*	
Earthquake	***Damping ξ***	***Sf***	***Rf***	***Sf***	***Rf***
	2%	1.30	0.30	1.30	0.30
San Fernando	5%	1.30	0.25	1.30	0.25
(Pac. Dam)	10%	1.30	0.25	1.25	0.25
	2%	1.65	0.55	1.60	0.55
Mexico	5%	1.70	0.50	1.65	0.55
(El Suchil)	10%	1.70	0.50	1.65	0.50

that, in general, for vertical static loads it is the cross-sectional area alone working in tension or compression that resists the loads, and that in the horizontal direction it is a combination of shear forces, flexure, or tension and compression, it could be expected that the damping ratio in the vertical direction would be lower then the damping ratio in the horizontal direction. In such a case, combining vertical and horizontal spectra for different damping ratios could result in a considerable increase of the effect of vertical accelerations in the response of structures. This point needs to be investigated further, since there is no documentation in the literature that covers this aspect.

3.8 Generation of synthetic ground motions to satisfy spectral requirements and cross-correlations

To demonstrate the application of the above described method, a complete example for the city of Montreal based on the horizontal code prescribed spectrum is presented. Montreal is classified in a seismic region corresponding to the high a/v group of earthquakes. A complete generation of three horizontal and three vertical synthetic accelerograms is presented. Following the generation of these time-histories, the correlation between the two components is discussed, and a method to establish an acceptable degree of correlation is proposed.

3.8.1 Shifted and Reduced Spectra

The shift factors and reduction factors discussed in the previous paragraph are used to generate vertical spectra based on the horizontal spectra specified in the code for the city of Montreal. For Montreal, the NBCC (1995) suggests a value for the horizontal PGA of 0.18 g. Referring to paragraph 3.6 of this chapter, we use a value of $S_f = 1.55$ and $R_f = 0.80$ for the high a/v group. Defining the code prescribed horizontal spectrum for $\xi = 5\%$ of critical damping, and generating the shifted and reduced vertical spectrum, we obtain the vertical target spectrum for the generation, as illustrated in Figure 3.6.

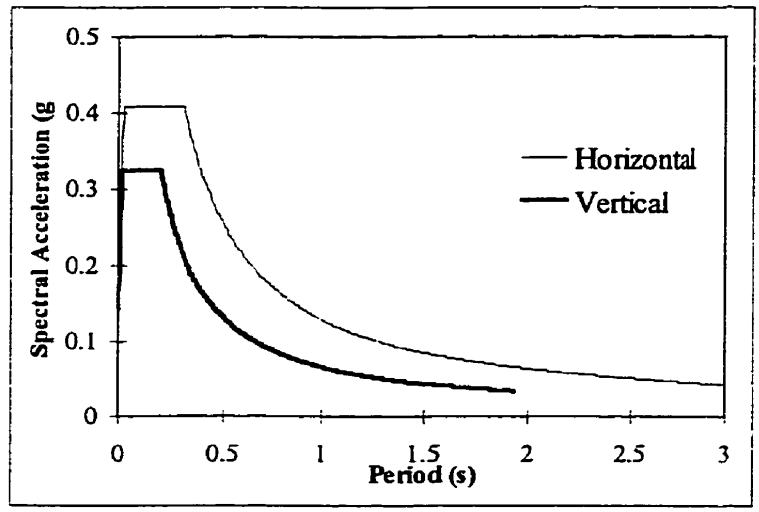

Figure 3.6 : Horizontal and vertical (shifted and reduced) spectra for Montreal

3.8.2 Intensity Function

Based on the horizontal and vertical spectra for each city, synthetic accelerograms are generated. The program SIMQKE (1976) was used to generate the time histories. In SIMQKE, an intensity function must be specified. This intensity function multiplies the generated stationary ground motion to simulate the different non stationary intensity zones of the accelerogram. The intensity function is comprised of three distinct areas :

1) build up zone
2) strong shaking zone
3) decay zone.

To define the intensity function, for a given seismic area, estimates of the total duration, as well as the duration of the build up zone and the decay zone are required. Based on the statistics compiled for the historical records chosen for our study, time function comparisons could be carried out.

These comparisons apply to the horizontal direction time function. For the vertical direction time function, it was decided to reduce the build up zone to account for the fact that the vertical component seems to build up faster. This assessment was made based on statistics presented in Tables 3.4, 3.5 and 3.6 that indicate that the time necessary to build up 5 % of the total energy (based on the Arias intensity), is in average 50% smaller for vertical components. This observation complies with previously reached conclusions in the literature that the vertical component could be compared to a sudden burst of energy. Hawkins and Inverson (1996) stated that in the Northridge (1994) earthquake, the vertical accelerations induced significant vibrations in the structure a few seconds prior the arrival of the horizontal strong shaking. In addition it was noted, by observing results on synthetic ground motions, that the build up zone corresponded approximately to 5 % of the total energy.

Following this observation, it was decided to use the same intensity function for the horizontal and vertical directions, except for the build up area that is reduced by 50% for the vertical direction.

Figure 3.7, shows the form of the intensity functions used for the generation. As can be seen in Figure 3.7, T_{IH} which corresponds to the horizontal build up time, is taken as two times T_{IV} which represents the vertical build up time.

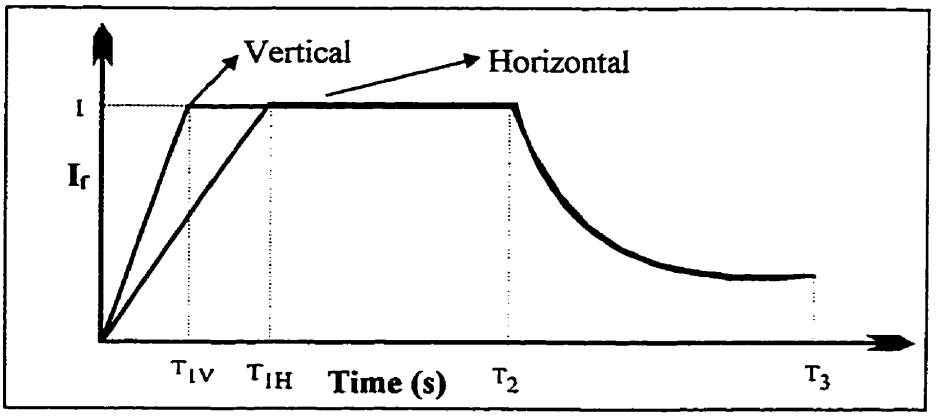

Figure 3.7 : Intensity functions

The build up function is taken as linear, while the decay function is exponential. The exponential decay is taken as :

$$I_f = e^{-0.3(t-T_2)} \qquad (3\text{-}1)$$

where t is the time, and T_2 is the beginning of the decay in s.

The generated accelerograms for Montreal must be typical of Eastern Canadian ground motions. In order to decide on the duration, historical records like the Saguenay (1988) earthquake were examined, as well as synthetic ground motions generated by Atkinson.

Figure 3.8 shows the intensity functions for both the horizontal and vertical directions for the generated strong motion for the city of Montreal.

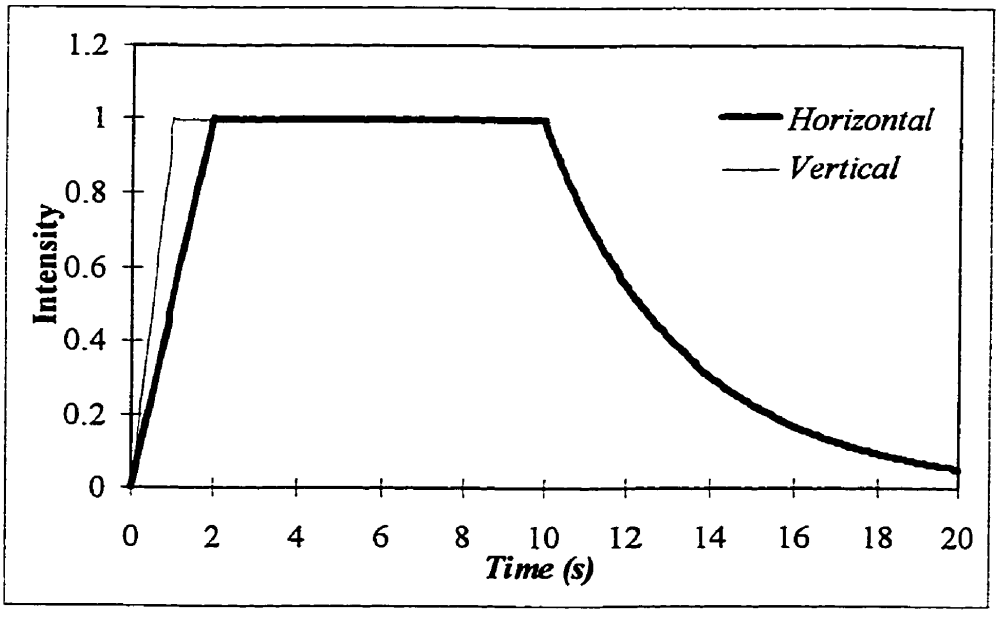

Figure 3.8 : Intensity Functions for Montreal

For the horizontal direction, the build up area is taken as 2 s, the constant strong shaking as 10 s, and the decay as 8 s. For the vertical direction, the same parameters are used, but the build up time is reduced to 1 s (50% of build up time in horizontal direction).

3.8.3 Generated synthetic ground motions

Three pairs of synthetic accelerograms were generated with SIMQKE (1976). The first controlling criteria was the spectrum compatibility, and all three pairs had compatible spectra. Following this first test, the effective durations were computed for comparison with other typical records for this area. The durations were quite reasonable, and the records were all considered as satisfactory.

Figures 3-9 and 3-10 show the acceleration spectra of the three horizontal, and three vertical respectively, synthetic ground motions, generated with SIMQKE (1976). The target spectra, based on NBCC (1995) are also plotted.

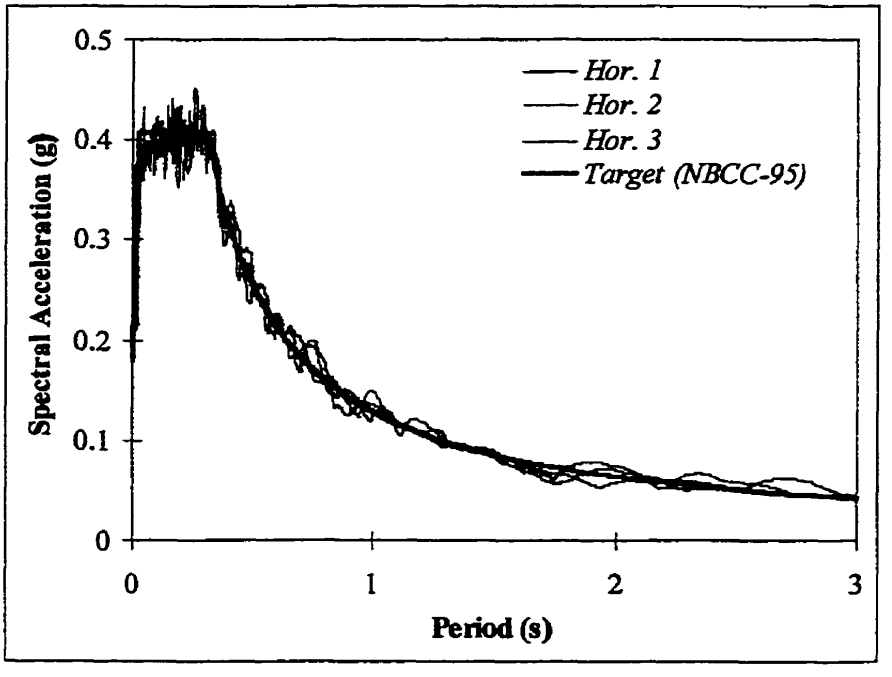

Figure 3.9 : Horizontal acceleration spectra for Montreal

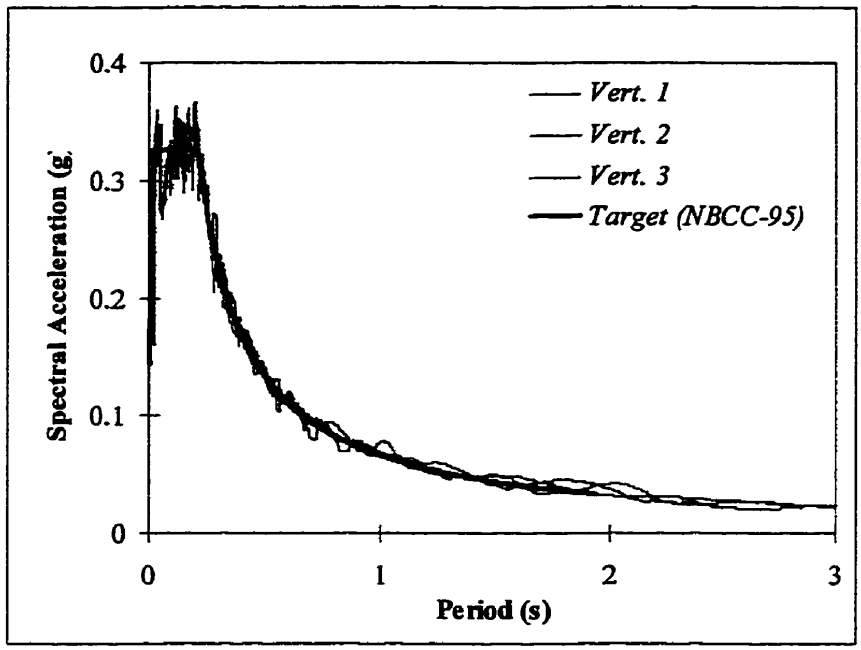

Figure 3.10 : Vertical acceleration spectra for Montreal

Figure 3.11 presents two accelerograms, a horizontal one, H1, and a vertical one, V1, generated with the above describe procedure for the city of Montreal.

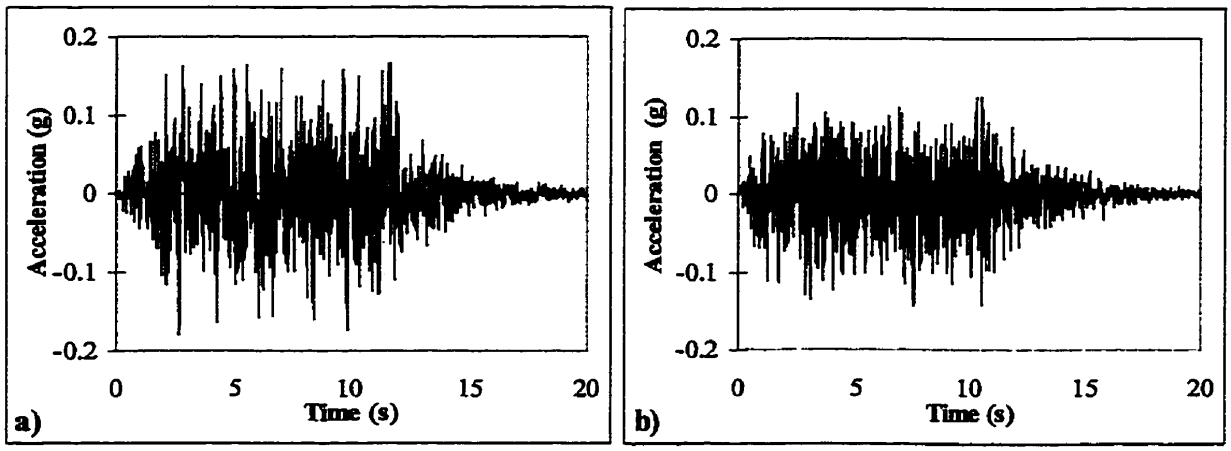

Figure 3.11: Synthetic accelerograms for Montreal

a) H_1: horizontal component b) V_1: vertical component

3.8.3 Correlation

Following the generation of the accelerograms, the correlation factor between all horizontal and all vertical records was computed, by dividing the vectorial product of the two accelerograms by the product of the norms of the accelerograms. Table 3-9 shows the correlation factors for the accelerograms computed for Montreal.

Table 3-9 : Correlation factors for Montreal accelerograms :

	H1	*H2*	*H3*
V1	*0.055*	*0.01*	*-0.04*
V2	*0.061*	*-0.01*	*-0.04*
V3	*0.026*	*-0.04*	*-0.03*

The accelerograms computed with SIMQKE (1976) by choosing different seed numbers show very low correlation amongst themselves. Considering that a correlation of $\theta = 0.2$ is realistic, based on results presented in this study in Tables 3.4, 3.5, 3.6, and on conclusions reached by Chen and Lee (1973), where a correlation of 0.2 is suggested after statistical analyses on the correlation of 100 historical records, we conclude that the accelerograms generated for Montreal might be too conservative especially for structures where the simultaneous interaction of both components is critical. Following this observation, it was decided to study a method to alter the existing records to increase the correlation to a more realistic value, and if possible to the suggested value of 0.2. A method proposed by Levy and Wilkinson (1973), consists of delaying the start of one of the two accelerograms, thus affecting the correlation.

Figure 3.11 shows the variation of the correlation as a function of the delay time t. The correlation is computed for accelerograms H1 and V3, for Montreal.

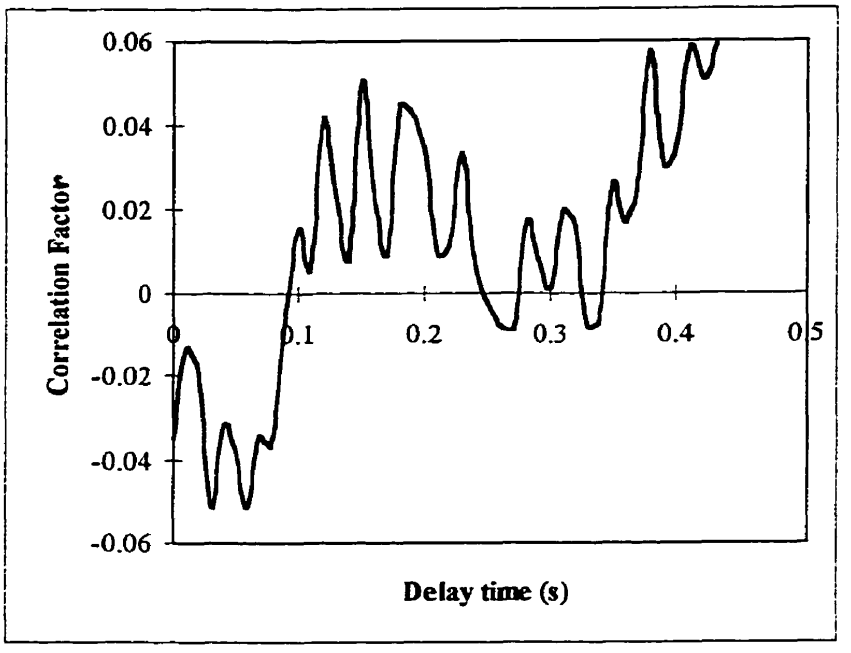

Figure 3.12 : Correlation factor for H_1 and V_3 records for Montreal

We can see that the correlation is not improved significantly as it does not exceed 0.06, which is quite low. Following this observation, it was decided to induce a stronger correlation in two accelerograms typical of Montreal, by generating the horizontal and vertical accelerograms with the same seed number. Once these two strongly correlated accelerograms are delayed in the same way as described above, a correlation of 0.2 or any other correlation for that matter could be attained.

Figure 3.12, shows the correlation factor for accelerograms H_1 and V_{1T}, where V_{1T} is generated with the same seed number. The correlation factor is plotted as a function of the delay time. For this case, we can see that a delay time of 0.035 s, which could be considered as insignificant as a change to the original accelerograms, yields a correlation factor of 0.2.

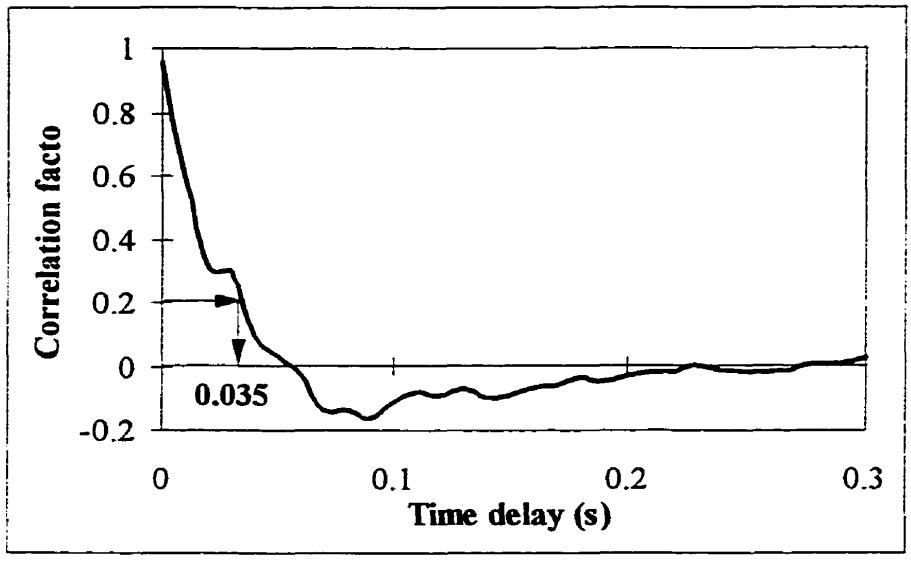

Figure 3.13 : Correlation factor for initially strongly correlated accelerograms

The suggested method is a simple way of inducing the desired amount of correlation in two synthetic accelerograms, but the exact effect of a low correlation on the response of structures solicited by two dimensional accelerograms is not yet clear. Further studies should be attempted to assess the exact effect of the low correlation between accelerograms generated by SIMQKE.

3.8.4 Peak Correlation Factor (PCF)

The correlation coefficients are computed for the entire record. Many structures that could be highly influenced by the simultaneous application of horizontal and vertical accelerations, are sensitive to the occurrence of simultaneous peaks. In fact, a pair of horizontal and vertical accelerograms, which have a high correlation factor, may not have any significant peaks that occur at the same time. On the other hand, a different pair of time histories, which present a low correlation factor over the entire record, may have three or four significant peaks that occur simultaneously, thus inducing greater damage to the structure than a highly correlated pair.

It is believed that the vertical accelerations alone are not responsible directly for great structural damage, but it is the combined effect of horizontal and vertical accelerations that can be critical for a structure. The following cases illustrate the fact that the most important aspect of the two dimensional earthquake excitation is in fact the occurrence of peaks in both directions :

1) When analyzing sliding structures, such as gravity dams for example, the horizontal acceleration induces inertia forces that must be resisted by the friction of the dam-foundation interface. A negative (upward) vertical acceleration does not increase the horizontal inertia forces, but reduces the weight of the structure, thus reducing the resistance to sliding.

2) When analyzing the shear strength of concrete columns, the effect is similar, since vertical accelerations affect the axial load. The concrete contribution to shear is a function of the axial load. When simultaneous horizontal and vertical peaks occur, the shear demand may be maximum when the shear strength is decreased by reduction of the concrete contribution.

To asses the importance of the peak simultaneity, a Peak Correlation Factor (PCF) was defined in the following manner :

- Normalize both horizontal and vertical accelerograms by their respective PGA.
- Run through the horizontal accelerations step by step, and eliminate all the values that are below the Peak Limit Acceleration (PLA), by putting them to 0. The PLA could be defined as an arbitrary value above which the horizontal acceleration is expected to be significant. The PLA could also be defined specifically for a structure, for example for a sliding structure it could represent the critical acceleration to induce sliding, or a fraction of it since the presence of the vertical acceleration will reduce it.

- Once the selection of the significant horizontal accelerations is made, compute the product, for each time step, of the horizontal and vertical normalized accelerations.
- The PCF is defined in equation (3-5).

The procedure to compute the time-history of the PCF is summarized by equations (3.2) through (3.5) :

$$\frac{[a_h(s)]}{PGAH} = [a_h(s)]_N \quad \text{and,} \qquad (3\text{-}2)$$

$$\frac{[a_v(s)]}{PGAV} = [a_v(s)]_N, \quad \text{where} \qquad (3\text{-}3)$$

- $[a_h(s)]$ and $[a_v(s)]$ are the horizontal and vertical accelerograms respectively,
- PGAH and PGAV are the horizontal and vertical PGA.
- The index N indicates that the time histories have been normalized to their PGA.

For s = 1 to S ,

where s is the time step number in the accelerogram, and where S * Δt = total duration with

Δ(t) taken as the time step of the accelerogram.

$$[a_h(s)]_{NS} = \begin{cases} = 0 & if \ [a_h(s)]_N \le (PLA) \\ = [a_h(s)]_N & if \ [a_h(s)]_N \rangle \ (PLA) \end{cases} \qquad (3\text{-}4)$$

$$[PCF(s)] = [a_h(s)]_{NS} \times [a_v(s)]_N \qquad (3\text{-}5)$$

$[PCF(s)]$, once the absolute of all the values is taken, is a S x 1 vector and all values are between 0 and 1.

A value of 1 in the vector indicates a simultaneous occurrence of the PGAV and PGAH.

The PCF offers a more representative parameter to assess the potential effect of the combined two-dimensional . The PCF is not an absolute measure of the effect of the combined accelerations on a structure, since a very damaging horizontal spike could occur precisely when the vertical acceleration is 0, but more of an indicator of the possibility of an important combined effect of horizontal and vertical accelerations.

The PCF is computed in chapter 5 of this study for a number of accelerograms used in the parametric analyses, and some comments on the significance of this parameter on the structural response are presented.

CHAPTER 4

Effects of Near-Fault Vertical Seismic Accelerations on the Dynamic Response of Steel Moment-Resisting Frames

4.1 Introduction

Following the January 17, 1994 Northridge, California earthquake, where a number of brittle weld fractures were observed in beam-column connections of more than 100 steel moment-resisting frames, many studies have investigated the possible role played by the high vertical accelerations recorded during this earthquake (Papazoglou et al. 1996, Broderick et al. 1994). In this chapter, the effects of vertical accelerations on the plastic hinge formation, the maximum story deflections, the rotational ductility demand, the induced strain rate, and the increase in column axial loads, are investigated for a 6-story steel building subjected to near-fault earthquake records typical of the Los Angeles region.

4.2 Description of analyzed structure

The 6-story structure studied in this chapter was first designed by Tsai and Popov (1988), and modified by Hall (1995). As shown in Fig. 1, the structure is rectangular in shape, and spans 37 m by 22 m. Lateral loads in the North-South direction are resisted by two exterior moment-resisting frames. The structure is designed according to the 1994 edition of the Uniform Building Code (ICBO 1994) for a building in Zone 4 and on soil type S2. Design loads include 3.8 kPa for dead load on the roof, 4.5 kPa for dead load on the floors, a roof live load of 1.0 kPa, and a floor live load of 3.8 kPa. In addition to the

static loads, the masses corresponding to each node are included in the dynamic analyses. The masses are activated in both the x and y directions, for both the frame and the external column representing the effects of the remaining structure.

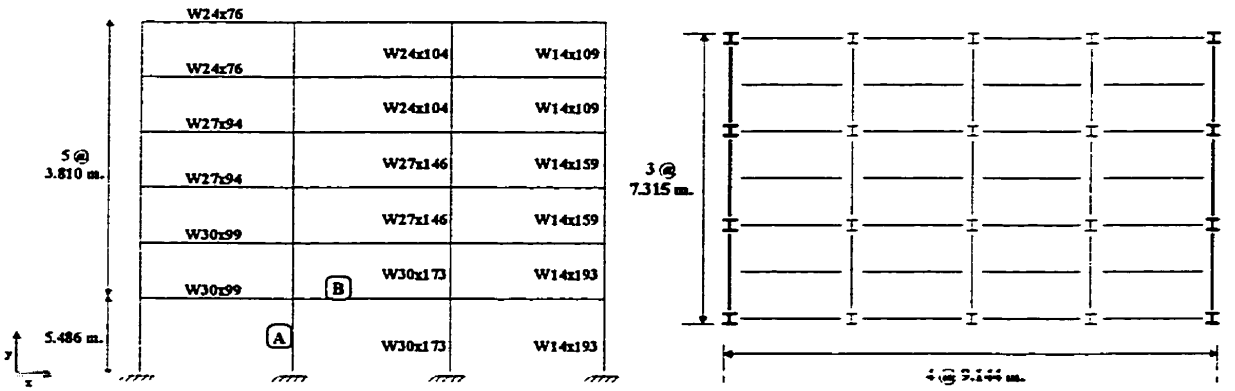

Figure 4.1 : Analyzed structure

The wind loads were calculated assuming a wind speed of 113 km/h and an exposure type B. The steel grade is assumed to be A36.

The sections comprising the beams and columns of the structure are indicated in Figure 4.1, and their properties are summarized in Table 4-1:

Table 4-1 : Properties of sections

	d (mm)	*Area* (mm^2)	I_{xx} (mm^4)	I_{yy} (mm^4)	*Zx* (mm^3)
External Columns					
W14 X 193	393.1	36 645	999 E6	388 E6	5 817 E3
W14 X 159	381.0	30 129	791 E6	311 E6	4 703 E3
W14 X 109	364.0	20 645	516 E6	187 E6	3 146 E3
Interior Columns					
W30 X 173	773.2	32 774	3 413 E6	249 E6	9 914 E3
W27 X 146	695.5	27 678	2 343 E6	184 E6	7 554 E3
W24 X 104	611.1	19 742	1 290 E6	108 E6	4 736 E3
Beams					
W30 X 99	753.1	18 774	1 661 E6	53.3 E6	5 113 E3
W27 X 94	684.0	17 871	1 361 E6	51.6 E6	4 556 E3
W24 X 76	608.0	14 452	874 E6	34.2 E6	3 277 E3

4.3 Modelling assumptions

The 2D analyses were performed using the Ruaumoko nonlinear dynamic analysis computer program (Carr, 1996). Only one exterior frame was modelled since the interior frames were simply connected.

A bilinear inelastic model was introduced to model the rotational hysteretic hinging at beam and column ends. Each member was assigned a plastic hinge length of 90% of its depth at each end, based on parametric analyses that showed that on average such a plastic hinge length yields reasonable values of the maximum computed moment at section ends.

A strain hardening ratio of 2 % is used and, as it will be further discussed in the paragraph presenting the results, a plastic rotation of $\theta = 0.03$ rad after which local buckling occurs, is considered a failure criteria for steel sections. At failure, a value of $M_{ult.} = 1.2\ M_p$ is considered reasonable, and is used here to obtain the strain hardening of 2 %. Equation (4.1), gives the expression of the strain hardening ratio r, assuming the length of the plastic hinge h to be equal to d.

The bilinear model is summarized in Figure 4.2. In this figure, $0.2\ M_p$ represents the moment increase due to strain hardening whereas θ_p is the plastic rotation corresponding to failure of the section.

The same equation can be expressed according to maximum plastic curvature by defining $\phi_p = \theta_p/d$.

$$r = \left(\frac{0.2\ M_p}{(\theta_p / d)} \right) \bullet \left(\frac{1}{EI} \right) \qquad (4\text{-}1)$$

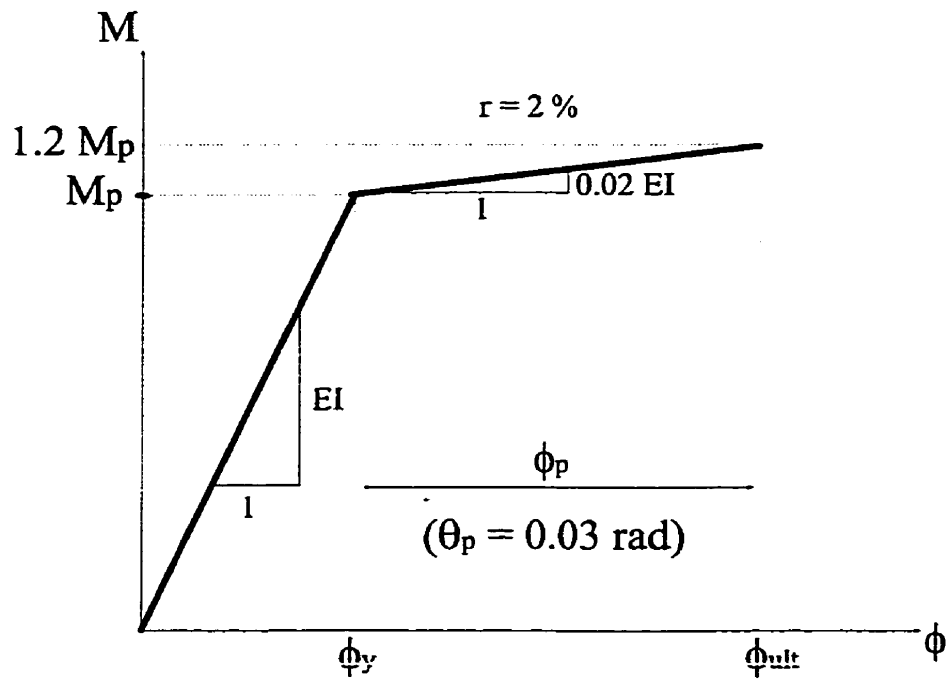

Figure 4.2 : Bilinear inelastic M-ϕ model

Shear deformations in panel zones were ignored, and only the response of the bare frame was included. The columns were assumed fixed at the ground level. A Rayleigh type damping of 5% critical was assigned based on the first two elastic modes of vibration of the structure.

To account for the combined effect of axial loads on the flexural strength, P-M interaction curves, such as defines by the LRFD (1993) code are introduced in the model. The curves are built using the following equations for the compression area :

$$\frac{C}{\phi \cdot C_y} + \frac{8}{9} \cdot \frac{M}{\phi \cdot M_p} = 1.0 \qquad (4\text{-}2)$$

and,

$$\frac{C}{2 \cdot \phi \cdot C_y} + \frac{M}{\phi \cdot M_p} = 1.0 \qquad (4\text{-}3)$$

where C is the compressive load, C_y the compressive axial yield force, M the moment and M_y the yielding moment. The curves intersect at values of moment $M = 0.9.M_p$ and axial load $C = 0.2\ C_y$.

For the axial tension portion of the interaction curves, a straight line is used, from the pure axial limit to the pure flexural limit, as shown in Figure 4.3.

Table 4.2 summarizes the procedure used to generate the P-M interaction curves for each section. The value of ϕ was taken equal to 1.0, since this study was more of an investigation of probable seismic behaviour, thus it was not relevant to introduce material strength reduction factors.

The plastic moment M_p, defined by equation (4-4), representing the moment necessary to plastify the complete section when the axial load is zero:

$$M_p = Z \cdot F_y \qquad (4\text{-}4)$$

where Z is the plastic section modulus, and F_y the steel yield strength.

The plastic moment for all members are computed with respect to the direction of the moment resistant frames, using the strong axis properties of the section. For the axial

direction, both the maximum tensile and compressive loads, corresponding to a complete plastification of the section are given by equation (4-5).

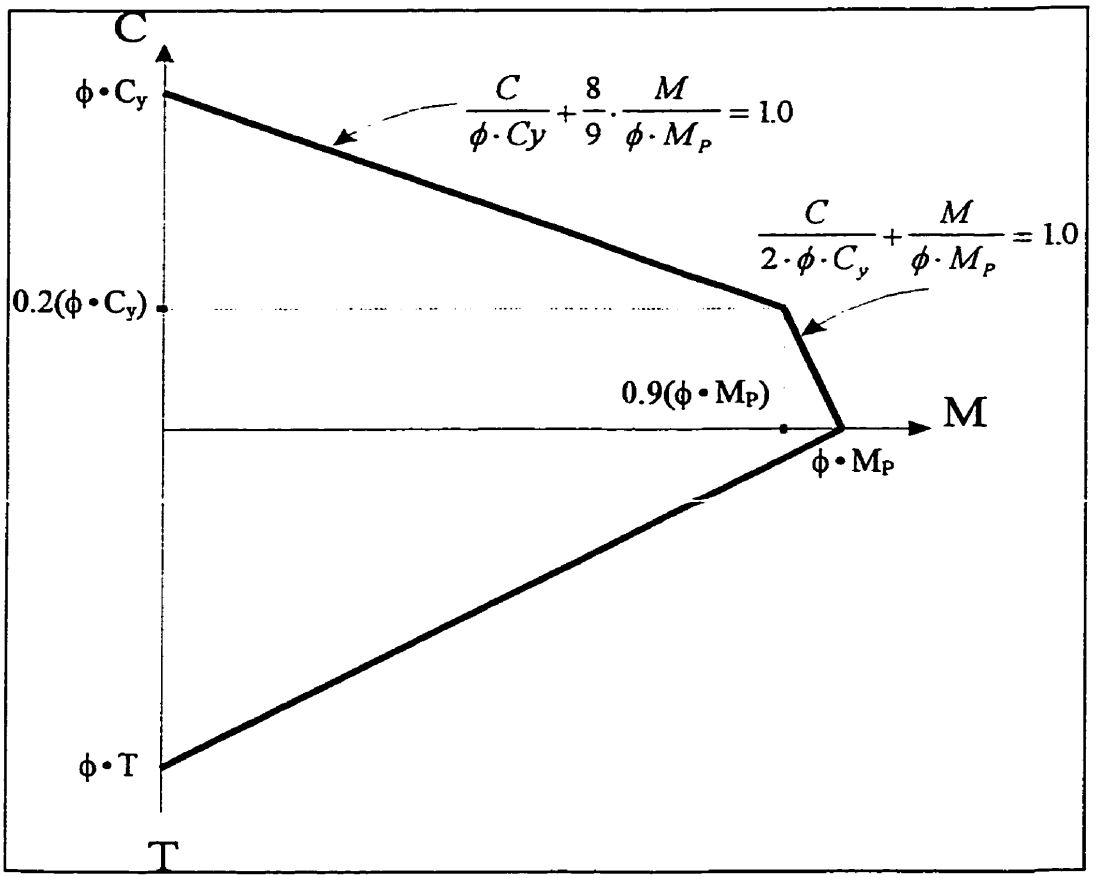

Figure 4.3: P-M interaction curve

$$\left|C_y\right| = \left|T\right| = A_S . F_y \qquad (4\text{-}5)$$

where,

C_y = compressive yield load of the section,

T_y = tensile yield strength of the section,

A_s = area of section, and

F_y = steel yield strength.

Considering these equations, the values of M_P, C_y and T_y are computed for the sections used. Results are presented in Table 4-2:

Rigid end offsets were defined to account for the actual size of the member's connections. The actual yield strength of the steel was taken at 290 MPa. Figure 4.4 illustrates the procedure used to define the rigid beam and column ends.

Table 4-2 : Strength limits of sections

External Columns	**Mp *(x10³ kN.mm)***	**C_y and T_y *(± kN)***
W14 x 193	1 687	10 627
W14 x 159	1 364	8 737
W14 x 109	912	5 987
Interior Columns		
W30 x 173	2 875	9 505
W27 x 146	2 191	8 027
W24 x 104	1 373	5 725
Beams		
W30 x 99	1 483	5 445
W27 x 94	1 321	5 183
W24 x 76	950	4 191

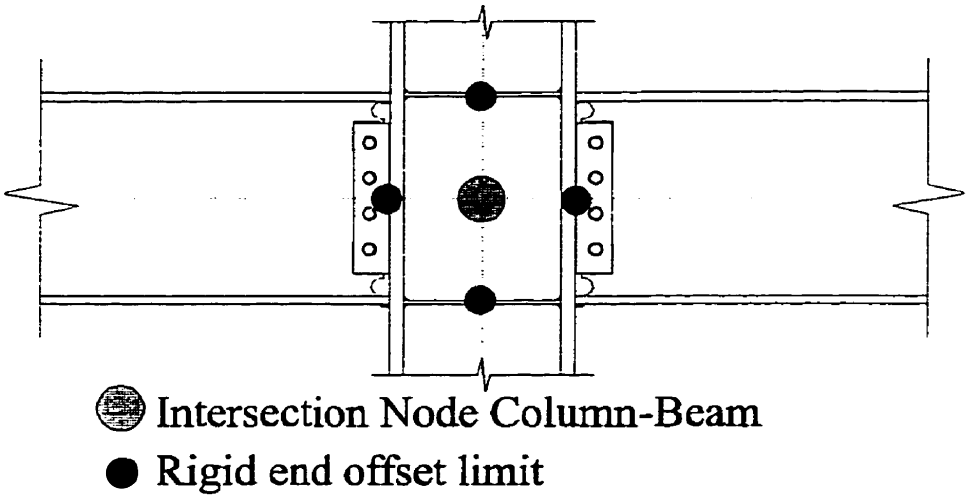

Figure 4.4 : Rigid end offsets

The analyses were performed for the total duration of each earthquake record, with a time step increment of 0.002 s. Second order P-Δ effects were included for both the frame and the interior portion of the structure. Half the building weight, and 0.5 kPa of live load were included in the seismic weights of each level. The gravity load effects caused by the interior portion of the building were taken in account by adding an external 6-story column, attached to the main building by hinged connections. At each level, the interior weight of the half the structure was added, as well as the vertical masses not included in the analyzed frame.

4.4 Characteristics of ground motions

Out of the 20 groups of accelerograms proposed by the S.A.C. steel project (Woodward-Clyde, 1997), 5 pairs of time-histories were chosen for the analyses. These accelerograms represent near-fault, extreme events, and are used to predict ground motions for a major earthquake in the Los Angeles area.

Horizontal and vertical accelerograms were used for each group. For all pairs of earthquakes, the vertical spectral acceleration peaks occur at smaller period values than those of the horizontal spectral acceleration peaks. The fundamental horizontal period of the structure was computed at T_h =1.3 s, and the vertical one at T_v = 0.09 s. For several earthquake records, the spectral ordinates at these periods are significant. Figure 4.5 shows the spectra of three selected records. Table 4.3 summarizes the characteristics of the 5 pairs of earthquake records. The records were selected to maximize the spectral accelerations at the predominant periods of the structure, in both the horizontal, S_{aH}, and vertical, S_{av}, directions.

Table 4-3 : Characteristics of ground motions.

Earthquake	*PGA Horiz. (g)*	*PGA Vert. (g)*	*Total Duration (s)*	S_{aH} for T_h = 1.3 s (g)	S_{av} for T_v = 0.09 s (g)	Ratio S_{aV}/S_{aH} at Th, Tv
NF1	0.90	0.75	50	0.85	1.30	1.53
NF13	0.62	0.85	15	1.40	2.10	1.50
NF21	0.79	0.65	40	1.55	1.90	1.23
NF23	1.68	0.72	40	4.50	1.25	0.28
NF27	0.90	0.71	40	1.90	1.25	0.66

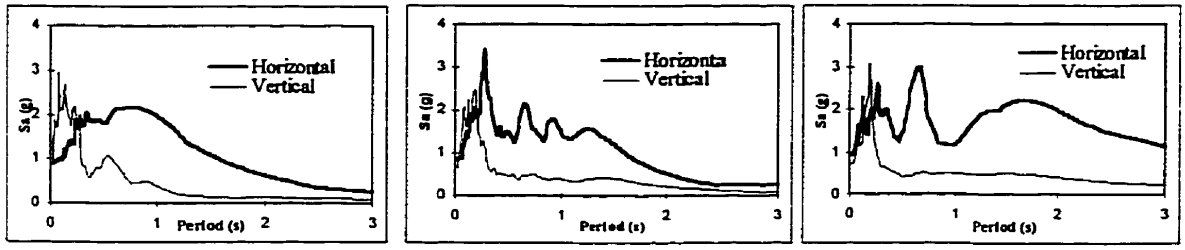

a) *b)* *c)*

Figure 4.5 : Elastic response spectra (ξ =5%):

a) NF 13, b) NF 21, c) NF 27 earthquake records

4.5 Numerical results

4.5.1 Maximum floor deflections

The envelope of maximum horizontal floor deflections is an important parameter when assessing the seismic response of buildings, since excessive deflections may cause loss of stability or excessive damage to inter-story elements. Soft story behaviour can also be detected from this parameter.

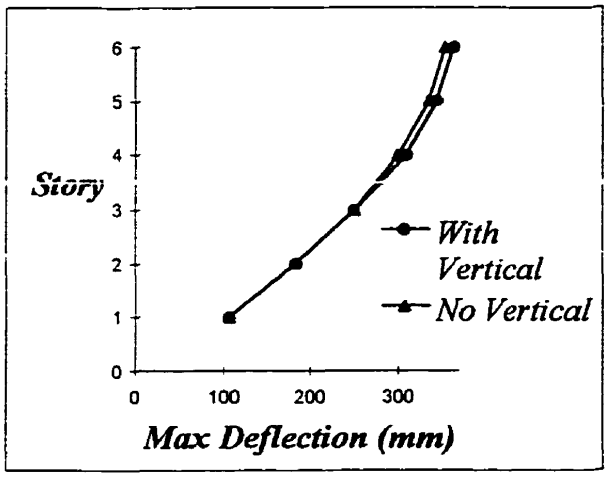

Figure 4.6 : Maximum story deflections (NF 21 earthquake)

As illustrated in Figure 4.6, the peak horizontal deflections were unaffected by the consideration of the vertical accelerations in the analysis. A maximum variation of 1 % out if all 5 records was noted, but no significant effect of the vertical accelerations could be found.

4.5.2 Rotational ductility demand in beams and columns

The rotational ductility demand, μ^{θ}, is a good indicator to characterize the severity of damage of a moment-resisting frame. Since the major energy dissipating mechanism is the

formation of rotational plastic hinges near the ends of beams and columns, this parameter is a direct measure of the structural seismic performance. The parameter μ^{θ} can be transformed into a plastic rotation by using the geometric properties of the section. It then becomes a failure criterion. Experimental data indicates that a plastic rotation of the order of 0.02 rad to 0.03 rad is sufficient to induce failure in beam-column connections.

The near-fault vertical accelerations were found to play a negligible role on the rotational ductility demand of both beams and columns (Figure 4.7). This contradicts some conclusions reported in the literature (Broderick et al. 1994), where an increase of 10 % in rotational ductility demand was attributed to the vertical accelerations.

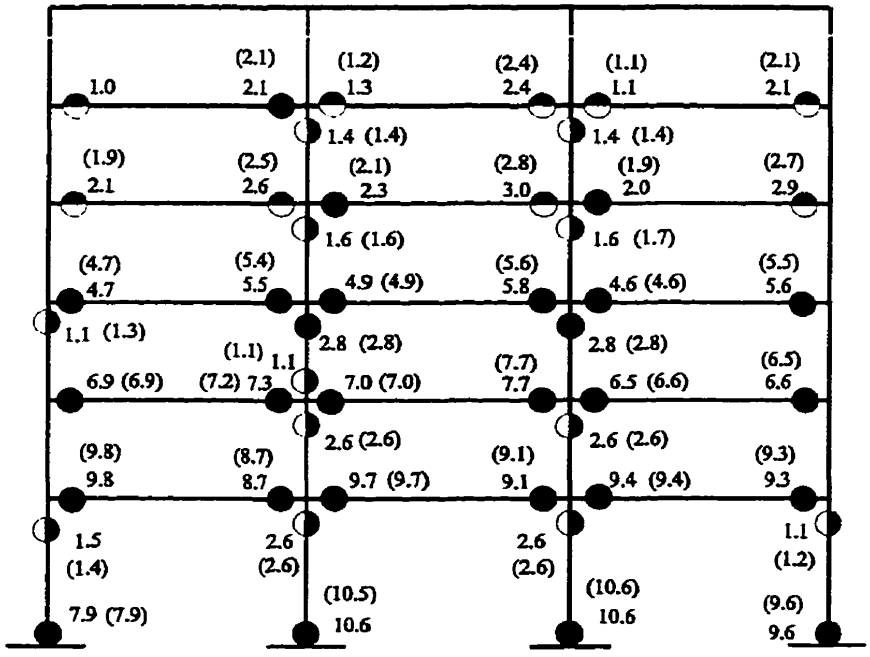

Figure 4.7 Rotational ductility demand (NF13 ground motion)

( ) : without vertical accelerations, ● : plastic hinge (both directions)

◓ : plastic hinge (one direction)

4.5.3 Axial loads in columns

The most important effect brought by vertical acceleration as noted in this study, is the increase of axial loads in columns. Figure 4.8 shows the high frequency and increase of maximum axial load, which increases to 2400 kN from an initial value of 1700 kN, when the vertical accelerations are included. In fact for both maximum compressive and tensile values, significant increases were attributed directly to the consideration of vertical accelerations in the analyses. As illustrated in Figure 4.9, compressive loads were increased by 85% on average over the 5 earthquakes for the top middle columns, reaching a maximum increase value of 115%, for earthquake NF21, where the axial compressive load reached 370 kN from an initial value of 170 kN. Tensile loads were increased by as much as 26.8% on average for top exterior columns. The mean, the maximum, and minimum axial load increases for the 5 earthquakes considered are summarized in Figure 4.9.

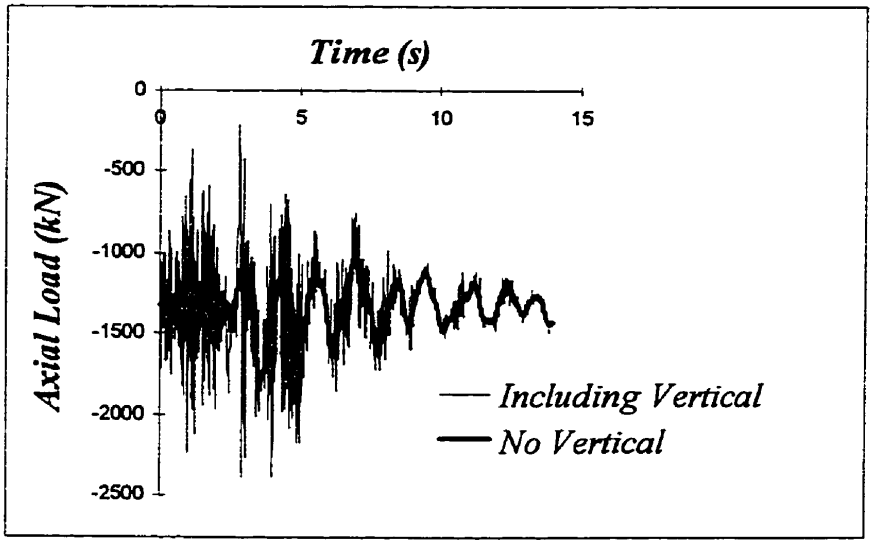

Figure 4.8: Column A : axial load time-history

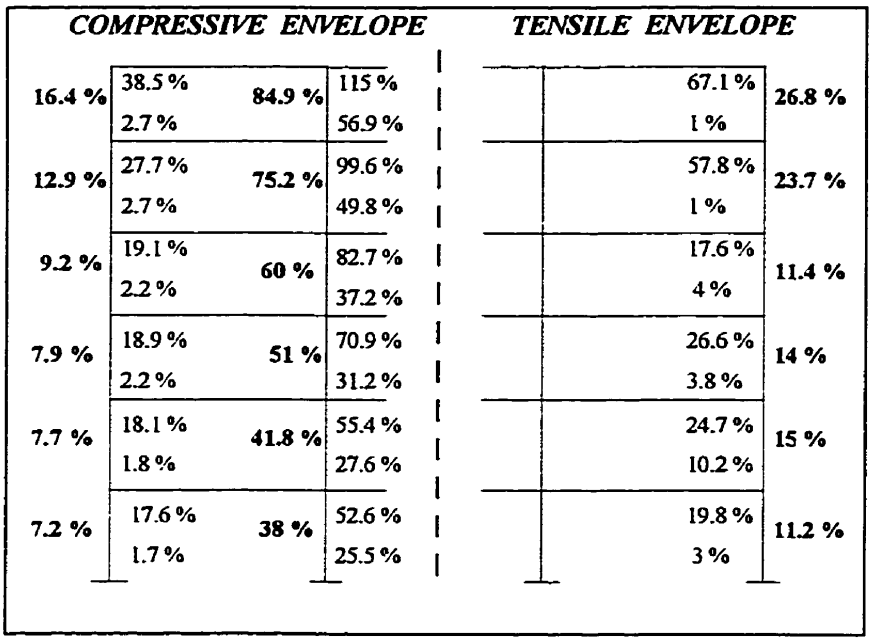

Figure 4.9 : Percentage of increase in axial loads

Bold numbers : Mean value over 5 records,

Normal numbers : Max and Min

The large increases noted for the compressive load of the interior columns of the frame is explained by the fact that design loads for these columns are not influenced as much by the overturning moments as are the exterior columns. Added to this, the vertically accelerated mass attributed to the interior columns is larger then that attributed to the exterior columns, since the tributary area of these columns is much larger.

The increase in maximum column axial loads is explained by the vibration of beams due to the vertical excitation. In fact, the period of the structure in the vertical direction is very close to the periods of large vertical spectral ordinates. The vibrations induced by vertical accelerations are at high frequencies, especially at the beginning of the earthquake. As the damage to the structure progresses, the frequency of vertical

vibrations is reduced, and in some cases after major yielding of the structure has taken place, the effect of vertical accelerations becomes insignificant.

4.5.4 P-M interaction curves for columns

The sequence of instantaneous P-M values obtained from the analyses (Figure 4.10) indicate that the large increase in column axial load does not modify significantly the structural response, nor does it increase yielding in the structure. This is explained by the fact that the columns are designed for very large bending moments and have large strength reserves in the axial direction. Nevertheless, the large increase in axial loads could lead to serious inadequacies for structural systems where members are designed mainly for axial load, like for example pined-braced structures. This could be assessed in a further study.

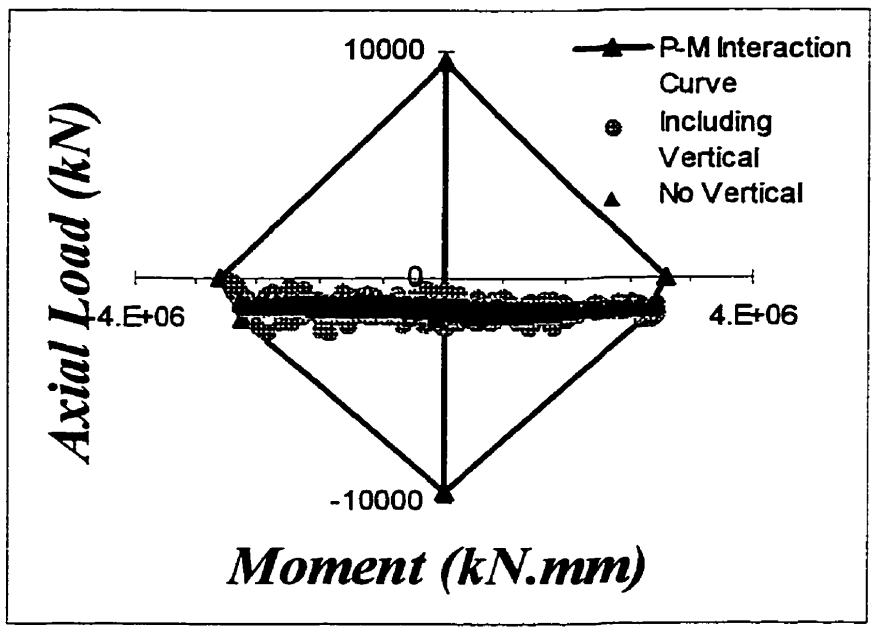

Figure 4.10 : P-M interaction for column A (see Figure 4.1) for NF1 earthquake

When considering the combined effect of vertical and horizontal accelerations, the phasing between these two solicitations must be assessed. The high frequency axial load fluctuation, attributed mainly to the vertical accelerations, and the bending moment variation at column and beam ends, attributed mainly to the horizontal accelerations, interact through the P-M interaction curves of the section.

As noted earlier, the rotational ductility demand, μ^{θ}, is unaffected by the presence of vertical accelerations despite the large increases of axial loads (Figure 4.11a). Examining more closely a single yielding phase, and plotting the corresponding time-history of the axial load, for both analysis cases, with, and without vertical accelerations, we can see that the axial load fluctuates at a higher frequency with the vertical acceleration (Figure 4.11b and Figure 4.11c). The mean value of the axial load during this phase is equal to the value of the static load. In fact, during a single flexural yielding phase, the axial load oscillates around the value of the static axial load of 1450 kN, spanning from a minimum value of 1150 kN in the first half of the yielding phase, to a maximum of 1900 kN which corresponds to an increase of approximately 30% .

During the first portion, where the axial load is decreasing, we see that when vertical accelerations are not included, the section starts yielding at a lower moment. Similarly, during the increase of the axial load in the second portion of the yielding cycle, the opposite can be observed; the section is yielding at a lower value for the analysis including vertical accelerations.

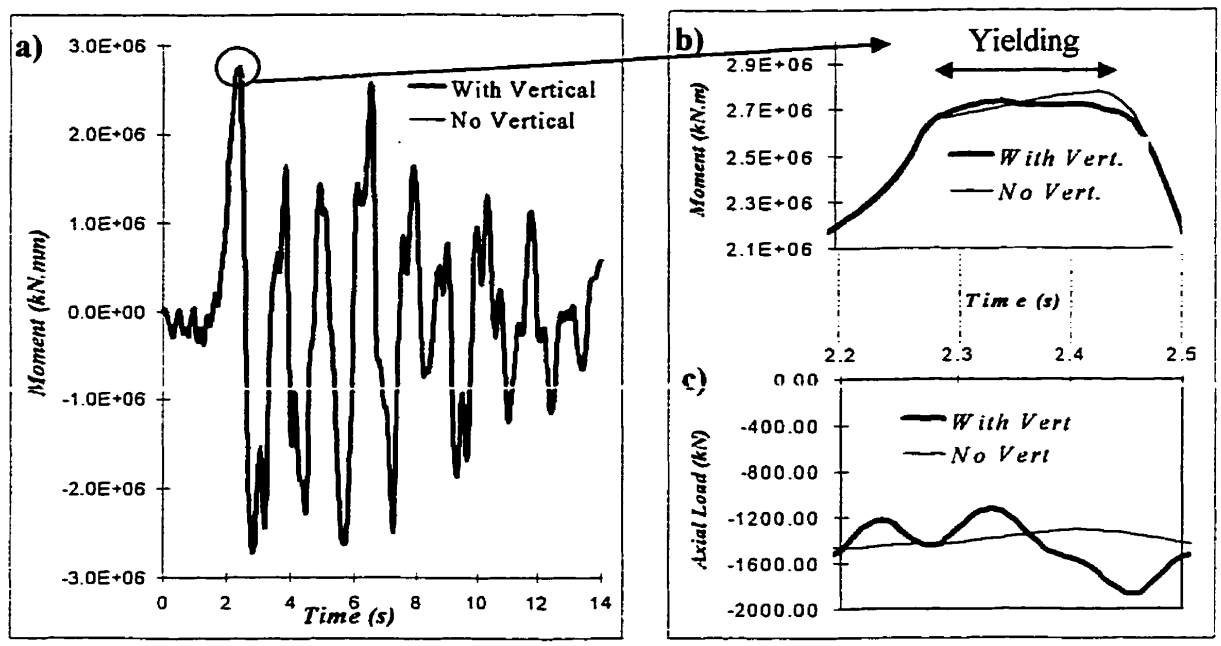

Figure 4.11 : Yielding phase :
a) Moment time-history, b) Yielding moment peak, c) Corresponding axial load.

Considering this, it could be expected that vertical accelerations may be more critical for structures which respond in the horizontal and vertical directions at approximately the same frequency. This phenomenon may be favored by time-histories where the predominant periods of ground motion in the horizontal and vertical directions are similar.

4.5.5 Strain rate

One of the most important characteristics of the high frequency vertical accelerations, is the increase in strain rate. It is well known that high strain rates affect the material properties of steel, increasing the elastic limit, thus increasing the plastic moment that a given section is able to develop. In classical capacity design approach, weld connections are designed according to the plastic moment, which is in fact the maximum theoretical moment that they have to carry. The strain rate effect increases the plastic moment. This can lead to brittle fractures in the connection weld, since welds are designed based on ultimate strength F_u which is not influenced as much by strain rate effects (and are usually of high strength brittle material).

To assess the effect of vertical accelerations on this potential failure mechanism, strain rate time-histories were computed, for typical beam element, by multiplying curvature time-histories at the beam ends, by the lever arms of the sections (Figure 4.12), and for a typical column element by using the axial strain time-history (Figure 4.13). With the absolute values of the strain rate time-history, and using the equation proposed by Wakabayashi et al. (1984), an estimate of the dynamic yield strength, F_{yd} time-histories can be calculated :

$$\frac{F_{yd}}{F_{ys}} = 1 + 0.0473 \cdot \log\left(\frac{\dot{\varepsilon}}{\dot{\varepsilon}_0}\right) \qquad (4\text{-}6)$$

where F_{yd} is the dynamic yield strength at a strain rate of $\dot{\varepsilon}$, and F_{ys} is the quasi-static yield strength under a strain rate of $\dot{\varepsilon}_0 = 50 \times 10^{-6}$ /s.

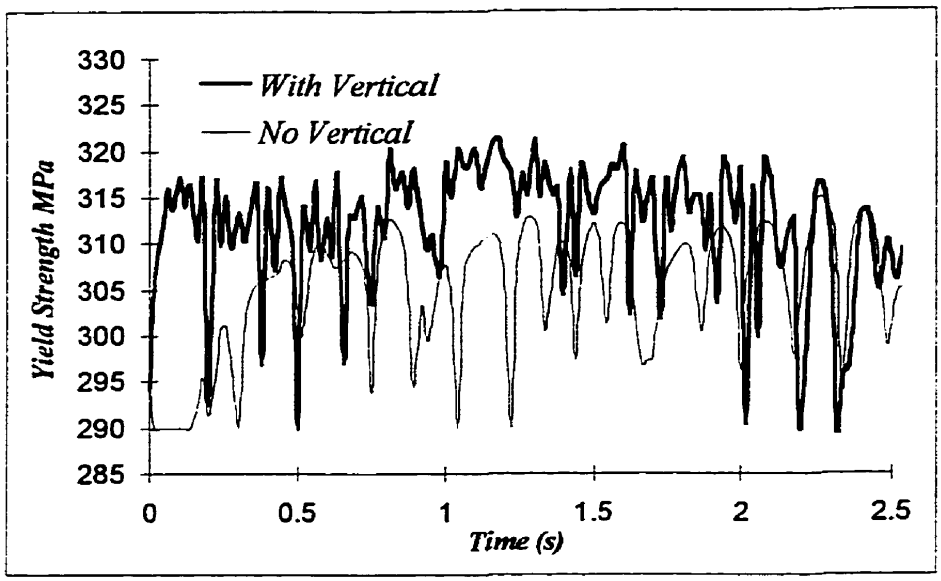

Figure 4.12: Yield strength, beam B under NF13 earthquake (see Figure 4.1)

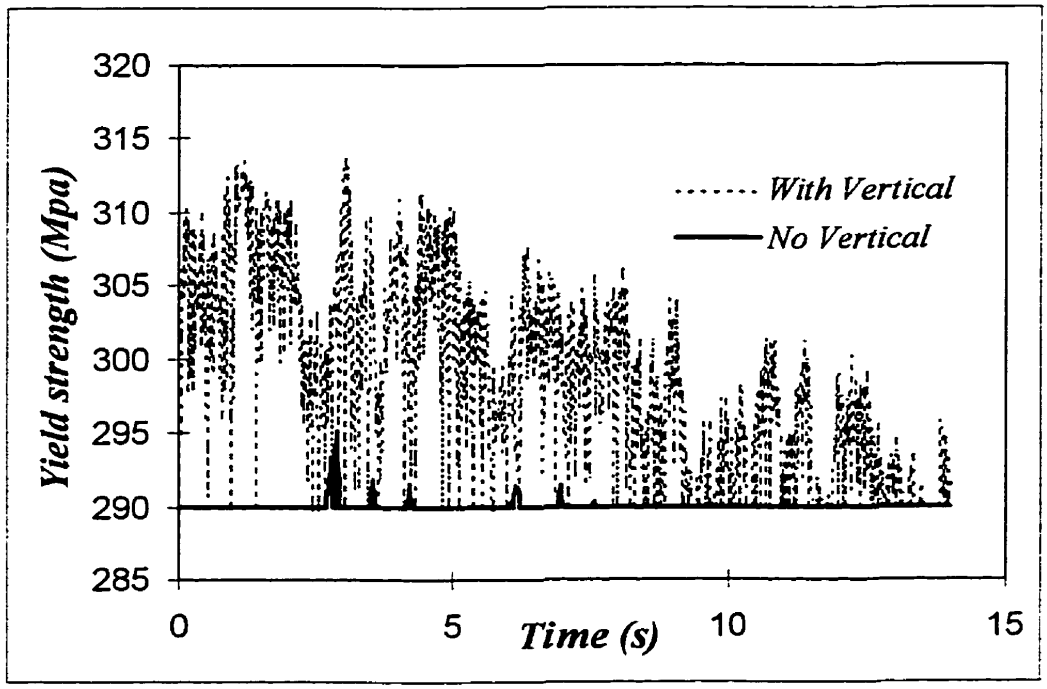

Figure 4.13 : Yield strength, column A under NF 13 earthquake (see Figure 4.1)

Figure 4.12 shows that on average the yield strength is increased from 290 MPa to 315 MPa with a maximum value of 320 MPa, which corresponds to a 10 % increase. This increase is more important at the beginning of the shaking, when the structure is still in the elastic range. In fact for the first 2 to 3 seconds, the yield strength is notably high when the vertical accelerations are included. Even when only the horizontal acceleration is used, high strain rate spikes can be observed. With the vertical acceleration, high strain rates are maintained constant at high values for a longer period of time. It is thus more probable that when a peak horizontally induced solicitation occurs, the steel will exhibit a higher yield strength, thus favoring brittle weld failure.

4.5.6 Mid-span beam vertical accelerations and deflections

Results obtained earlier show that, although vertical accelerations induce important beam vibrations at mid-span, they do not significantly affect the demand in rotational ductility at the beam-column connections. Nevertheless, important beam vibrations can cause important non structural damage, and can also represent great danger for occupants of buildings during earthquakes.

The excessive deflections, but especially the impressive vertical accelerations felt at mid-span especially for the higher stories, could cause human injury, tumbling of furniture and other appliances.

Figure 4.14 shows the vertical accelerations obtained at mid-span of the 5th story middle beam under the NF13 earthquake. We can see that the acceleration reaches a maximum value of 1.75 g, and multiple cycles with amplitudes equal to or superior to the gravitational acceleration can be observed during the earthquake. It can clearly be understood, that such accelerations acting in the upwards direction theoretically cause every unattached object to "float" for a small amount of time. This seems to offer an

explanation to why many earthquake survivors report having felt important vertical accelerations.

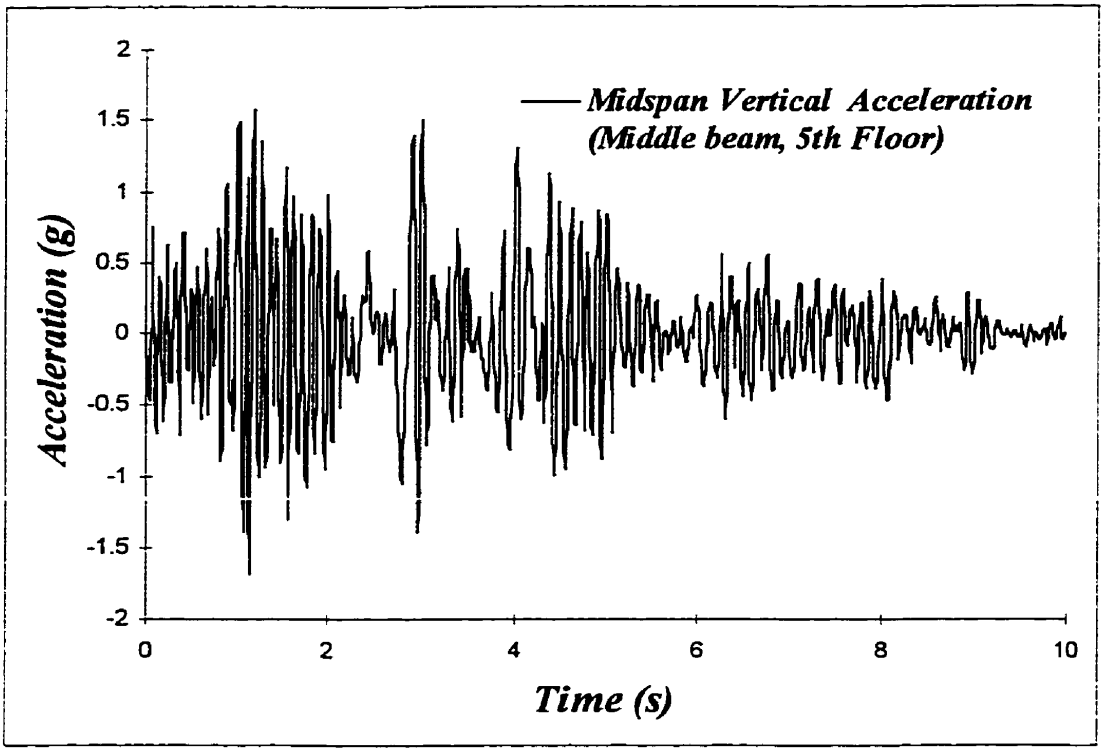

Figure 4.14: Mid-span vertical beam accelerations (NF 13 earthquake)

Examining the beam mid-span deflections shown for the same location in Figure 4.15, we see that they do not reach excessive values as could be expected from the important accelerations that are observed. A maximum beam deflection of 12.5 mm, corresponding to a value of L/560 was achieved. This is consistent with the fact that the vertical accelerations are a high frequency solicitation, thus yielding small displacements.

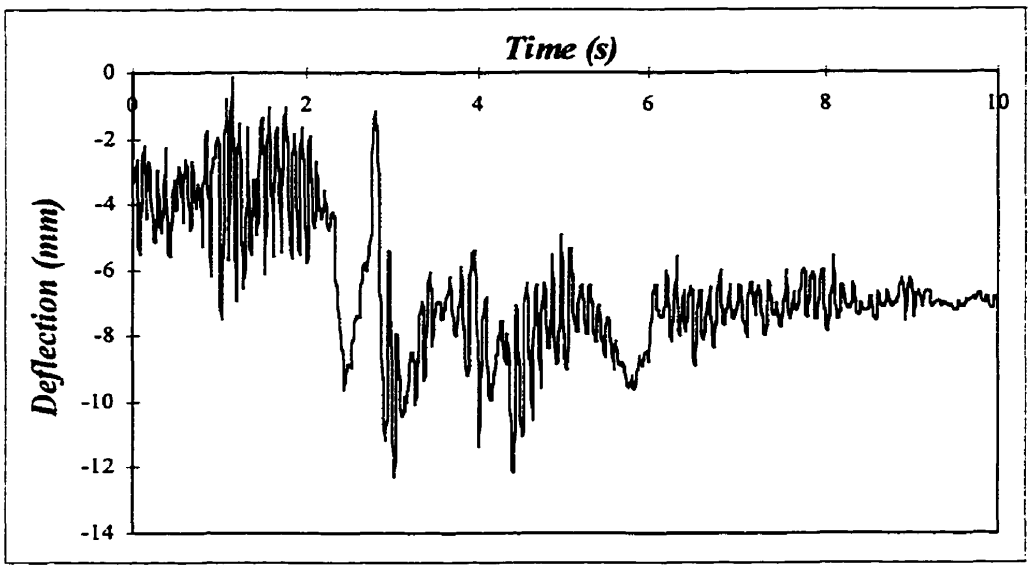

Figure 4.15 : Mid-span vertical beam deflection (middle beam 5th floor) for NF 13 earthquake

4.6 Conclusion

Based on the results of inelastic dynamic analyses on a 6-story moment resisting frame obtained in this study, the following conclusions can be drawn :

1) The analyses show that the effect of vertical accelerations on steel moment resisting frames is more important when the structure is responding in the elastic domain. As the yielding progresses the effect of vertical accelerations is filtered out, and becomes insignificant.

2) The numerical results obtained in this study show that the effect of vertical accelerations on the seismic response of moment-resisting frames is negligible in a general sense under near-fault ground motions. In fact, the demand in rotational ductility and the

maximum story deflections, which represent the major indices to assess the seismic performance of such structures, are not sensitive to vertical accelerations.

3) Substantial increases in axial loads were directly attributed to vertical accelerations. These increases reached higher values for the interior, top story columns. These axial loads did not induce instability or yielding problems for the structure, mainly because elements are designed for high moments, thus have large strength reserves in the axial direction. These increases may represent a critical factor for other types of structures, like for example pinned-braced structures, where the elements work mainly as truss elements and bare larger axial loads.

4) Examining the yield phases, it is noted that due to the high frequency of the vertical accelerations, the axial load is both slightly increased and diminished during a single flexural yielding phase when the vertical accelerations are included in the analysis. The effect of vertical accelerations may therefore be more important when the response in the vertical and horizontal directions are in phase with similar frequency content. This behaviour could be favored by ground motions with similar predominant periods in both directions.

5) The vertical accelerations substantially increase the strain rate, consequently increasing the probable yield strength of the base material, and therefore favoring the occurrence of brittle weld failures.

6) Significant vertical accelerations of floor beams were computed during the analyses. This would induce serious shaking of occupants, as well as non-structural damage to delicate equipment (computers, laboratories...).

CHAPTER 5

Analysis of a Sliding Structure Subjected to Horizontal and Vertical Ground Motion

5.1 Introduction

The evaluation of gravity dam safety throughout North America has sparked great interest in the definition and choice of accelerograms to perform dynamic analyses. A great deal of information is available concerning the horizontal component ground motions, and guidelines such as those of the ACE (1990) offer engineers computational methodologies to estimate the seismic performance of such structures. Nevertheless, more recently, a debate has emerged on the importance of vertical accelerations in the assessment of dam safety. This debate was triggered by the fact that in recent ground motion records large vertical accelerations were observed. The main question is weather or not the inclusion of vertical accelerations in the analyses is significant, and if so how to define the vertical response spectrum and related accelerogram.

In this chapter, dynamic analyses are performed on a gravity dam a) to determine the importance of vertical accelerations in the overall response, b) to evaluate the adequacy of vertical ground motions generated by using the method proposed in chapter 3, and c) to assess the importance of controlling the correlation between the synthetic horizontal and vertical components when using a multi-directional time-history.

5.2 Definition of analyzed structure

The structure used in the analyses is a rigid representation of the Paugan Dam. Figure 5.1a shows the original section (adapted from Ghrib et al., 1997), while Figure 5.1b summarizes the modelization used in the analyses along with the computed loads and masses. After replacing the openings by an equivalent concrete section, it is 47.6 m in height. The trapezoidal section of the dam is 10.95 m wide at the top and 40.7 m. at the base. The reservoir level is 50.6 m above the base of the original section. Figure 5.1 shows the equivalent rigid section analyzed. The loads considered in the analyses are the dead load, W, the hydrostatic forces acting horizontally on the upstream face of the dam, H_{st}, and the uplift force acting at the base of the dam, U. The uplift force was computed using a trapezoidal shape of uplift pressure with 50.7 m of water pressure upstream, and 10 m downstream to account for the pressure induced by the flow through the opening.

In addition to these loads, the dam is subjected to seismic inertia forces through horizontal and vertical masses. The horizontal and vertical mass of the dam M, computed assuming a concrete density of 2300 kg/m^3 is 2827.4 kN.s^2/m. In the horizontal direction, the added water mass, M_{ao}, accelerated with the dam is computed using Westergaard's approach. Using equation 5-1 proposed by Chopra and Zhang (1991) the added water mass is computed as :

$$M_{ao} = 0.54 \cdot \rho \cdot h^2 = 1382.6 \quad kN.s^2 / m \qquad (5\text{-}1),$$

where ρ is the density of water, and h the upstream water level.

The effect of the water mass vibrating vertically due to the reservoir's bottom motion is neglected in this study.

To resist the applied forces, the friction provided along the dam-foundation interface is determined by using a friction angle of $\phi = 45°$, for both static and dynamic friction coefficients.

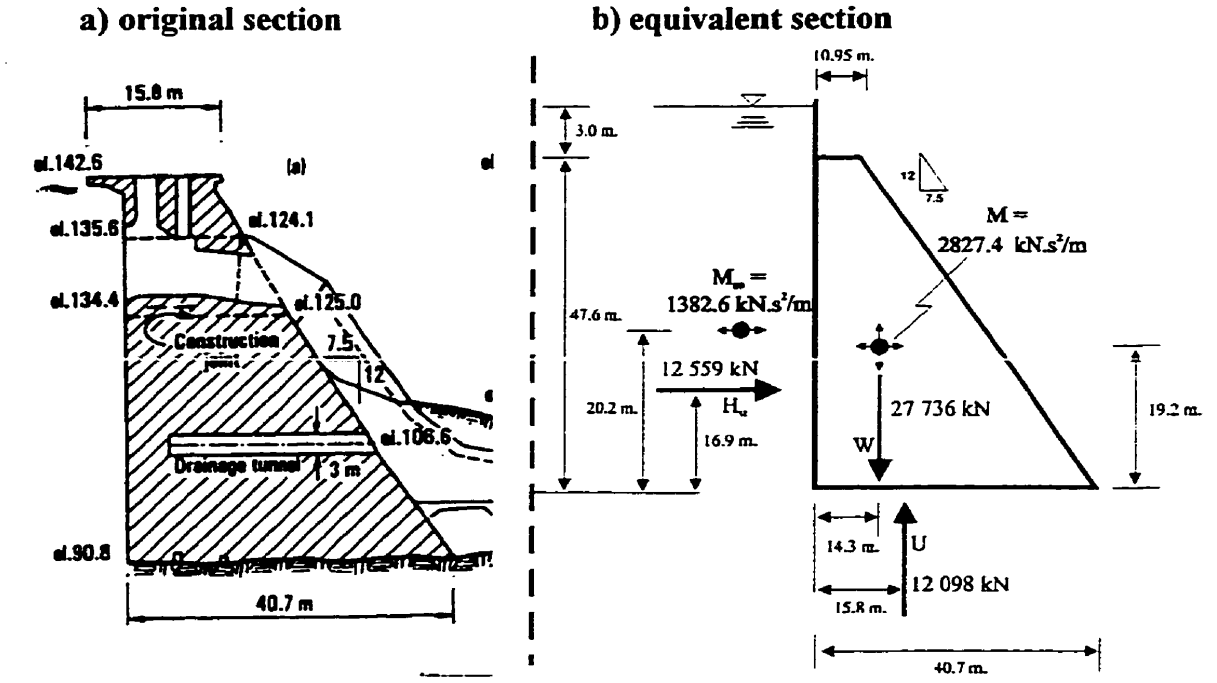

Figure 5.1 : Paugan Dam

The mobilized friction force is computed using the free body diagram of the dam and balancing all forces, when the dam is not sliding. When the dam is sliding, and neglecting vertical inertia forces, the mobilized friction force is taken as the maximum available frictional strength computed from:

$$F_R = (W - U) \cdot \tan\phi \qquad (5\text{-}2)$$

Figure 5.1 and Table 5-1 summarize the geometric properties, as well as the loads and masses of the equivalent section representing Paugan Dam.

Table 5-1 : Loads and masses (Paugan Dam)

W (kN)	*Hst (kN)*	*U (kN)*	*M (kN.s²/m)*	*Mao (kN.s²/m)*
27 736	12 559	12 098	2 827.4	1382.6

A first assessment of the dam's sensitivity to earthquake induced sliding can be obtained by computing the horizontal critical acceleration to initiate sliding without considering vertical accelerations.

Considering the vertical acceleration to be 0, thus keeping the weight of the dam W constant, the critical horizontal acceleration for inducing downstream sliding can be computed with the following equation :

$$a_c = \frac{1}{(M + M_{ao})}(\tan\phi(W - U) - H_{st}) \qquad (5\text{-}3),$$

which yields a value of $a_c = 0.731$ m/s^2 or 0.0745 g for Paugan dam.

As will be discussed in the paragraph defining the ground motions, this dam is sensitive to sliding when solicited by earthquakes corresponding to the expected horizontal peak ground acceleration of 0.25 g, corresponding to a probability of $5 \cdot 10^{-4}$ for the geographic location of the dam (Ghrib et al., 1997).

5.3 Sliding including vertical ground motions

In the analyses, since the main concern was the assessment of the safety with respect to sliding, the dam structure was considered as a rigid monolith supported without bond on a planar surface.

Since the study was not predominantly to assess the detailed response (stresses, cracking...) of the dam but more to evaluate the effect of vertical accelerations, only the downstream sliding of the dam is considered. Referring to Chopra et al. (1991), it can be drawn that downstream sliding occurs before upstream sliding and before both downstream and upstream tipping for all common gravity dams.

Seismic sliding analysis using rigid body dynamics ignores the spectral amplification that could occur when the ground motion's predominant period is close to the predominant period of the dam. However this approach still yields satisfactory results, giving a good idea of the potential sliding that could occur when the dam is solicited by an earthquake.

The equations developed by Chopra (1991), which consist of treating the problem as a time history of pseudo-static responses, is a simple and reliable way to compute the sliding response of rigid bodies subjected to seismic accelerations.

The SIV computer program was developed within the scope of this research project to assess the downstream sliding of rigid gravity dams under combined horizontal and vertical accelerations (Christopoulos 1998).

The program computes at every time step the downstream sliding critical acceleration, and compares it with the input seismic acceleration. The weight of the structure fluctuates

since it is affected by the vertical seismic accelerations according to equation (5-4), thus yielding a time dependent critical acceleration.

$$W(t) = M.(g + a_v(t)) \qquad (5\text{-}4)$$

where $a_v(t)$ is the vertical ground acceleration at time t.

During the analyses, an upward vertical acceleration spike exceeding the value of the gravitational acceleration g is possible. To avoid numerical instability caused by the floating state of the structure, the value of $(g+a_v(t))$ was limited to a minimum value of 0.000001 where g and $a_v(t)$ are expressed in m/s^2. The program SIV then indicates a floating state by a warning to the user.

As long as the critical downstream sliding acceleration is not exceeded, the dam is responding in "stick mode", no sliding is occurring, and the horizontal acceleration of the rigid block is equal to the horizontal ground acceleration. When the critical acceleration, at a given time step, is exceeded by the horizontal ground acceleration, the rigid block starts sliding and the sliding mode is engaged.

The program does not permit upstream sliding, thus sliding can only occur if the downstream critical acceleration is exceeded. The critical acceleration, a_c, which corresponds to the acceleration at which the soliciting inertia forces added to the hydrostatic forces are greater then the available resistance provided by friction on the base surface, can be computed, taking in account both components , horizontal and vertical, by the following equation :

$$a_c = \frac{\left[M.(g + a_v(t)) - U\right].\tan\phi - H_{st}}{(M + M_{ao})} \qquad (5\text{-}5)$$

When a_c is exceeded, the rigid block is in motion, and the following dynamic equation of equilibrium must be satisfied at each time step :

$$\left(M + M_{ao}\right).\ddot{s}(t) = -M.a_h(t) + H_{st} - H_d - F_R \qquad (5\text{-}6)$$

where $\ddot{s}$ is the sliding acceleration of the block, H_d the hydrodynamic forces computed using Westergaard's added mass of water, and F_R the maximum values of available friction on the dam surface.

Changing this equation around and introducing the two input parameters $a_h(t)$ and $a_v(t)$, respectively the horizontal and vertical ground accelerations, we have :

$$\ddot{s}(t) = -a_h(t) + \frac{(H_{st} - \left[M.(g + a_v(t)) - U\right].\tan\phi)}{(M + M_{ao})} \qquad (5\text{-}7)$$

A Newmark $\beta = 1/6$, linear acceleration step-by-step scheme was used to compute sliding velocity and displacements:
Within a time step h, delimited by the initial point with the subscript 0, and the final point with the subscript 1, the variation of the sliding acceleration, $\ddot{s}$, after a time τ is obtained with the following equation:

$$\ddot{s}(\tau) = \ddot{s}_0 + \left(\frac{\ddot{s}_1 - \ddot{s}_0}{h}\right).\tau \qquad (5\text{-}8)$$

The sliding velocity, $\dot{s}$, and sliding displacements, s, are given respectively by equations (5-9) and (5-10):

$$\dot{s}_1 = \dot{s}_0 + \frac{h}{2}.(\ddot{s}_0 + \ddot{s}_1) \tag{5-9}$$

$$s_1 = s_0 + \dot{s}_0.h + \ddot{s}_0.\frac{h^2}{3} + \ddot{s}_1.\frac{h^2}{6} \tag{5-10}$$

Once sliding is instigated, it will only stop if two conditions are met:

a) the horizontal acceleration is inferior to the critical acceleration, and

b) the sliding velocity at the end of a time step is negative.

When both conditions are met, the rigid body falls in stick mode, and a correction is added to the previous time step displacement. The correction takes in account that during a time step where at the end the velocity is computed negative, a certain amount of sliding occurs before the velocity becomes negative. As can be noted in Figure 5.2, the amount of sliding that must be added is that which occurs during the h_a portion of the time step h.

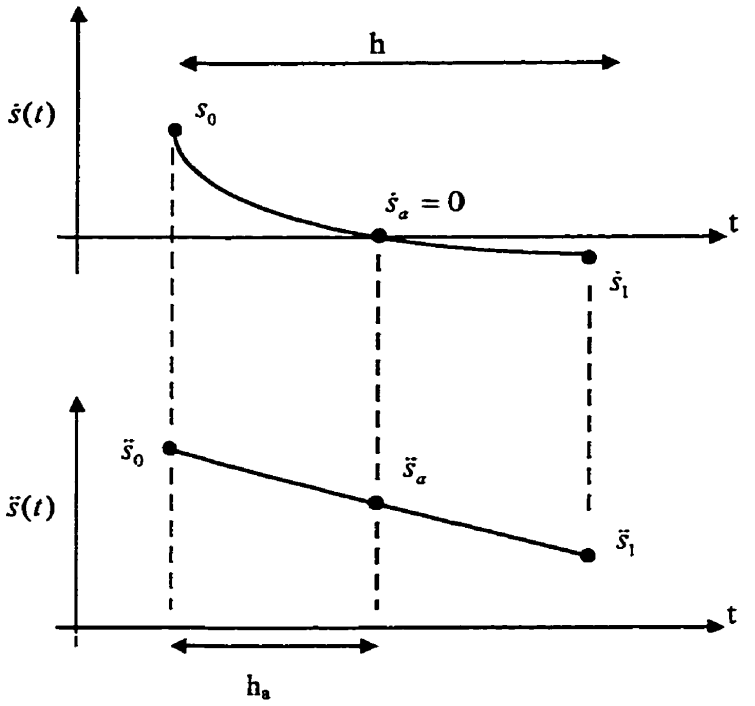

Figure 5.2 : Correction of displacement

Referring to equations (5-8), (5-9) and (5-10), and putting the velocity $\dot{s}_a$ equal to 0 at time h_a, we can express h_a in the following manner :

$$h_a = -\frac{2 \cdot \dot{s}_0}{(\ddot{s}_0 + \ddot{s}_a)} \qquad (5\text{-}11)$$

Defining A as the slope of the acceleration $\ddot{s}(t)$ during the time step h , such as

$$A = \frac{\ddot{s}_1 - \ddot{s}_0}{h} \qquad (5\text{-}12)$$

the value of $\ddot{s}_a$ can be obtained with the following equation :

$$\ddot{s}_a = \sqrt{(\ddot{s}_0)^2 - 2 \cdot A \cdot \dot{s}_0} \qquad (5\text{-}13)$$

Having established $\ddot{s}_a$, the correction to be added to the sliding displacement, s_{cor}, can be computed with the following equation :

$$s_{corr} = (\dot{s}_0 . h_a) + (\ddot{s}_0 . \frac{h_a^2}{3}) + (\ddot{s}_a . \frac{h_a^2}{6}) \qquad (5\text{-}14)$$

The program uses the above mentioned procedure to compute the instantaneous, and total cumulative sliding of the dam structure.

The program also computes the sliding safety factor, F_s, defined in equation (5-15) at each times step. The safety factor time-history, $F_s(t)$, is another indicator of sliding potential during an earthquake. This factor is often preferred to the evaluation of the total sliding, because in terms of safety, this factor should always be greater then 1, if sliding is to be avoided. It is difficult, and quite peculiar to interpret what a computed value of total sliding displacement could mean in terms of safety of a dam. It is more common to target an acceptable safety factor then an acceptable residual sliding displacement value.

$$F_s = \frac{F_{Resisting}}{F_{Soliciting}} = \frac{\left[M \cdot (g + a_v) - U\right] \cdot \tan\phi}{(M + M_{ao}) \cdot a_h + H_{st}} \qquad (5\text{-}15)$$

Computing the position of the resultant of vertical forces at the base of the dam is also a good indicator of the stress distribution at the base of the dam. When the resultant is centered, it is an indicator of more uniformly distributed compressive stresses on the base. When the resultant, computed by equilibrium of moments, is moved towards the

downstream side of the dam during an earthquake, tensile stresses could be initiated upstream promoting crack propagation along the base.

To evaluate the effect of vertical accelerations on this safety indicator, the position of the resultant, d, is computed at each times step. This value, is then normalized by the length of the base in such a way that the value varies from -1 when the resultant is at the furthest point upstream, to +1 when it is at the furthest point downstream, and yields a value of 0 when it is located in the middle of the base, as illustrated in Figure 5.3.

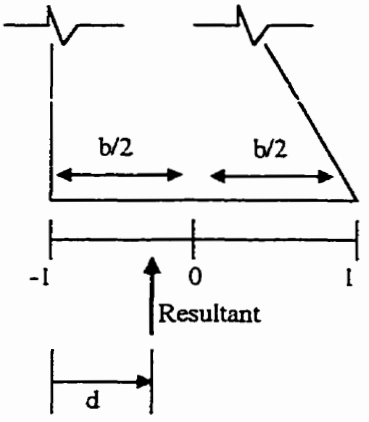

Figure 5.3: Position of resultant

The position of the resultant, d, measured from the upstream corner of the base is computed with the following equation for the Paugan Dam :

$$d = \frac{16.9H_{st} - a_h \cdot (20.2M_{ao} + 19.2M) + (14.3M(g + a_v)) - (15.8U)}{(M \cdot (g + a_v) - U))} \qquad (5\text{-}16)$$

Once the distance d is computed, it is transformed as a fraction of the base, b, and expressed with reference to the middle of the base. This transformed position of the resultant p, is computed according to equation (5-17).

$$p = \frac{(d - \frac{b}{2})}{b/2} \qquad (5\text{-}17)$$

The position of the resultant could be used as an indicator of whether or not the face of the dam will experience, during the earthquake, tensile stresses at either end. The most important measure is the maximum position of the resultant when it is moved downstream. When it exceeds the middle third, tensile stresses (crack) develop at the upstream face. The value corresponding to the middle third of the base, in terms of parameter p defined by equation (5-17), is p = ± 1/3. Moreover if the position of the resultant is outside of the base, important rocking motions could take place, indicating potential overturning instability.

To assess the correlation of the two components of the ground motion used in the analyses, the peak correlation factor (PCF) defined in Chapter 3 is also computed in the program, at every time step. On the time-history of the PCF, the maximum value, mean value, as well as the number of time steps where the PCF is greater then 0.05 are also computed.

A copy of the Turbo Pascal code, of the SIV computer program (SIV.pas) is included in appendix A.

5.4 Choice of historical and synthetic ground motions

The analyses of the Paugan Dam were performed for two types of ground motions: historical records, and synthetic accelerograms. The study focuses mainly on the Canadian seismic environment, which consists of two distinct regions with different characteristics for Eastern and Western Canada. For each of these regions, six pairs of horizontal and vertical historical earthquakes were chosen amongst the records presented in Chapter 3 from the McMaster data bank. For the Eastern region, earthquakes were taken from the high a/v group, whereas for the western region earthquakes from the intermediate and low a/v groups were used.

Synthetic accelerograms were generated using the velocity response spectra compatibility option of the SIMQKE (1976) program. At first, the mean horizontal spectrum, for each of the two groups, was derived from the historical accelerograms. These spectra were used to generate six horizontal accelerograms for each group. For the vertical synthetic motions, three different approaches were used.

The first one consisted of simply calibrating each horizontal accelerogram by 2/3 to obtain the corresponding vertical accelerogram. The second method consisted of reducing the horizontal mean target spectrum by a value of 2/3 and generating, based on this reduced spectrum, the corresponding vertical ground motion. The third method consisted of performing the shift and reduction method developed in Chapter 3, and using for each of the groups the values of the reduction factor R_f, and shift factor S_f derived in the statistical analyses of Chapter 3.

5.4.1 Historical records

The historical records were chosen amongst the initial McMaster data bank. Since the horizontal peak ground accelerations (PGAH) were quite scattered, all records were scaled to a PGAH of 0.25 g. The vertical accelerograms were scaled using the same scaling factor that brought the PGAH to 0.25 g, thus keeping unchanged the V/H ratio of PGA's of the historical records.

Tables 5-2 and 5-3 summarize the earthquake records chosen for each of the two groups (eastern and western). The eastern group records are particular recordings of western events that have characteristics typical to the east. This may seem paradoxal, but combining the appropriate distance to the source and magnitude, could yield earthquakes with high a/v ratio typical of eastern Canada.

Table 5-2 : Eastern group historical records

	Earthquake	Date	Location	Initial PGAH (g)	PGAV (g) corresponding to PGAH of 0.25 g
1	Helena Montana	31/10/35	Carrol College	0.146	0.152
2	Nahanni, Can.	23/12/85	Inverson 1	1.010	0.430
3	Oroville, CA	01/08/75	Seism. Station	0.084	0.341
4	San Fernando	09/02/71	Pacoima Dam	1.075	0.165
5	Parkfield. CA	27/06/66	Tremblor No.2	0.269	0.123
6	Lytle Creek	12/09/70	Wrightwood	0.198	0.090

Table 5-3: Western group historical records

	Earthquake	Date	Location	Initial PGAH (g)	PGAV (g) corresponding to PGAH of 0.25 g
1	Kern County	21/07/52	Taft Linclon	0.179	0.146
2	Mexico City	19/09/85	El Suchil	0.105	0.120
3	San Fernando	09/02/71	3470 Wilshire	0.132	0.106
4	San Fernando	09/02/71	3550 Wilshire	0.132	0.104
5	San Fernando	09/02/71	4680 Wilshire	0.117	0.140
6	Mexico City	19/09/85	La Villita	0.123	0.119

The mean absolute acceleration spectra were plotted in Figure 5.4 and Figure 5.5 for both the horizontal and vertical ground motion components. Comparing with the entire group spectra presented in Chapter 3, we can see that they remain quite similar.

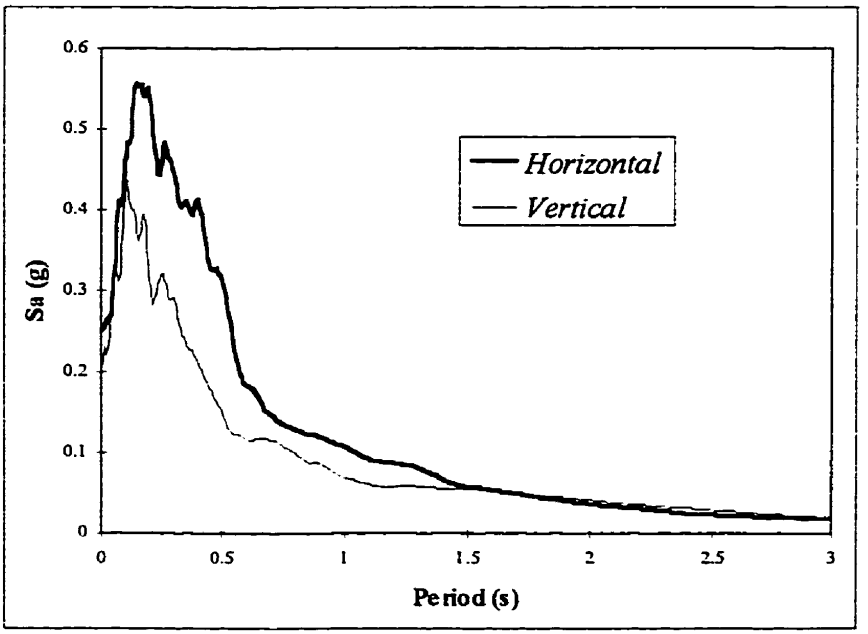

Figure 5.4: Eastern group mean acceleration spectra

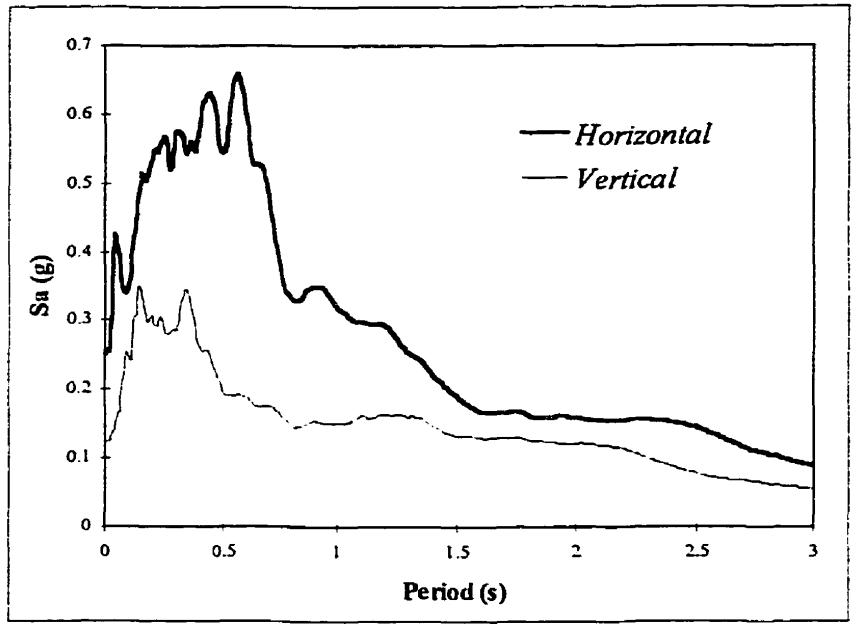

Figure 5.5: Western group mean acceleration spectra

5.4.2 Synthetic records

5.4.2.1 Horizontal Accelerograms

Six horizontal accelerograms were generated for each group, using the mean spectra derived from the historical earthquakes of each group. All six earthquakes were generated from the same response spectrum, with the SIMQKE (1976) program. Each earthquake is unique because the seed number is changed before each generation.

One of the most sensitive points when generating synthetic ground motion with SIMQKE is surely the duration that the user specifies when defining the intensity function. SIMQKE is sensitive to short durations on one hand, and on the other hand an effort to respect the historically observed duration must be made. For the western earthquakes, it is much easier to respect both criteria, but for eastern earthquakes, the short durations cause some hardship. The difficulty lies in choosing a duration that does not cause numerical problems in the program but is the shortest possible. The method used to attain

this, is plain trial and error. After three iterations, in which the time function was changed, and the durations computed and compared with the mean historical durations, a final intensity function was chosen.

Further in this chapter, in Tables 5-10 and 5-11, the computed duration indices for both groups of earthquakes are presented.

It is interesting to note here, that during these iterations some observations were made concerning the effect of changing the duration of synthetic motion. In fact, two phenomena control the effect of the duration on the structural response. The first, is that when the duration is reduced, the number of time steps at which the structure can slide is reduced, almost proportionally to the reduction of the duration of strong motion. The second, is the fact that the target spectrum remains unchanged when the duration is modified. To respect the same target spectrum, with a shorter duration, implies a greater amount of energy in a shorter duration earthquake than a longer one, which in turn will increase the amount of sliding occurring in each sliding phase. It is difficult to assess which of the two phenomena will have a greater effect on the structural response when the duration is changed. Further studies should be done on this aspect.

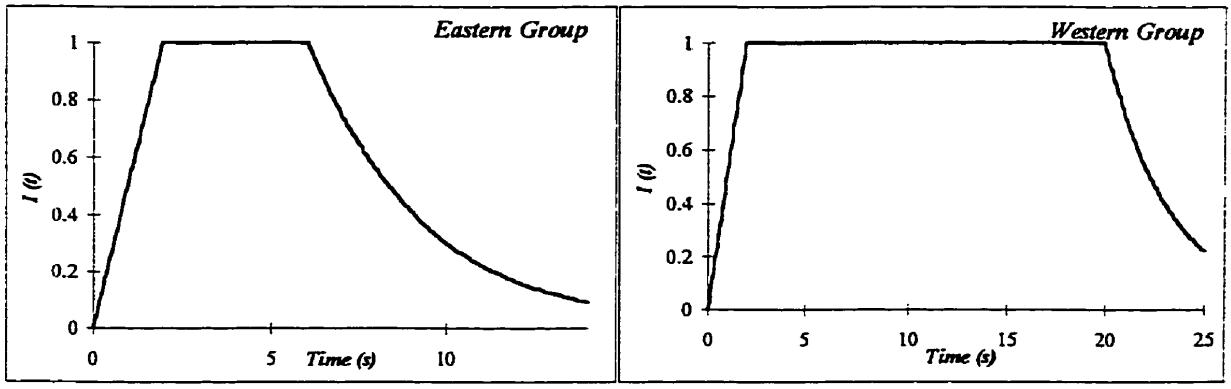

Figure 5.6 : Intensity functions for generation of synthetic accelerograms

The six eastern and six western synthetic horizontal earthquakes are called, respectively EH1 through EH6, and WH1 through WH6. The mean spectra for each of the synthetic group of time histories are given in comparison to the historical spectra in Figures 5-7 and 5-8.

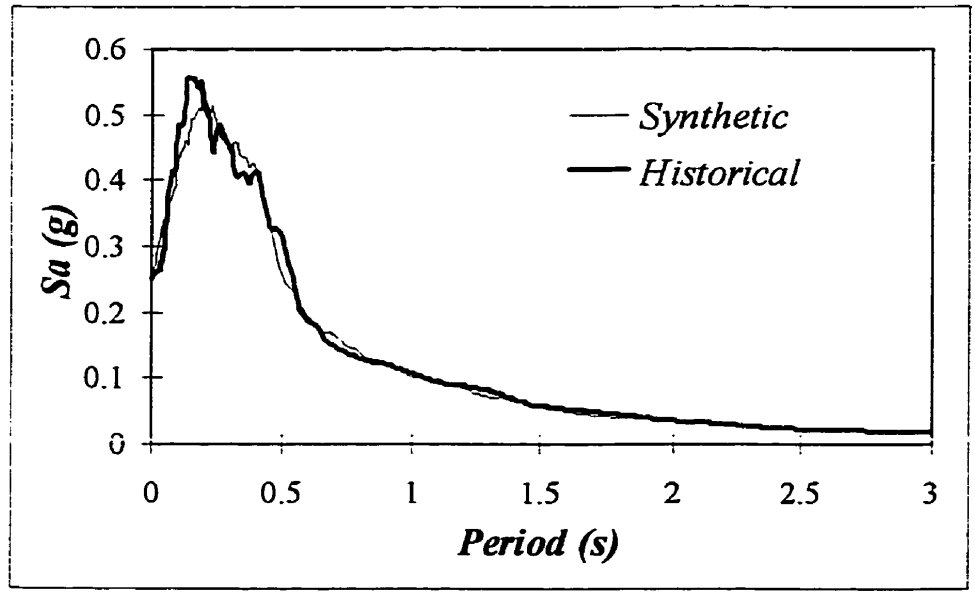

Figure 5.7 : Mean horizontal acceleration spectra : historical and synthetic eastern group

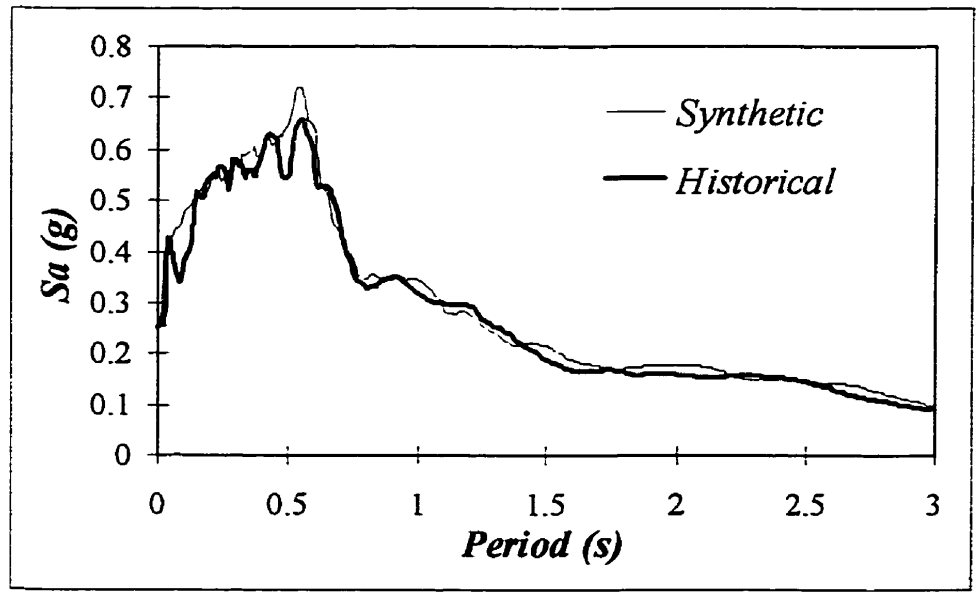

Figure 5.8: Mean horizontal acceleration spectra : historical and synthetic western group

5.4.2.2 Vertical component : calibration of horizontal time history

With this procedure each horizontal time history is simply multiplied by 2/3 to generate a vertical accelerogram. Once the vertical accelerograms are created, two load combinations are examined in the analyses :

a) a horizontal accelerogram with the vertical record that was derived from the same horizontal accelerogram, and

b) a horizontal accelerogram combined with a vertical accelerogram derived from a different horizontal accelerogram taken from the same group of earthquakes.

5.4.2.3 Vertical component : reduction of horizontal spectrum (reduced only)

This method of generation, which is also the most commonly used in practice, consists of calibrating the horizontal response spectrum to two thirds of its value to obtain the vertical spectrum. Once the vertical target spectrum is defined, the same procedure of generation with SIMQKE (1976) is used to generate the time-histories. The value of 2/3 is used because it is the most commonly accepted ratio of V/H peak ground accelerations. Although this method takes into account the lower values of vertical accelerations compared to the horizontal ones, it does not consider the difference in frequency content.

5.4.2.4 Vertical component : shift and reduced method

The method used to generate the vertical spectrum is based on the statistical analyses presented in chapter 3. This method uses a reduction factor and a shift factor on the horizontal spectrum to generate the vertical one. In this approach, the frequency content of the vertical spectrum is shifted towards the higher frequencies.

Figures 5-9 and 5-10 present for each group of earthquakes a comparison of the vertical spectra generated according to the above described methods (**a**. pondering the horizontal accelerogram, **b**. reducing the horizontal spectrum to obtain the vertical one, then

generating, and **c.** reducing and shifting the horizontal spectrum to obtain the vertical one, then generating) with the vertical target spectra.

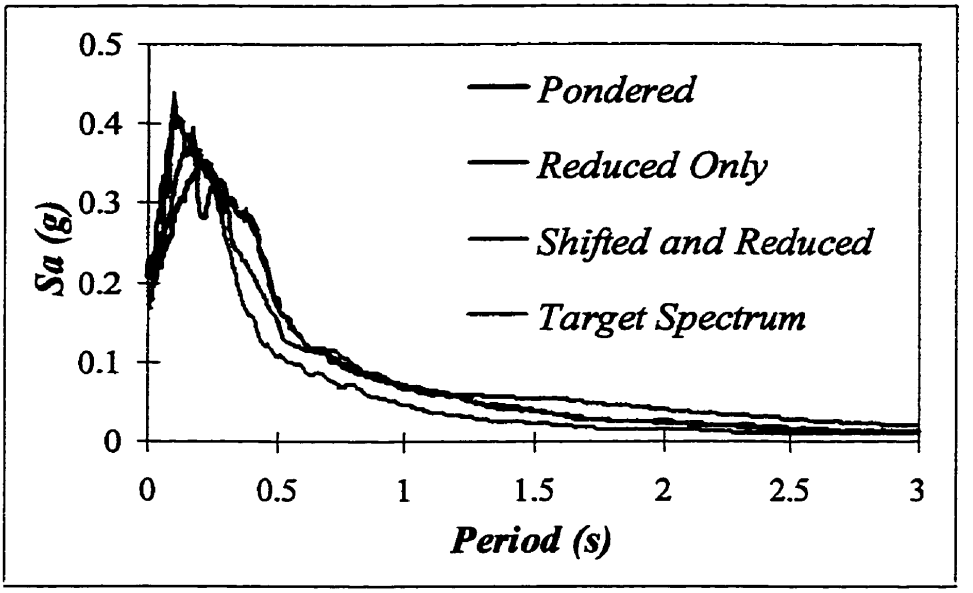

Figure 5.9 : Mean vertical spectra, for three methods of generation compared to the historical spectrum, for eastern group

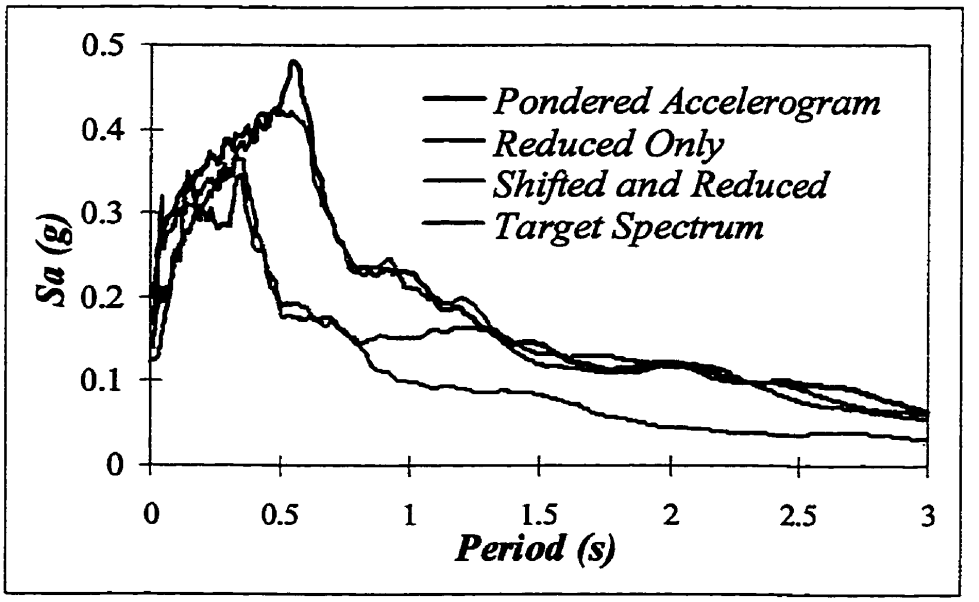

Figure 5.10 : Mean vertical spectra, for three methods of generation compared to the historical spectrum, for western group

From the results we can see that the shifted and reduced method is the one that yields the best approximation of the historical target spectrum. We can see that the shift factor forces the synthetic spectrum to fit the lower period spectral peaks that characterize vertical accelerations. The difference is more notable for the western group, since the western group horizontal predominant period is higher then the predominant period corresponding to the eastern group. We can see that the two first methods, the calibration method and the reduced only method yield a substantially overestimate the target spectrum for the western group.

5.5 Results

5.5.1 Description of results

As described in section 5.3, the SIV program computes instant sliding, total sliding, safety factor against sliding (time-history), position of resulting base force (time-history), as well as the time-history of the peak correlation factor (PCF). From these results, the minimum value of the safety factor is determined. This sliding safety factor is then compared with a sliding safety factor computed using a pseudo-static approach based on equation (5.15), where a_h and a_v are directly specified as a function of the PGAH and PGAV to avoid any time history calculation. For the PCF, the average over the accelerogram, the maximum value, as well as the number of time steps where it exceeds a predetermined value, chosen at 0.05 in this study, are computed.

The synthetic ground motion results are mostly used to evaluate the accuracy of different generation methods. They are also used to determine important factors and criteria that must be met to consider the synthetic ground motion as representative of a real earthquake bi-directional ground motion.

5.5.2 Historical earthquakes

5.5.2.1 Total Sliding

A comparison of the total sliding induced to the dam when only the horizontal ground motion is used, shows that for the western group historical earthquakes the value is much larger then for the eastern earthquakes. This is due to the difference in frequency content between the eastern, higher frequencies, and western, lower frequencies characteristics as well as the difference in duration. In fact, it has been shown by numerical analyses and experimental shake table tests (Tinawi et al. 1998) that the sliding is influenced more by the duration of acceleration pulses, which is directly related to the frequency content, than by the PGA.

The authors report that for some cases analyzed an acceleration pulse 5 times longer causes a total sliding 25 times larger, for the same PGA. A comparison is also made between eastern and western North American (ENA, WNA) earthquakes. The authors concluded that for a same value of PGA, a value of total sliding three to four times greater is expected for the WNA earthquakes.

In fact, the mean value of the total sliding for Paugan dam, as computed in this project, for the eastern group (horizontal excitation), is 11.65 mm, whereas for the western group it is 71.04 mm. This represents a total sliding 6 times larger for the western group, and this, with the same PGA of 0.25 g. The results presented in Tables 5-4 and 5-5, also show that the total sliding is substantially influenced by the presence of the vertical acceleration in the analyses for both groups.

Examining the total sliding results with vertical accelerations, for both groups, we can note once more that the value is much larger for the western group. For the western

group, the increase induced by vertical accelerations is smaller, since the mean total sliding reaches a value of 88.01 mm as compared to a value of 71.04 mm when the vertical component was omitted, representing a 24 % increase. For the eastern group, the total sliding reaches a value of 22.10 mm when the vertical accelerations are included, as compared to a value of 11.65 mm when the vertical component was omitted, which counts for an increase of 89 %.

The difference between the groups in the total sliding displacements increase due to the inclusion of the vertical excitation, can be explained by two physical phenomena that consider the simultaneous character of the bi-directional input :

a) In the eastern group, ground motion in both directions, but specifically in the vertical one, is at a higher frequency than that of the western group. This creates a " a floating state", which numerically represents the high frequency at which the weight of the structure is relieved, thus increasing the number of occurrences where sliding could be instigated. Physically this could be compared to the state at which an object placed on a home appliance machine, vibrating at a high frequency would loose all friction at the contact surface and slowly start sliding. Moreover, when the frequency content of both motions is very similar, the probability that both solicitations will be in phase is greater, which can lead to larger sliding displacements attributed directly to the presence of the vertical acceleration. This point is more thoroughly brought to light in a subsequent paragraph. The difference between the reduced (only) spectrum method, which yields horizontal and vertical time-histories with similar frequency content, and the shifted and reduced spectrum method, which accounts for the vertical acceleration's higher frequency content, are compared with the synthetic ground motions.

b) the PGAV, is greater for the eastern group then the western group since the reduction factor, R_f, derived from the statistical analyses of Chapter 3, is equal to 0.8 for the high a/v group, and only 0.55 for the intermediate and low groups.

Figures 5-11 and 5-12 show the total sliding displacements with and without vertical accelerations accumulated during the earthquake, respectively for the Parkfield (1966) California record at Tremblor, typical of the eastern group, and the San Fernando (1971) California record at 3470 Wilshire, typical of the western group. The cumulative sliding displacement responses indicate that the vertical accelerations increase sliding by a) increasing the number of sliding events, and b) by increasing the magnitude of sliding displacements within a sliding events that are already present without the vertical accelerations.

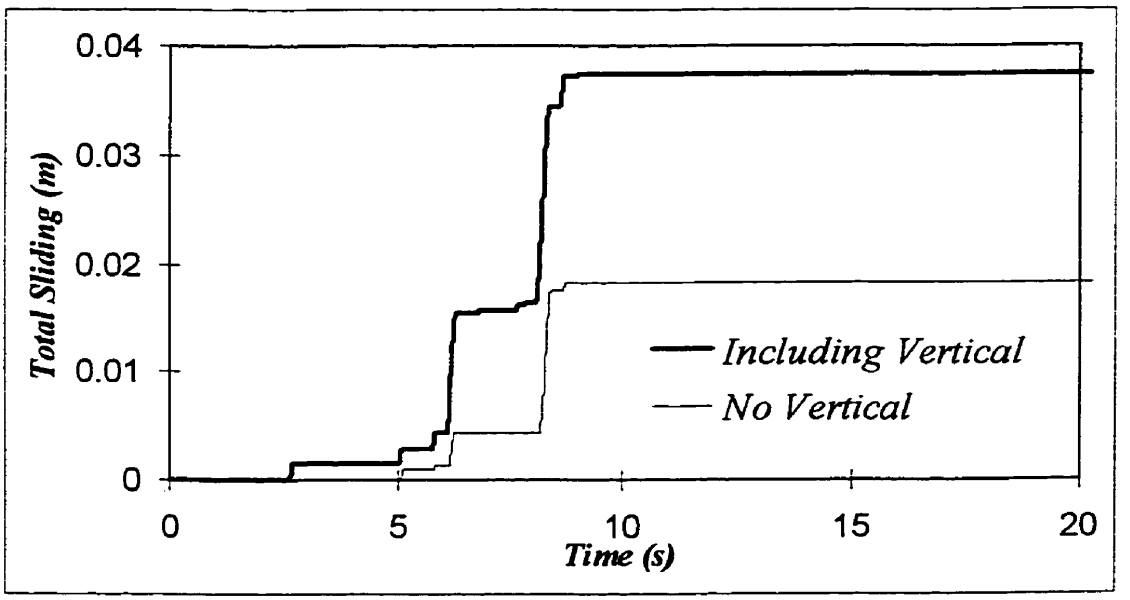

Figure 5.11 : Total sliding for Parkfield (1966) record (eastern group)

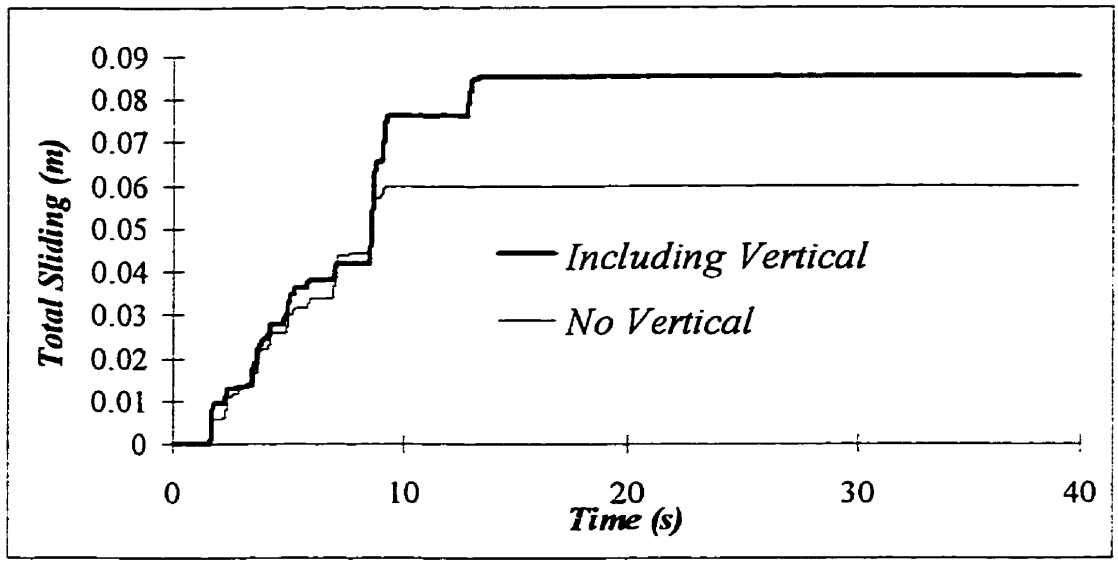

Figure 5.12 : Total sliding for San Fernando record (western group)

5.5.2.2 Safety factor against sliding F_s

From sliding the safety factor time-history computed by the program, the minimum values for each earthquake are presented in Tables 5-4 and 5-5. On average the safety factor decreases by 21% for the eastern group, and by 5 % for the western group when the vertical accelerations are included.

For the individual records, the safety factor was found to decrease by as much as 60 % for the Nahanni record, in the eastern group, and by as much as 14 % for the 3470 Wilshire record, in the western group. Figure 5.13 shows an example of safety factor time-history.

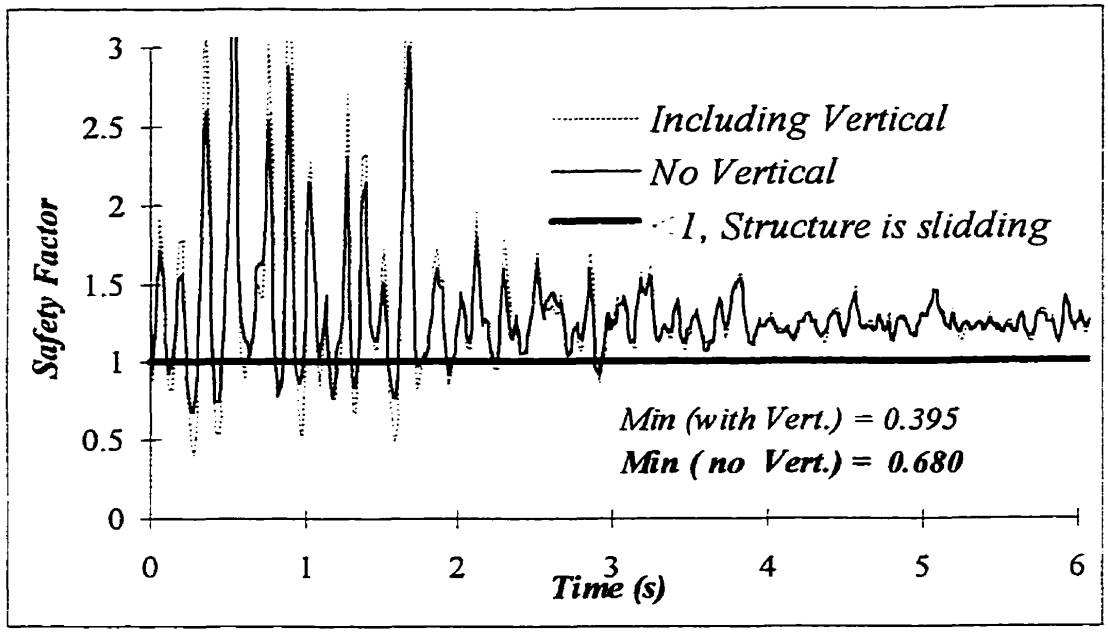

Figure 5.13 : Safety Factor time-history for Oroville record

One of the objectives of this study was to assess the widely used 30 % "rule of thumb" concerning the combination of horizontal and vertical earthquake induced forces when performing pseudo-static safety factor calculations. In practice, engineers combine 100% of the maximum horizontal force with 30% of the maximum vertical force, to account for the fact that the PGA in both directions cannot occur at the same time.

Using the horizontal PGA of 0.25g, and the vertical PGA corresponding to each earthquake, the pseudo-static safety factors were computed using the 30% rule. Two sliding safety factors were computed, F_{S1} and F_{S2}:

a) F_{S1} is computed using 100% Horizontal (PGAH) with 30% Vertical (PGAV)

b) F_{S2} is computed using 100% Vertical (PGAH) with 30% Horizontal (PGAH)

As reported in Tables 5-4 and 5-5, the sliding safety factor F_{S1} using the 30% rule yields satisfactory results. It seems to correspond quite well to the lowest safety factor occurring during the time-histories, as computed with the program.

For the eastern group, the mean, over the six earthquakes of the lowest value of the sliding safety factor is 0.58, whereas the mean pseudo-static F_{S1} value is 0.60. For the western group, the mean value of the lowest sliding safety factor obtained from the time-histories is 0.69 compared to the mean F_{S1} value of 0.64. The total sliding displacements for the western group is four times larger then the total sliding in the eastern group. However, when considering the analyses with the vertical component, the mean lowest sliding safety factor for the eastern group is only 16 % smaller then the mean lowest safety factor of the western group. This strengthens the idea that it is not necessarily the maximum acceleration value, which takes place once during the record, that has a significant meaning to induce large sliding displacements. It is more the duration of the pulses as well as the number of pulses above a critical value that affect the magnitude of residual displacements.

Examining the values of F_{S2}, we note that for the eastern group this safety factor is very close to the F_{S1} factor, and in some cases is even less. For the western group, the F_{S2} factor is on average 25% greater then the F_{S1} factor, and does not control the pseudo-static calculation. These results are consistent with the idea that the vertical accelerations play a more important role in the sliding response in eastern type ground motions.

Based on this evidence, it is suggested that both F_{S1} and F_{S2} factors be computed when determining the safety factor against sliding for structures in Eastern North America.

It is also common in practice to use the sliding safety factor as a design criterion instead of computing the total sliding. In fact it is quite incongruous to speak of large dams

where safety issues are very sensitive, by referring to a probable total displacement. The computed displacements are simply indicators of the degree of safety of the dam, since it is still far from being clear what an acceptable total sliding is. The most common approach consists of establishing an acceptable sliding safety factor, usually above 1, and strengthening the structure to meet this criterion. Nonetheless, one must be aware of the fact that the design ground motion, with its subjectively related return period, can well be exceeded, even by 3 times the PGA value according to Heidebrecht (1992). In such case, it is complementary to treat the safety against sliding by estimating the total sliding displacement. This approach accounts for the seismic characteristics of the region, i.e. frequency content, V/H ratio and duration, as well as the proclivity of the dam to sliding.

Table 5-4 : Total sliding displacements and safety factor for eastern group

	Total Sliding displ. (m)			*Safety Factor (min. from time-history)*			*30% rule*	
Quake	*No Vert*	*With Vert*	*% incr.*	*No Vert*	*With Vert*	*% decrease*	*Fs 1*	*Fs 2*
Helen	0.00675	0.01583	134.5	0.775	0.734	5.29	0.628	0.729
Nahan	0.00244	0.00689	182.4	0.683	0.276	59.59	0.523	0.220
Oroville	0.01667	0.04077	144.6	0.680	0.395	41.91	0.559	0.393
PacDam	0.01822	0.03742	105.4	0.780	0.635	18.59	0.623	0.707
Tremblor	0.01832	0.02247	22.7	0.683	0.667	2.34	0.639	0.781
Wright.	0.00750	0.00924	23.2	0.812	0.779	4.06	0.659	0.878
AVER.	0.01165	0.02210	89.7	0.736	0.581	21.01	0.605	0.618

Table 5-5 : Total sliding displacements and safety factors for western group

	Total Sliding displ. (m)			*Safety Factor (min. from time-history)*			*30% rule*	
Quake	*No Vert*	*With Vert*	*% incr.*	*No Vert*	*With Vert*	*% decrease*	*Fs 1*	*Fs 2*
Taft	0.03205	0.04478	39.7	0.739	0.649	12.18	0.630	0.740
Suchil	0.06442	0.07603	18.0	0.770	0.784	-1.82	0.640	0.786
3470	0.05975	0.08535	42.8	0.775	0.667	13.94	0.645	0.811
3550	0.05721	0.07395	29.3	0.683	0.641	6.15	0.645	0.813
4680	0.16270	0.18448	13.4	0.696	0.661	5.03	0.632	0.749
LaVillita	0.05013	0.06346	26.6	0.683	0.739	-8.20	0.640	0.788
AVER.	0.07104	0.08801	23.9	0.724	0.690	4.72	0.639	0.781

5.5.2.3 Position of resultant

Table 5-6 shows the maximum and minimum positions of the resultant at the base of the dam for both groups of earthquakes.

The middle third is exceeded in the downstream direction (+), for all of the earthquake records when the vertical accelerations are omitted from the analyses for both earthquake groups. In the upstream direction, the position of the resultant is not detrimental to the structural behaviour, since the horizontal hydrostatic forces limit the possibility of inducing tensile stresses in the downstream portion of the base.

For the western earthquake group, the average of the maximum positive position of the resultant is 0.87, whereas it is 0.851 for the eastern earthquake group. When the vertical accelerations are included in the analyses, the maximum position of the resultant in the downstream direction (+) is increased, to 0.922 for the western earthquake group, and 1.312 for the eastern earthquake group. The vertical accelerations seem to play a more important role in the eastern earthquake group.

Table 5-6 : Position of Resultant (-1,+1)

EASTERN GROUP					*WESTERN GROUP*				
Quake	*Max No V*	*Max with V*	*Min No V*	*Min with V*	***Quake***	*Max No V*	*Max with V*	*Min No V*	*Min with V*
Helen	0.780	0.839	-0.321	-0.321	*Taft*	0.840	0.991	-0.321	-0.319
Nahan	0.946	2.440	-0.148	-0.167	*Suchil*	0.788	0.757	-0.321	-0.319
Oroville	0.934	1.855	-0.284	-0.287	*3470*	0.779	0.952	-0.321	-.0324
PacDam	0.773	0.996	-0.321	-0.321	*3550*	0.946	1.010	-0.246	-0.245
Tremblor	0.946	0.975	-0.217	-0.224	*4680*	0.919	0.984	-0.321	-0.323
Wright.	0.724	0.763	-0.321	-0.322	*LaVillita*	0.946	0.835	-0.137	-0.143
AVER.	0.851	1.312	-0.269	-0.273	***AVER.***	0.870	0.922	-0.278	-0.279

Values equal or superior to one, are indicators of potential rocking motions that can cause overturning instability. However, the peak values of the position of the resultant on the base of the dam are only reached for very short periods of time, and destructive displacements are unlikely to be mobilized.

It is also interesting to note that the static resultant of the base reaction is located approximately at a value of + 1/3 corresponding to the downstream middle third limit of the kern.

5.5.2.4 *Horizontal-Vertical Interaction and Peak Correlation Factor*

The peak correlation factor (PCF), as defined in Chapter 3, is a more detailed estimation of the H and V components correlation then the global correlation as expressed by the cosine of the angle in space between the two accelerograms.

Three indicators obtained from the time history of the PCF were examined. The average value over the whole earthquake, the maximum value, and the number of time steps where the PCF exceeded the value 0.05.

Examining these values for each group in tables 5.7 and 5.8, we can see that the average value of the PCF is greater for the earthquakes in the western group than the eastern group. The total duration of the historical records is used in computing the PCF.

Considering that many records present very low accelerations for periods of time at the beginning and at the end of the earthquake, it can be inferred that the insignificant accelerations padding the strong motion at the start and end of the accelerogram, influence the average correlation for the whole historical record. This renders the correlation measure meaningless for the few seconds of strong shaking where the structural damage will occur. Nonetheless, this parameter will further be discussed when

analyzing results from analysis with synthetic earthquakes, where the duration is identical for all records. It must be pointed out at this stage, that the PCF was initially defined to assess the 30% "rule of thumb" when combining the horizontal and vertical accelerations. Considering that a value of the PCF equal to 1 implies the simultaneous occurrence of the horizontal and vertical PGA. In the same way, a value of 0.3 or 30% represents the occurrence of 30% of the vertical PGA when the horizontal PGA is reached or vice-versa. To a certain extent, it could be assumed that above a certain level of vertical and horizontal accelerations, the sliding effect induced on the structure by two combinations of horizontal and vertical accelerations having the same PCF could be somehow similar. Figure 5.14 presents the curve defining the critical sliding accelerations. The critical sliding acceleration varies from a value of H_{crit} = 0.072 g when only the horizontal acceleration is considered, to a value of V_{crit} = 0.108 g, when only the vertical acceleration is considered, for the case study of the Paugan dam. It must be noted that sliding can occur with a vertical acceleration above 0.108 g without any horizontal acceleration ! The average PGAV is approximately 0.16 g for the historical records considered, when calibrated for a PGAH of 0.25 g. It can be seen that the importance of the effect of the vertical accelerations could have been foreseen on such a plot.

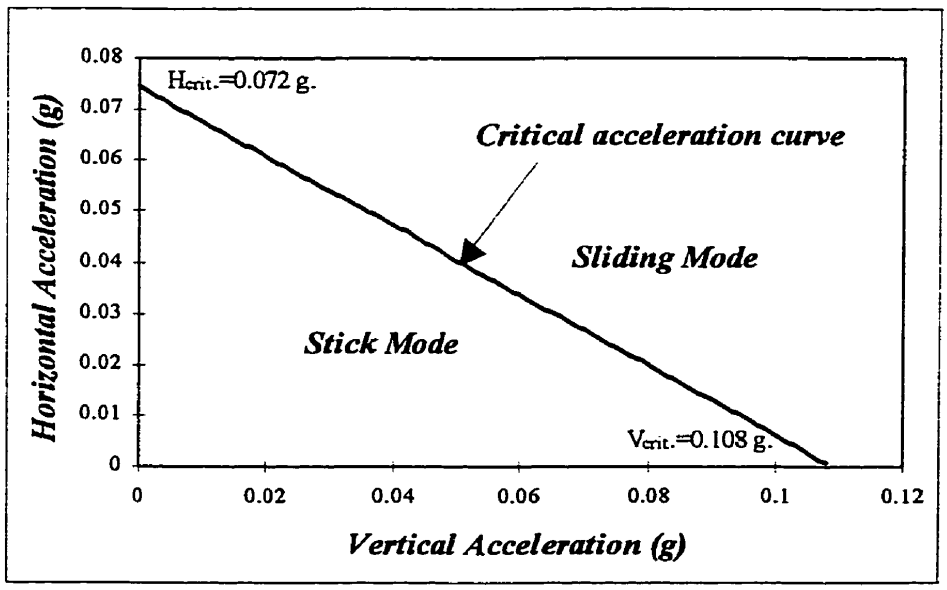

Figure 5.14: Critical sliding acceleration (V-H interaction)

To understand the meaning of the PCF, we can plot curves of equal PCF values or ``ISO-PCF `` curves in reference to the critical acceleration curve presented in Figure 5.14.

Figure 5.15 shows that as the PCF cut-off limit is increasing, the distance from the critical acceleration curve is also increasing along with the potential sliding energy transmitted to the structure. The curve corresponding to a PCF cut-off value of 0.05 seems to best correspond the a criterion above which the combined effect of horizontal and vertical accelerations on the structure may have a significant effect.

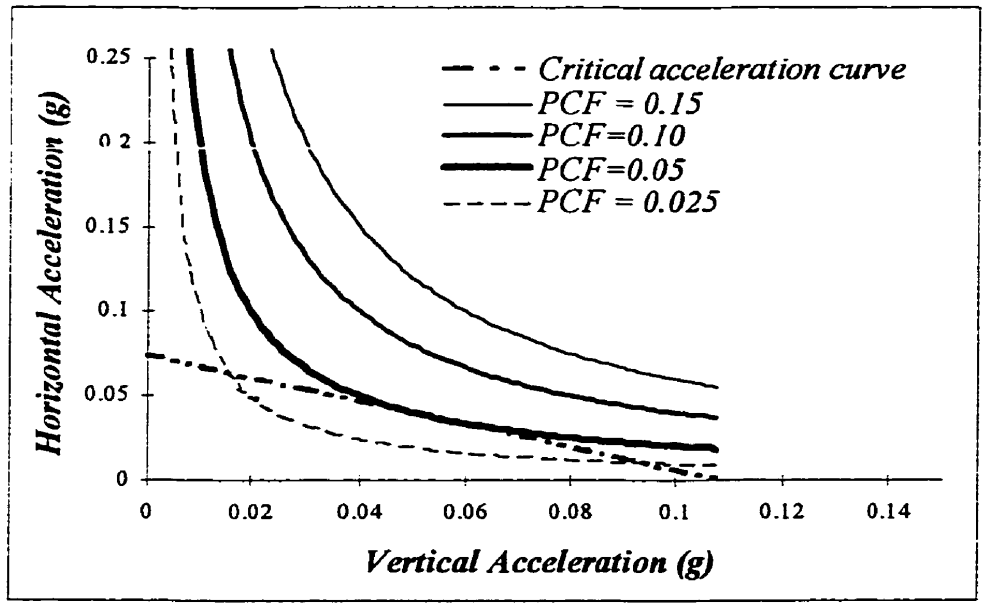

Figure 5.15 : ``ISO-PCF`` curves

Considering this, it was decided to compute the number of time steps for each accelerogram where the PCF is superior to 0.05 as an indicator of the combined effect of vertical and horizontal accelerations on the sliding response of the dam. Looking at Table 5-7 and Table 5-8, for both earthquake groups, the average of the maximum value of the PCF is close to 0.5, which could be due to a combination of 100% of the horizontal PGA, with 50% of the vertical one or an equivalent combination.

The number of time steps where the PCF is superior to 0.05, indicates the difference between the eastern and western groups. The mean value is 84 for the east and reaches 446 for the west. This is an indicator, before even running the sliding analysis of the potential effect of a combined horizontal and vertical accelerogram on the sliding response of an earthquake.

It must be noted that while the PCF is quite different between the eastern and western group of earthquakes, the classic correlation indicator, for example the cosine of the angle θ between the horizontal and vertical accelerograms remains approximately the same for both groups, at a value close to 0.2.

Table 5-7 : Statistics on the PCF (eastern group)

Peak Correlation Factor

Quake	*Average*	*Max*	*Occurrences > 0.05*
Helen	0.0030	0.5381	88
Nahan	0.0025	0.3851	26
Oroville	0.0169	0.6967	91
PacDam	0.0078	0.4874	140
Tremblor	0.0042	0.3600	56
Wright.	0.0108	0.6478	104
AVER.	0.008	0.5192	84.2

Table 5-8 : Statistics on the PCF (western group)

Peak Correlation Factor

Quake	*Average*	*Max*	*Occurrences > 0.05*
Taft	0.0154	0.4468	412
Suchil	0.0117	0.5103	317
3470	0.0179	0.6786	581
3550	0.0144	0.6440	461
4680	0.0115	0.4678	370
LaVillita	0.0184	0.5271	535
AVER.	0.015	0.5458	446.0

5.5.3 Synthetic earthquakes

5.5.3.1 Horizontal earthquakes only

Table 5-9 indicates that the synthetic records for the eastern group yield residual sliding displacements very similar to those obtained with the historical records corresponding the same group. However, the western group synthetic records give sliding displacements that are not at all comparable with the historical records of the same group. The spectrum compatibility of synthetic records is satisfactory for the western group. However, the sliding of the dam is entirely a non-linear phenomenon. To better assess the characteristics of the synthetic accelerograms, the predominant period, the root mean square of the accelerogram (RMSA), and the Arias intensity, were computed for the synthetic records and compared to the historical records.

Table 5-9 : Synthetic earthquake results (horizontal only)

(sliding in meters)

Eastern Group		*Western Group*	
Quake	***H alone***	***Quake***	***H alone***
EH1	0.01102	*WH1*	0.11479
EH2	0.01244	*WH2*	0.13277
EH3	0.00974	*WH3*	0.16830
EH4	0.01174	*WH4*	0.16197
EH5	0.01298	*WH5*	0.13451
EH6	0.01449	*WH6*	0.14484
AVER.	**0.01207**	**AVER.**	**0.14286**
Historical	**0.01165**	**Historical**	**0.07104**
difference %	**3.59**	**difference %**	**101.3**

Tables 5-10 and 5-11 present the values of these indices for the eastern and western groups, respectively.

For the eastern group all the indices are reasonably close to the historical values. It could be concluded that the ENA synthetic motions are quite representative of the historical

accelerograms. For the western group (Table 5-11), it is quite evident that although spectrum compatibility has been achieved, the generated motions have different characteristics. The predominant period is much lower for the synthetic accelerograms than for the historical accelerograms. It is in fact quite close to the predominant period corresponding to the eastern group motion. Added to this, the Arias intensity and the RMSA are much higher for the western synthetic records than for the historical ones.

Table 5-10 : Characteristics of ground motions for eastern earthquake group (PGAH = 0.25 g)

	Synthetic							*Historical*
	EH1	**EH2**	**EH3**	**EH4**	**EH5**	**EH6**	***Average***	***Average***
Time of Occurrence of PGA (s)	4.73	3.30	3.99	2.31	1.92	4.19	3.41	4.54
Mc Cann-Shaw duration (s)	6.33	7.09	6.16	6.38	6.47	7.09	6.59	4.79
Bracketted duration (s)	8.01	7.09	7.24	7.20	8.47	7.80	7.64	4.64
Trifunac (s)	6.26	6.05	5.93	6.19	6.45	6.53	6.24	4.89
Hudser (s)	6.44	6.72	6.04	6.51	6.44	6.50	6.44	5.48
Predominant period (s)	0.092	0.117	0.095	0.119	0.121	0.103	0.11	0.18
RMSA (g)	0.043	0.046	0.043	0.040	0.042	0.045	0.04	0.03
Arias Intensity (g^2.s)	0.026	0.029	0.025	0.023	0.025	0.028	0.03	0.02

Table 5-11 : Characteristics of ground motions for western earthquake group (PGAH = 0.25 g)

	Synthetic							*Historical*
	WH1	**WH2**	**WH3**	**WH4**	**WH5**	**WH6**	***Average***	***Average***
Time of Occurrence of PGA (s)	14.98	16.56	12.80	14.08	6.26	7.96	12.11	8.48
Mc Cann-Shaw duration (s)	19.85	18.83	19.16	19.42	20.12	18.54	19.32	18.40
Bracketted duration (s)	21.31	21.73	21.53	21.95	20.89	20.93	21.39	23.23
Trifunac (s)	17.71	17.03	17.41	17.97	17.50	16.58	17.37	21.72
Hudser (s)	18.70	19.01	18.36	18.95	18.40	17.86	18.55	23.79
Predominant period (s)	0.112	0.101	0.130	0.122	0.118	0.129	**0.12**	**0.30**
RMSA (g)	0.073	0.074	0.075	0.073	0.071	0.068	**0.07**	**0.04**
Arias Intensity (g^2.s)	0.133	0.137	0.142	0.134	0.125	0.117	**0.13**	**0.07**

Figure 5.16 shows an example of western synthetic and horizontal accelerograms. These are quite different in frequency content, and also in energy content, since the synthetic record has more peaks near the PGA value then the historical record. A good elastic spectrum compatibility does not necessarily yield the detailed acceleration pulse's same characteristics. For historical records, one or two major acceleration pulses can dictate the whole response of a structural system in terms of maxima. The spectrum being a measure of elastic maximum accelerations at different periods for a single DOF system, a single important pulse at a particular predominant period can greatly influence the shape of the spectrum.

The synthetic earthquakes, derived from a stationary process, seem to be more evenly distributed events, large accelerations more frequently encountered. In fact, the effect caused by a single acceleration pulse in a historical record, will be attained in a synthetic record by spreading out this effect along the whole record, either by dynamic amplification (frequency content) or increase of amplitudes. The spectrum compatibility criterion is a necessary one, but not always sufficient to ensure the reliability of structural response, specially for nonlinear sliding systems.

In Figure 5.17, we can clearly see that the sliding is evenly distributed over the length of the record for the synthetic accelerogram, whereas it is concentrated in three major sliding events for the historical record. This concurs with what was discussed earlier, that the historical records are dominated and greatly influenced by a low number of important acceleration pulses.

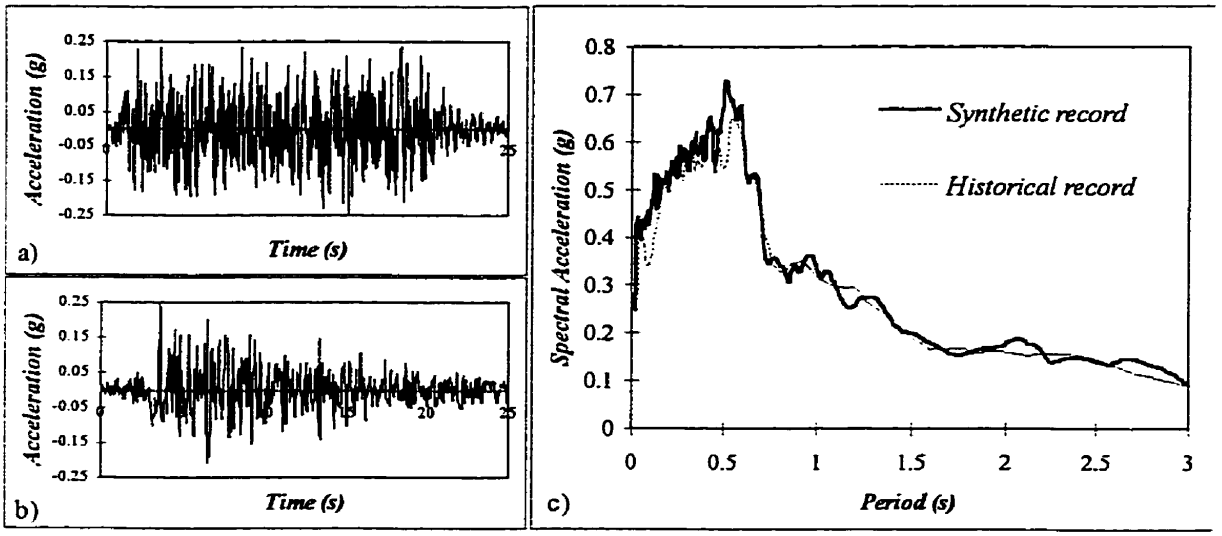

Figure 5.16 : Synthetic versus historical ground motions for western group

a) accelerogram for WH1 synthetic record; b) accelerogram for Taft Lincoln record; c) respective acceleration spectra.

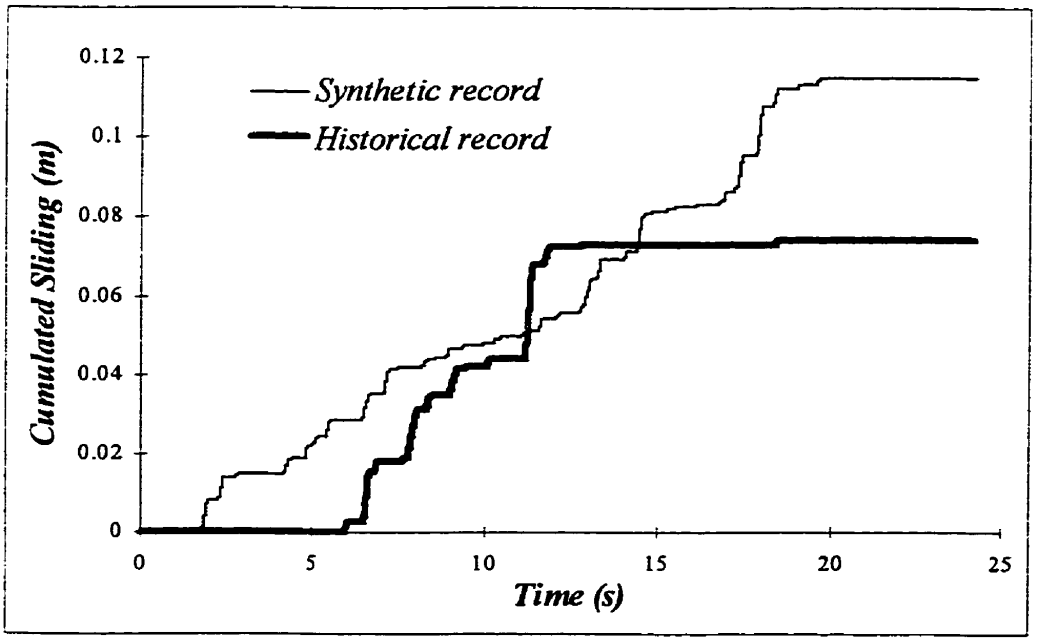

Figure 5.17 : Comparison of cumulated sliding displacements for western records (synthetic vs historical)

Considering this, and considering the drastic effect that the characteristics of the synthetic motions have on the sliding response of the analyzed structure, it is quite difficult to draw solid conclusions on the effect of the vertical ground excitation on the structural behaviour. However for the eastern earthquake group, where the synthetic motions are much more reliable in terms of similarities to the historical motion characteristics, the different generating methods for the vertical ground motions can be compared more reliably.

5.5.3.2 Vertical component

Table 5-12 indicates that the eastern vertical components for the three synthetic accelerograms generation methods increase the total sliding displacements induced to the dam.

Table 5-12 : Total sliding eastern synthetic records (with vertical)

	Total Sliding (m)				**% increase**	
Quake	*H alone*	*1- (HV)*	*2- (H+R)*	*3- (H+RS)*	*H+R*	*H+RS*
H1	0.01102	0.07550	0.01810	0.01619	64.25	46.91
H2	0.01244	0.08122	0.01720	0.02180	38.26	75.24
H3	0.00974	0.09036	0.01380	0.02260	41.68	132.0
H4	0.01174	0.06388	0.01540	0.01732	31.18	47.53
H5	0.01298	0.08231	0.01740	0.01821	34.05	40.29
H6	0.01400	0.07728	0.01850	0.01989	32.14	42.07
AVER.	**0.01199***	**0.07843***	**0.01673***	**0.01934***	**40.26**	**64.01**

1- method 1: pondering of H; *2*-method 2: reduced H spectrum; *3*-method 3: shift and reduced H spectrum
* **mean historical records results** (Table 5-4) - (H alone): 0.01165 m; (H+V): 0.02210 m.

Table 5-13 : Total sliding western synthetic records (with vertical)

	Total Sliding (m)				% increase	
Quake	*H alone*	*1- (HV)*	*2- (H+R)*	*3- (H+RS)*	*H+R*	*H+RS*
H1	0.11479	0.35890	0.16640	0.16152	44.96	40.71
H2	0.13277	0.34062	0.17299	0.16570	30.29	24.80
H3	0.16830	0.38526	0.22134	0.19501	31.52	15.87
H4	0.16197	0.41031	0.19595	0.17219	20.98	6.31
H5	0.13451	0.30688	0.14730	0.17097	9.51	27.11
H6	0.14484	0.31621	0.22250	0.18703	53.62	29.13
AVER.	**0.14286**	**0.35303**	**0.18775**	**0.17540**	**31.81**	**23.99**

1- method 1: pondering of H; *2*-method 2: reduced H spectrum; *3*-method 3: shift and reduced H spectrum
* **mean historical records results** (Table 5-5) - (H alone): 0.07104 m; (H+V): 0.08801 m.

The results are presented for both groups of earthquakes, but the eastern results are further analyzed because they are more representative and realistic as previously discussed.

Using the horizontal accelerogram calibrated at 2/3 (HV method) to approximate the vertical component is totally unrealistic and unrepresentative of the real interaction of horizontal and vertical seismic accelerations. The perfect correlation between the two accelerograms yields an exaggerated effect of the vertical accelerations. The mean total sliding displacements computed using this approximation of the vertical component is 78.43 mm, where for the historical record the mean total sliding displacements was 22.10 mm for the eastern group (Table 5-4).

For eastern records, the shifted and reduced method (H +RS) yields slightly better results then the reduced only method (H+R), if the comparison is made with the historical results, presented earlier. However both methods slightly underestimate the effect of the vertical accelerations in comparison to the results computed with the historical records. Nonetheless, it could be concluded that the difference is not of major importance, since the results are very close considering the degree of precision of the calculations and the simplifying hypotheses required to compute sliding displacements. It may not seem

justifiable, considering the computational effort that is implied, to use the shifted and reduced method, based on the total sliding displacement results. It must be pointed out that although the final residual sliding displacement may be similar, the time-history of the dam motion is much closer to the historical one if the shifted and reduced method is used instead of the reduced only method.

It must be reminded that the calculations were performed assuming a rigid block model of the sliding structure. When performing the shift method, the spectrum peak is shifted to shorter periods, to account for the higher frequency characteristics of vertical accelerations. It could be expected that, considering the short natural period of the dam structure in the vertical direction, a more important dynamic amplification could occur for the shifted method. This effect would be more reliably described by the shifted vertical accelerogram. This needs to be investigated further for flexible structural systems.

5.5.3.3 Sliding Safety factor

Table 5-14 and Table 5-15 indicate that the sliding safety factors are slightly overestimated for the eastern earthquake group when the vertical accelerations are included, and slightly underestimated for the western group. As noted in the previous paragraph, the 30% combination rule used in the context of pseudo-static calculations is a good estimation of the minimum sliding safety factor derived from time-history calculations.

It is interesting to note that for the western earthquake group, where the total sliding displacements were found to be highly overestimated by the synthetic records, the synthetic and historical sliding safety factors are quite similar.

Table 5-14 : Sliding safety factor (eastern earthquake group)

	Safety Factor MIN			% decrease	
Quake	*H alone*	*H + R*	*H + RS*	*H + R*	*H + RS*
H1	0.683	0.723	0.650	-5.86	4.83
H2	0.683	0.560	0.645	18.01	5.56
H3	0.683	0.684	0.730	-0.15	-6.88
H4	0.821	0.739	0.729	9.99	11.21
H5	0.683	0.642	0.698	6.00	-2.20
H6	0.775	0.745	0.729	3.87	5.94
Average	**0.721**	**0.682**	**0.697**	**5.311**	**3.077**
Average (HIST)	**0.736**	**0.581**	**0.581**	**21.01**	**21.01**
Average (30%)	**FS1**	**0.605**			
	FS2	**0.618**			

Table 5-15 : Sliding safety factor (western earthquake group)

	Safety Factor MIN			% decrease	
Quake	*H alone*	*H + R*	*H + RS*	*H + R*	*H + RS*
H1	0.714	0.664	0.643	7.00	9.94
H2	0.683	0.595	0.628	12.88	8.05
H3	0.683	0.594	0.646	13.03	5.42
H4	0.683	0.594	0.590	13.03	13.62
H5	0.683	0.644	0.648	5.71	5.12
H6	0.683	0.647	0.593	5.27	13.18
Average	**0.688**	**0.623**	**0.625**	**9.488**	**9.222**
Average (HIST)	**0.724**	**0.690**	**0.690**	**4.928**	**4.928**
Average (30%)	**FS1**	**0.639**			
	FS2	**0.781**			

For the synthetic records, the minimum, or close to minimum sliding safety factors might be occurring much more frequently during the whole span of the record, as compared to values derived from the historical records. For historical records, low safety factors occur only a few times during the record. This could be noticed, in Figure 5.16, by inspection of a historical and a synthetic accelerogram for the western group.

5.5.3.4 Position of resultant

Tables 5-16 and 5-17 show the position of the resultant on the dam base, computed for the three methods used to generate the vertical component of ground motion.

The maximum position of the resultant under only synthetic horizontal motion, is identical to the average position of the resultant computed for the historical accelerograms. This result is due to the fact that both historical and synthetic accelerograms were calibrated for a PGAH of 0.25 g.

Consistent with previously reached conclusions, it is evident that the ponderation of the horizontal accelerogram method of generating the vertical component of ground motion (HV) is unacceptable. The average maximum position of the resultant reaches a value of 1.4373 for the eastern earthquake group for the HV method, while the historical accelerograms yielded average values of only 0.922. The "perfect" correlation between the two components, as mentioned previously in this study, induce unrealistic responses for all parameters examined.

It is also shown in these results that the shifted and reduced method yields results that are slightly closer then the historical records response. However, the difference being so small, both results are considered good approximations of the historical response. Similar conclusions on the different generation methods can be reached when looking at the results for the western earthquake group (Table 5-17). Nonetheless, as previously stated, a substantial difference exists between the results obtained with the synthetic records and the historical records for the western earthquake group. The reasons for this difference is stated earlier in this chapter.

Table 5-16 : Relative position of resultant (eastern earthquake group)

	Position of Resultant (-1;+1) *maxima from computed time-history*			
Quake	*H alone*	*HV*	*H + R*	*H + RS*
H1	0.9240	1.4681	0.8368	1.0100
H2	0.9462	1.4681	1.2199	1.0300
H3	0.9462	1.4681	0.9453	0.8670
H4	0.7160	1.4681	0.7959	0.8452
H5	0.9462	1.4681	1.0480	0.9195
H6	0.7805	1.2830	0.8430	0.8277
Average	0.8768	1.4373	0.9482	0.9166
Average (HIST)	0.8700	0.9220	0.9220	0.9220

Table 5-17: Relative position of resultant (western earthquake group)

	Position of Resultant (-1;+1) *maxima from computed time-history*			
Quake	*H alone*	*HV*	*H + R*	*H + RS*
H1	0.8867	1.3197	0.9759	0.9994
H2	0.9462	1.4681	1.1191	1.0541
H3	0.9462	1.4681	1.1254	0.9881
H4	0.9462	1.4681	1.1300	0.9632
H5	0.9462	1.2030	1.0071	0.9771
H6	0.9462	1.4681	1.0030	1.1297
Average	0.9363	1.3992	1.0601	1.0186
Average (HIST)	0.8510	1.3120	1.3120	1.3120

CHAPTER 6

Conclusion

6.1 Summary

In this present study, related to the incidence of vertical seismic excitations on the structural response of civil engineering structures, three major research axes were considered: a) the characteristics of the vertical earthquake component, b) the effect of vertical accelerations on steel moment-resisting frames, and c) the effect of vertical excitations on the sliding response of a gravity dam.

At first, a review of previously published work on vertical seismic accelerations covering a) the seismological aspect, b) historical evidences, c) experimental evidences, d) numerical evidences, and e) code practice, is presented.

The study on the characteristics of the vertical accelerations was performed on a series of historical accelerograms that were subdivided according to the NBCC (1995) definition of the a/v ratio. This ratio of the peak ground acceleration, a_g, expressed in g, over the peak ground velocity, v_g, expressed in m/s, is a measure of the frequency content of the excitation. A high a/v value is representative of eastern North American ground motions, whereas the low and intermediate values of this ratio represent western North American events. On these series of historical accelerograms, indices such as different measures of duration, predominant period, as well as spectral ordinates were computed and compared. Based on these results, a method consisting of shifting and reducing the horizontal spectrum to obtain the vertical one was proposed.

The non-linear analyses on a 6-story steel moment-resisting frame structure were performed for earthquakes typical of near-fault Californian ground motions. Special attention was given on determining the effect of the vertical excitation on the rotational ductility demand, but other response parameters, such as the increase in the axial load and the strain rate effects were also examined.

The effect of the vertical accelerations on the sliding response of gravity dams was approached by a case study of the Paugan dam (50 m), subjected to historical and synthetic records typical of eastern and western earthquakes. The synthetic horizontal accelerograms were generated based on the mean acceleration response spectra of the historical earthquakes, whereas the vertical synthetic accelerograms were generated with three distinct methods. The first method consisted in simply calibrating the horizontal accelerogram by a value of 2/3. The second method consisted in calibrating the horizontal spectrum to obtain the vertical one, then generating the vertical accelerogram, and the third consisted in shifting and reducing the horizontal spectrum to obtain the vertical one before generating the vertical accelerogram. The analyses were performed with a computer program developed in the scope of this study to compute the sliding displacements as well as other performance indicators (i.e sliding safety factors). This program considers both horizontal and vertical input accelerations to compute the sliding response of the dam, using rigid body dynamics.

6.2 Conclusions

The following major conclusions can be outlined from the research work performed in this thesis:

Characteristics of vertical earthquake components

- As reported in the literature, the horizontal and vertical accelerations have different characteristics with respect to a) frequency content, b) attenuation, c) amplitude of ground motion, d) energy content, and e) build up time. Vertical accelerations can be described as impulsive, high frequency accelerations with a lower amplitude but a faster build up time than horizontal accelerations.

- For shorter distances to the fault, the horizontal and vertical accelerations have more similar characteristics, whether it is in frequency content or in amplitude values. As the distance from the fault increases, the vertical accelerations, propagating mainly as P-waves, attenuate and differentiate themselves more and more from the horizontal accelerations propagating mainly as S-waves.

- The a/v classification seems to have a significance for the characteristics of the vertical component, especially when the intermediate and low a/v groups are joined together representing western North American earthquakes, in opposition to the high a/v group representing eastern North American earthquakes.

- The widely used value of 2/3 is a good approximation of the vertical PGA to the horizontal PGA ratio. Nonetheless, the wide range of values computed from historical earthquakes show that in many cases the vertical PGA can exceed the horizontal one by a large amount. Therefore great precaution is suggested when assessing the inertia forces induced by vertical accelerations for structures that are directly sensitive to these forces (i.e. cantilevers, large span beams, etc.)

- When examining the response spectra, the value of 2/3 is inadequate to describe the relationship between the horizontal and the vertical components, because they have spectral peak ordinates at different period values. The shifted and reduced method is a

reliable and simple way to estimate the vertical spectrum from the corresponding horizontal one.

- The shift factor suggested following this study, is 1.55 irrespective of the a/v ratio of the earthquake. The reduction factors are 0.8 for the high a/v group, and 0.55 for both the intermediate and low a/v earthquake groups.

- The percentage of critical damping used in the analysis does not affect the shift and reduction factors. It is therefore possible to generate a vertical spectrum with the shifted and reduced method for a given amount of critical damping, and then calibrate the results to fit a different value of damping.

- All along this study, the question of correlation and coherency between horizontal and vertical accelerations has emerged under different forms. In the literature and in our statistical analyses of historical earthquake records, a correlation factor of 0.2 is considered as a reasonable one. The accelerograms generated with SIMQKE (1976) with different seed numbers present a correlation factor close to zero.

- When computing the correlation of the horizontal and vertical components, the correlation on the whole duration of the accelerogram is tainted with values of accelerations that are insignificant for the structure. Thus a correlation factor can be high over the entire length of an earthquake, but it does not necessarily mean that the significant few peaks which govern the structural response are correlated.

<u>Seismic response analysis of a moment-resisting frame including vertical acceleration</u>

- Vertical accelerations do not seem to affect the global response of steel moment resisting frames, nor to increase the demand in rotational ductility as sometimes

reported by some in the literature.

- The effect of vertical accelerations is more important when the structure is responding elastically. Gradual yielding of the structure filters the effects of high frequency vertical accelerations, and renders the structure insensitive to them.

- Substantial increases in the column maximum axial loads were directly attributed to the vertical accelerations. They are not critical for moment resisting frames, since this structural system offers large reserves in the axial direction because the sections are mainly designed to resist important moments. Nonetheless, for structures designed mainly for axial load, these increases could be critical.

- The strain rate is substantially increased by the inclusion of vertical accelerations. The increase of the base steel yield moment due to the increased strain rate will influence the design of columns at the panel zone area, as well as welds in the connections.

Dynamic sliding response of a gravity dam subjected to historical and synthetic vertical horizontal and vertical ground motion

- The analyses considering only the horizontal component of ground motion, for both the synthetic and the historical records, showed that the higher frequency content of the eastern group earthquakes cause a smaller total sliding displacement then the western type earthquakes.

- The sliding response of gravity dams is sensitive and substantially affected by the vertical component of ground motion. For the group of eastern historical earthquakes, the inclusion of vertical accelerations in the analyses caused an increase

of 89% in the total sliding displacement. For the western historical earthquake records , the increase due to the vertical accelerations was 24%.

- When generating synthetic accelerograms to perform sliding response analyses, many indices (duration, predominant period of strong shaking, energy content...) must be examined and controlled, even if the spectrum compatibility is adequate. Similar spectral responses can be obtained from different accelerograms. For problems where the non-linear response is predominant, spectrum compatibility is not a sufficient condition to judge on whether or not a synthetic motion is acceptable and representative of historical events.

- The PCF is a measure of the potential interaction at peak values of two ground motion components. The PCF values were much greater for the western earthquake group than for the eastern group, indicating a higher potential total sliding displacement under the combined effect of horizontal and vertical excitations. This factor is a measure of correlation between two accelerograms based on the anticipated structural response. The correlation angle θ is a correlation factor based solely on the accelerograms. While the PCF was quite different between the historical eastern and western earthquake groups, the correlation angle θ was similar for both groups at approximately 0.2.

- The shifted and reduced method and the reduced method, both based on alterations of the horizontal spectrum to obtain the vertical one, yielded similar and satisfactory predictions of the effect of vertical accelerations on the total sliding displacement of the dam. Nonetheless, the detailed time-history of sliding displacements was much more similar between the historical records and the records obtained from the shifted and reduced method then with the reduced only method. Furthermore, in an analysis where dynamic amplification could occur, it is believed

that the shifted and reduced method would yield better results, because it describes more reliably the vertical spectral peaks.

- Calibrating a horizontal accelerogram to estimate the vertical component of ground motion is unacceptable, since the perfect correlation between the two components is too severe on the structural response.

- The 30% "rule of the thumb", which considers 100% of horizontal PGA induced forces combined with 30% of vertical PGA induced forces, for computing the dam sliding safety factor in a pseudo-static analysis, was evaluated. It was found that the 30% rule to assess the pseudo-static seismic safety of a dam structure, is a good approximation of the minimum safety factor encountered during step-by-step analyses. For eastern type earthquakes, it is strongly suggested to compute both possibilities: a) 100% horizontal seismic forces simultaneously with 30% vertical seismic forces, and b) 100% vertical seismic forces simultaneously with 30% horizontal seismic forces, when evaluating the safety factor.

- Strong motion generation to assess the sliding response of dams using SIMQKE (1976), seems to be adequate for eastern type earthquakes. The duration must be controlled. In this study, through trial and error, a realistic time function was defined. This time function yielded duration indices similar to those of the historical records, and the related sliding displacements were also quite similar.

- For western type earthquakes, the characteristics of the accelerograms generated with SIMQKE (1976) seem to diverge somewhat from the characteristics of the historical records for the same group. This needs to be further investigated, but it is not as significant as it would be for the eastern earthquake group, since there exists a great amount of historical records for this type of earthquakes.

6.3 Recommendations for future work

It is quite evident that despite important research initiatives on this topic during the past few years, a great deal of work needs to be done, before the problem of vertical accelerations is better understood, let alone completely resolved.

Following this study, the following topics for further interest and research were noted:

- Make a widespread effort to include in the numerous numerical analyses on all types of structures that are performed throughout the scientific community, analyses that investigate the effect of vertical seismic accelerations. This would broaden the vision that engineers have concerning vertical accelerations, demystify this problem, and point out numerous cases where these high frequency solicitations can play a major role.

- Assess the effect of low correlation (as when generated from SIMQKE (1976) with different seed numbers) between horizontal and vertical accelerograms on the structural response.

- Examine the effect of increased axial load due to vertical ground excitation on pin-braced steel structures.

- Perform dynamic analyses on dam structures, but permitting dynamic amplification in the vertical direction, and assess the performance of the shifted and reduced method, in comparison with the reduced only method. Such a study could assess whether or not the extra computing effort necessary to increase the representativity of synthetic vertical ground motion by applying the shifted and reduced method is justified.

- Further explore the PCF concept by computing statistics on this factor. Determine whether or not this parameter could be used as a criterion for assessing the damage potential of multi-directionnal accelerograms, and could be used for generating realistically correlated synthetic ground motions (in terms of structural response).

- Broaden the study of the shifted and reduced method to a larger number of earthquakes.

- Develop code type pseudo-static calculation method to include inertia forces induced by vertical ground motions in building response analysis.

References

ABE, K., and WATANABE, H. 1996. A study on amplification factors of earthquake motions observed at a granite site and relationships between their vertical and horizontal motions. Eleventh World Conference on Earthquake Engineering, Mexico, Paper No. 1242.

ACE (CANADIAN ELECTRICAL ASSOCIATION) 1990. Safety assessment of existing dams for earthquake conditions.-Volume A: ground motion parameter maps. Report prepared by ACRES International Ltd for the ACE. ACE No. 420 G 547.

AGBABIAN, M. S., HIGAZY, E. M., ABDEL-GHAFFAR, A. M., and ELNASHAI, A.S. 1994. Experimental observations on the seismic shear performance of RC beam-to-column connections subjected to varying axial column force. Earthquake Engineering and Structural Dynamics, 23: 859-876.

AISC. 1993 Load and Resistance Factor Design Specification for Structural Buildings. AISC, Inc. Chicago, Il.

AMIRBEKIAN, R., and BOLT, A. 1995. Vertical shaking variability from wave scattering in alluvial basins. Proceedings of the Fifth International Conference on Seismic Zonation, Nice, France, Presses Académiques, pp. 941-948.

ARIAS, A. 1969. A measure of Earthquake Intensity. Seismic Design of Nuclear Power Plants. Ed. by R. Hansen, Cambridge, Massachusetts Institute of Technology.

ASANO, M., and TORII, S. 1992. The design and analysis of a building with atrium and large cantilever., Tenth World Conference on Earthquake Engineering, Madrid, Spain, pp. 4071-4077.

ATKINSON, G. M., and SOMERVILLE, P. 1994. Calibration of time history simulation methods. Bulletin of the Seismological Society of America, 84 (2): 400-414.

ATKINSON, G.M., and SOMERVILLE, P.G. 1994. Notes on ground motion parameters for eastern north America : duration and H/V ratio. Bulletin of the Seismological Society of America, 83: 587-596.

BARDET, J. P., and DAVIS, C. 1996 Engineering observations on ground motion at the Van Norman Complex after the 1994 Northridge Earthquake. Bulletin of the Seismological Society of America, 86 (1B): S333-S349.

BOLT, B. A. 1973. Duration of strong ground motion. Proceedings of the Fifth World Conference on Earthquake Engineering, Rome, Italy, 1, 6-D, Paper no. 292.

BORJA, R. I., WU, W.-H., SMITH, H.-A. 1993. Nonlinear response of vertically oscillating rigid foundations. ASCE Journal of Geotechnical Engineering, 119 (5): 893-911.

BOZORGNIA, Y., NIAZI, M., CAMPBELL, K.W. 1995. Characteristics of free-field vertical ground motion during the Northridge earthquake. Earthquake Spectra, 11 (4): 515-525.

BOZORGNIA Y., NIAZI, M., CAMPBELL, K.W., 1996. Relationship between vertical and horizontal response spectra for the Northridge Earthquake. Eleventh World Conference on Earthquake Engineering, Mexico, Paper No. 893.

BRODERICK, B. M., ELNASHAI, A. S., AMBRASEYS, N. N., BARR, J. J., GOODFELLOW, R. G., and HIGAZY, E. M. 1994. The Northridge earthquake of 17 January 1994 : Observations, Strong Motion and Correlative Response Analysis, Research Report ESEE-94/4, Imperial College, London, U.K..

BRUNA, R., and RIERA, J. D. 1988. Towards the simultaneous generation of the three components of the seismic acceleration on rock surface. Nuclear Engineering and Design. North-Holland, Amsterdam, 110: 153-163.

CARR, A.-J. 1996. Ruaumoko - Inelastic Dynamic Analysis program. Department of Civil Engineering, University of Canterbury, New Zealand.

CHEN, C., and LEE, J. P. 1973. Correlation of Artificially Generated Three Component Time-Histories. Proceedings of the Second International Conference on Structural Mechanics in Reactor Technology, Berlin, Germany, Paper No. K1/8.

CHOPRA, A.-K., and ZHANG, L. 1991. Earthquake-Induced Base Sliding of Concrete Gravity Dams. ASCE Journal of Structural Engineering, 117 (12): 3698-3719.

CHRISTOPOULOS, C. 1998. SIV Program (Sliding Including Vertical)

DESPEYROUX, J. 1982. The El Asnam earthquake of 10 October 1980: characteristics of the main shock and lessons to be drawn for earthquake engineering. Engineering Structures, 4: 139-146.

FILIATRAUT, A., and TREMBLAY, R. 1997. Seismic Retrofit of Steel Moment Resisting Frames with Passive Friction Energy Dissipating Systems. Proceedings of the Northridge Earthquake Conference, Los Angeles. 8 pp.

GHOSH, A. K., 1988. On site specific design response spectra. Nuclear Engineering and Design. North-Holland, Amsterdam, 106: 275-287.

GHRIB, F., LÉGER, P., and TINAWI, R. 1995. Une approche progressive de vérification sismique des barrages en béton d'Hydro-Québec. Rapport No. EPM / GCS 1994-19.

GHRIB, F., LÉGER, P., TINAWI, R., LUPIEN, R., VEILLEUX, M. 1997. Seismic safety evaluation of gravity dams. The International Journal on Hydropower and Dams, Volume Four, Issue Two, pp. 126-138.

GUPTA, R. K., and HUTCHINSON, G. L. 1993. Horizontal and vertical response of torsionally coupled buildings. Engineering Structures,16 (11): 11-24.

HALL, J.-F. 1995. Parameter study of the response of moment-resisting steel frame buildings to near-source ground motions. Technical Report SAC95-05.

HEIDEBRECHT, A. C., TSO, W. K., and ZHU, T. J. 1992. Engineering implication of ground motion A / V ratio. Soil Dynamics and Earthquake Engineering, pp. 133-144.

HUDSON, M.B., SKYERS, B.D., LEW, M. 1996. Vertical strong ground motion characteristics of the Northridge Earthquake. Eleventh World Conference on Earthquake Engineering, Mexico, Paper No. 728.

ICBO. 1994. Uniform Building Code - Vol. 2. International Conference of Building Officials, Whittier, California.

IVERSON, J. K., and HAWKINS, N. M. 1994. Performance of precast / prestressed concrete building structures during Northridge earthquake. PCI Journal, 39 (2): 39-55.

JIWEI,W., DAJUN, D., and DI, Z. 1994. A study of earthquake response in a 15- story reinforced-concrete frame-tube model in shaking table test. The Structural Design of Tall Buildings, 3: 201-214.

KIDO, K., SUGIMURA, MORITAM M., and HIRAKI, K. 1997. Dynamic analysis of Hitokura dam during the 1995 Hyugoken-Nambu earthquake. Commission Internationale Des Grands Barrages, Dix-neuvième Congrès des Grands Barrages, Florence, pp. 689-708.

KITAGAWA, Y., OHTA, T., KAWAMURA, S., YOKOTA, H., NAKAE, S. and TERAMOTO, T. 1996. Design earthquake ground motion for dynamic analysis of building. Eleventh World Conference on Earthquake Engineering.

KOHZU, I., and SUITA, K. 1996. Single or few excursion failure of steel structural joints due to impulsive shocks in the 1995 Hyogoken Nambu earthquake. Eleventh World Conference on Earthquake Engineering, Mexico, Paper No. 412.

LACHET, C., BOUCHON, M., THEODULIDIS, N., and BARD, P-Y. 1995. Horizontal to vertical spectral ratio and geological conditions. Tenth European Conference on Earthquake Engineering, Balkema, Rotterdam, pp. 285-289.

LAWSON, J. 1994. Reflections on the effect of vertical seismic acceleration. PCI Journal, 39 (4): 40-41.

LÉGER, P., and LECLERC, M. 1996. Evaluation of earthquake ground motions to predict cracking response of gravity dams. Engineering Structures, 18, (3): 227-239.

LEVY, S., and WILKINSON, J. P. D. 1973. Generation of artificial time-histories, rich in all frequencies from given response spectra. Proceedings of the Second International Conference on Structural Mechanics in Reactor Technology, Berlin, Germany, Paper No. K1/7.

LIAUW, T. C., TIAN, Q. L., CHEUNG, Y. K. 1988. Structures on sliding base subject to horizontal and vertical motions. ASCE Journal of Structural Engineering, Vol.114, No.9, pp. 2119-2129.

MAKRIS, N., and CONSTANTINOU, M. C. 1992. Experimental study and analytical prediction of response of spring-viscous damper isolation system. Tenth World Conference on Earthquake Engineering, Madrid Spain, Balkema, Rotterdam, pp. 2467-2471.

McCANN, M. W., and SHAW, H. C. 1979. Determining strong-motion duration of earthquakes. Bulletin of the Seismological Society of America, 69 (4): 1253-1265.

MOHAMMADIOUN, G., and MOHAMMADIOUN, B. 1996. Vertical/Horizontal ratios for strong ground motion in the near field and soil non-linearity. Eleventh World Conference on Earthquake Engineering, Mexico, Paper No. 899.

OHNO, S., KONNO, T., ABE, K., MASAO, T., IIZUKA, S. and UEBAYASHI, H. 1996. Ground motions for aseismic design. Eleventh World Conference on Earthquake Engineering, Mexico, Paper No. 1791.

ORABI, I. I., and AHMADI, G. 1988. Response of structures subjected to horizontal-vertical random excitations. Soil Dynamics and Earthquake Engineering, 7 (1): 9-14.

PAGLIETTI, A., and PORCU, M. 1995. Extra load in columns due to floor rocking under vertical seismic motion. Tenth European Conference on Earthquake Engineering, Madrid, Spain, Balkema, Rotterdam, pp. 1259-1264.

PAK, R. Y. S., and GUZINA, B. B. 1995. Dynamic characterization of vertically loaded foundations on granular soils. ASCE Journal of Geotechnical Engineering, 121 (3): 274-286.

PAPAZOGLOU, A.J., and ELNASHAI, A.S. 1996. Analytical and Field Evidence of the Damaging effect of Vertical Earthquake Ground Motion. Earthquake Engineering and Structural Dynamics, 25: 1109-1137.

PARVEZ, S. M., and SHIMAZU, T. 1987. The behaviour of beams in reinforced concrete frames under the combined action of vertical and horizontal loadings. Journal of Structural and Construction Engineering, (transactions AIJ), 372: 72-85.

PAZ, M. 1994. International Handbook of Earthquake Engineering. Codes, Programs and Examples. Chapman & Hall, U.S.A, 545 pp.

PENZIEN, J., and WATABE, M. 1974. Simulation of 3-Dimensional Earthquake Ground Motions. Bulletin of the International Institute of Seismology and Earthquake Engineering, pp. 103-114.

SAADEGHVAZIRI, M., and FOUTCH, D. A. 1991. Dynamic behaviour of RC/ highway bridges under the combined effect of vertical and horizontal earthquake motions. Earthquake Engineering and Structural Dynamics, 20: 535-549.

SAC Joint Venture Steel Project Phase 2. 1997. Suites of time histories. Woodward-Clyde Federal Services, Pasadena, California, Draft Report March 1997.

SHIOI, Y., and SAKAJIRI, N 1996. Seismic damage to civil engineering structures by the 1994 far-off Sanriku earthquake. Eleventh World Conference on Earthquake Engineering, Mexico, Paper No. 854.

SUGIMOTO, H., NARUSE, K., and SEKO, Y. 1992. Design of 3-D earthquake isolation floor applied to a large room housing computers. Tenth World Conference in Earthquake Engineering, Madrid, Spain, Balkema, Rotterdam, pp. 2295-2299.

TAKAHASHI, K., OHNO, S., TAKEMURA, M., OHTA, T., HATORI, T., SUGAWARA, Y., and OMOTE, S. 1992. Observation of earthquake strong-motion with deep borehole. Generation of vertical motion propagating in surface layers after S-wave arrival. Eleventh World Conference on Earthquake Engineering, Mexico, VII-137-142.

TAYEBI, A. K., 1994. An evaluation of spectrum-compatible accelerograms for nonlinear analysis of short-period structures located in Eastern Canada. M. Eng. Thesis, McGill University, 144 p.

TINAWI, R., LÉGER, P., LECLERC, M., and CIPOLLA, G. 1998. Shake table tests for the seismic response of concrete gravity dams. 11th European Conference on Earthquake Engineering, Paris, France, pp. 11.

TRIFUNAC, M. D., and BRADY, A. G. 1975. A study on the duration of strong earthquake ground motion. Bulletin of the Seismological Society of America, 65 (3): 581-626.

TSAI, K.-C., and POPOV, E. P. 1988. Steel Beam-Column Joints in Seismic Moment Resisting Frames. Report No. UCB/EERC-88/19, Earthquake Engineering Research Center, University of California, Berkeley, Ca.

UNIFORM BUILDING CODE (1991).

WAKABAYASHI, M., NAKAMURA, T., IAWA, S., and HAYASHI, Y. 1984. Effects of strain rate on the behaviour of structural members. Proceedings of the Eighth World Conference on Earthquake Engineering, San Francisco, Ca, IV: 491-498.

YAMANOUCHI, H., and HASEGAWA, T. 1996. Seismic performance of model structures designed by old and new Japanese seismic design codes, against 1995 Kobe earthquake ground motions. Eleventh World Conference on Earthquake Engineering, Mexico, Paper No. 878.

APPENDIX A

SIV PROGRAM
(turbo pascal language)

```
Program SIV;
{Sliding Includind Vertical}
{MARCH,JUNE 1998}
{Constantin Christopoulos}
{File SIV.pas}

Uses CRT;

VAR

NPOINTS: Integer;
{Number of points in accelerogram}
File1: String[20];

FINP,FSLI,FACC,FPCF,FXPCF,FLEV,FFAS : TEXT;

DUM1,DUM2,DUM3,DUM4,DUM5,DUM6,DUM11 : SINGLE;
DUM7 : CHAR;
DUM8,DUM9,DUM10 : Double;
{Dummy variables to adapt input file to this program}
W: SINGLE;
{weight of dam}
Wao:SINGLE;
{weight of water displaced with dam, westergaard forces}
M:SINGLE;
{mass of dam}
Mao:SINGLE;
{mass corresponding to Wao}
Hst:SINGLE;
{static push of water horizontal}
U:SINGLE;
{static uplift vertical}
mu:SINGLE;
{coefficiant of friction}
DTA:SINGLE;
{time step of original accelerogram }
DTC:SINGLE;
{computing time step, specified by the user}
```

```
{-------------------------}
PROCEDURE Files ;
{This procedure opens the input file and creates}
{the output files .SLI, .ACC, .PCF, .LEV }
{-------------------------}

BEGIN
Clrscr;
Writeln('    quel est le nom du fichier d"entr,e?');
WRiteln('**le fichier d"entr,e doit ^tre un fichier ASCII');
Writeln('avec l"extension .PRN !! ne pas inclure l"extension!!');

Write('   >');
Readln (file1);
Assign(FINP,File1+'.prn');

Reset (FINP);

Assign(FSLI,(File1+'.SLI'));

Rewrite(FSLI);

Assign (FACC,(File1+'.ACC'));
Rewrite(FACC);

Assign (FXPCF,(File1+'.XPC'));
Rewrite(FXPCF);

Assign (FPCF,(File1+'.PCF'));
Rewrite(FPCF);

Assign (FLEV,(File1+'.LEV'));
Rewrite(FLEV);

Assign (FFAS,(File1+'.FAS'));
Rewrite(FFAS);


End; {Files}

{-------------------------}
FUNCTION JD(HOR,VER,b:SINGLE):SINGLE;
{This function computes the lever arm of the resultant }
{force, when the H and V accelerations are specified}
{it computes the distance from the upstream corner in terms}
{of percentage of the base length b= 40.7 m (Paugan Dam)}
{-------------------------}
BEGIN

JD:=(((Hst*16.9)-HOR*(20.2*Mao+19.2*M)+(14.3*M*(9.81+VER))-(15.8*U))/(M*(9.81+VER)-U))/b;
```

```
END;{JD}

{-------------------------}

PROCEDURE ACC;
{This procedure interpolates the values of the original }
{accelerogram, and creates the file FACC which contains }
{the values of the accelerograms, both H and V at a time step}
{equal to the computing time step specified by the user}
{*******************************************************}
{At the same time as the accelerations are computed, this proc.}
{also computes the lever arm of the resultant, the Safety Factor FS}
{and the peak correlation factor PCF}
{-------------------------}

VAR
q: INTEGER;
AH1,AH2,AH12,AV1,AV2,AV12 :DOUBLE;
e:DOUBLE;
DTR: LONGINT;
{ratio of acc. time step over desired computing time step}
PGAH,PGAV : DOUBLE;

s: SINGLE ;
Chi,FS : DOUBLE;

XPCF,Norm:DOUBLE;


BEGIN

Readln(FINP,DUM1);
Readln(FINP,DUM2);
Readln(FINP,NPOINTS);
Readln(FINP,DTA,DUM4);
Readln(FINP,DUM5);
Readln(FINP,DUM6);
Readln(FINP,DUM7);
Readln(FINP,DUM8);


{-----------------------------------------}
Readln (FINP,DUM11,AH1,AV1);
{-----------------------------------------}

  PGAH:=0;
  PGAV:=0;

  Repeat
```

```
Writeln(FACC,(AH1/100):10:5,(AV1/100):10:5);

{computing lever arm e}
  e:=JD((AH1/100),(AV1/100),40.7);
  Writeln(FLEV,e:10:10);


{computing FS }


{**********************}

  s:=1;

  Chi:= 9.81+(AV1/100);
   If (M*Chi-U)<=0 then
        Chi:=((U/M)+0.00000001);

  IF (AH1> 0) and (ABS((M+Mao)*AH1/100)>Hst)  then
        s:=-1;

  FS:=(s*(M*Chi-U)*mu)/(Hst+(M+Mao)*(-AH1/100));
  Writeln(FFAS,FS:5:3);

{**********************}


{computing PGA values }

  IF ABS(AH1/100)>PGAH Then
        PGAH:=ABS(AH1/100);

  IF ABS(AV1/100)>PGAV Then
        PGAV:=ABS(AV1/100);


{computing PCF (not pondered by the PGA's of the 2 accelerograms)}

XPCF:=ABS(AH1/100*AV1/100);
Writeln(FXPCF,XPCF:10:7);


{-------------------------------------------------}
Readln(FINP,DUM11,AH2,AV2);
{-------------------------------------------------}

   DTR:=Round(DTA/DTC)-1;

   If DTR=0 then
```

```
BEGIN

END

ELSE

Begin
     For q:=1 to DTR DO
       Begin
         AH12:=((AH2-AH1)/DTA)*(q*DTC)+AH1;
         AV12:=((AV2-AV1)/DTA)*(q*DTC)+AV1;
         Writeln(FACC,(AH12/100):10:5,(AV12/100):10:5);

       {computing lever arm e}
       e:=JD((AH12/100),(AV12/100),40.7);
       Writeln(FLEV,e:10:10);


       {computing FS  }
   {**********************}

   s:=1;

       Chi:= 9.81+(AV12/100);
        {If (M*Chi-U)<=0 then
         Chi:=((U/M)+0.00000001);}

       IF (AH12>0) and (ABS((M+Mao)*AH12/100)>Hst)  then
         s:=-1;

       FS:=(s*(M*Chi-U)*mu)/(Hst+(M+Mao)*(-AH12/100));
       Writeln(FFAS,FS:5:3);

       {**********************}

       {computing PGA values PGAH and PGAV}
        IF ABS(AH12/100)>PGAH Then
          PGAH:=ABS(AH12/100);
        IF ABS(AV12/100)>PGAV Then
          PGAV:=ABS(AV12/100);


     {computing PCF (not pondered by the PGA's of the 2 accelerograms)}

      XPCF:=ABS(AH12/100*AV12/100);
      Writeln(FXPCF,XPCF:10:7);

       End;{for}
End;{else}
```

```
    AH1:=AH2;
    AV1:=AV2;
  Until EOF(FINP);

{-------------------------}

Reset(FXPCF);
Norm:=PGAH*PGAV;
If Norm=0 then
  Writeln(FPCF,'Les accelerations verticales sont nulles')
  Else
  Begin
   Repeat

  Readln(FXPCF,XPCF);
  Writeln(FPCF,(XPCF/Norm):10:6);

  Until(EOF(FXPCF));
  End;{else}



Close(FINP);

Close(FXPCF);
Close(FPCF);
Close(FLEV);
Close(FFAS);
Close(FACC);

Reset(FACC);

END;{ACC}



{-------------------------}
PROCEDURE UserINP;
{This procedure asks the user to specify the parameter values}
{-------------------------}
BEGIN
Clrscr;

{Writeln ('D,sirez entrer vos donn,es sous forme de fichier?')
Writeln ('O/N ? (O) > ');
Readln(Var);
If Var := O}
```

```
Write('  Entrez le poids du barrage en kN > W= ');
Readln(W);

Writeln(' ');
Write('  Entrez Wao en kN > Wao= ');
Readln(Wao);

Writeln(' ');
Write('  Entrez la force de soulŠvement U en kN > U= ');
Readln(U);

Writeln(' ');
Write('  Entrez la force hydrostatique en kN > Hst= ');

Readln(Hst);
Writeln(' ');
Write('  Entrez le coefficiant de friction dynamique > mu= ');

Readln(mu);
Writeln(' ');
Writeln('  Entrez le pas dt d'integration d.sir, en s. ');
Write  ('  de la forme 0.1 , 0.01, 0.001, ... etc   > dt= ');


Readln(DTC);
Writeln(' ');
End; {UserINP}


{-------------------------}
PROCEDURE Masses;
{This procedure computes the masses based on the inputed weights}
{-------------------------}
BEGIN
M:=(W/9.81);
Mao:=(Wao/9.81);
End; {Masses}


{-------------------------}
PROCEDURE Sliding;
{This computes the sliding displacement of the defined structure}
{submited to the horizontal and vertical accelerograms}
{-------------------------}
VAR
i: INTEGER;
Chi: DOUBLE;
Car: CHAR;
AJUST: REAL;
NEG:Boolean;
```

```
S1,S2,ST,Si1,Si2,Sii1,Sii2 : DOUBLE;
H1,V1,H2,V2 : REAL;

A: DOUBLE;
B: DOUBLE;
DTCOR: DOUBLE;

r:char;


Begin
 NEG:=False;
  S1:=0 ;
  Si1:=0;
  Sii1:=0;
  ST:=0;


  Reset(FACC);
  Readln(FACC,H1,V1);

 REPEAT

  Readln(FACC,H2,V2);

  Chi:=(9.81+V2);
  If (M*Chi-U)<=0 then
   Chi:=((U/M)+0.00000001);


 IF (H2<0) and (H2<-((mu*(M*Chi-U)-Hst)/(M+Mao))) Then
 {Sliding Mode is activated}



 Begin

   Si1:=0;
   Sii1:=0;

   Repeat

        NEG:=False;

        Chi:=(9.81+V2);
         If (M*Chi-U)<=0 then
           Chi:=((U/M)+0.00001);

        Sii2:=((Hst-(M+Mao)*H2-(M*Chi-U)*mu)/(M+Mao));
        Si2:=(Si1+(DTC/2)*(Sii1+Sii2));
```

```
        S2:=(Si1*DTC)+(Sii1*(DTC*DTC)/3)+(Sii2*(DTC*DTC)/6);

        If Si2<0 then

         Begin

          Neg:=True;
          {correction on acceleration and displacement}
          A:=((Sii2-Sii1)/DTC);
          B:=(Sii1*Sii1-(2*A*Si1));

          Sii2:=-SQRT(B);
          Si2:=0;

          DTCOR:=-2*Si1/(Sii1+Sii2);

          S2:=((Si1*DTCOR)+(Sii1*(DTCOR*DTCOR)/3)+(Sii2*(DTCOR*DTCOR)/6));

         End;

   ST:=ST+S2;

   Writeln (FSLI,S2:10:5,ST:10:5);

   Si1:=Si2;
   Sii1:=Sii2;

   H1:=H2;
   V1:=V2;

  If NOT EOF(FACC) THEN
  Readln(FACC,H2,V2)

 Until (NEG=TRUE);

End{sliding mode}

ELSE
 Begin
   Sii1:=0;
   Si1:=0;
   S1:=0;
   S2:=0;

   Writeln (FSLI,S2:10:5,ST:10:5);
```

```
    Si1:=Si2;
    Sii1:=Sii2;


  End;{else}


Until EOF(FACC);

End;{Sliding}


{++++++++++++++++++++++++++++++++++++++++}
{++++++++++++++++++++++++++++++++++++++++}
{CORE OF THE PROGRAM}
{++++++++++++++++++++++++++++++++++++++++}
{++++++++++++++++++++++++++++++++++++++++}

BEGIN

Clrscr;
Files;
UserINP;
Masses;

Acc;

Sliding;

Close(FACC);
Close(FSLI);

END.
{PROGRAM SIV}
```